AD-A051 968 STANFORD UNIV CA LAB FOR RATIONAL GEOMECHANICS F/G 8/13
SEASONAL CREEP OF SILTY CLAY SOIL AND THE FORMATION OF SMALL GU--ETC(U)
DEC 77 A E SOTO, R UPP, A M JOHNSON DAAG29-75-C-0025

UNCLASSIFIED ARO-13336.1-GS NL

1 OF 2
AD
A051 968

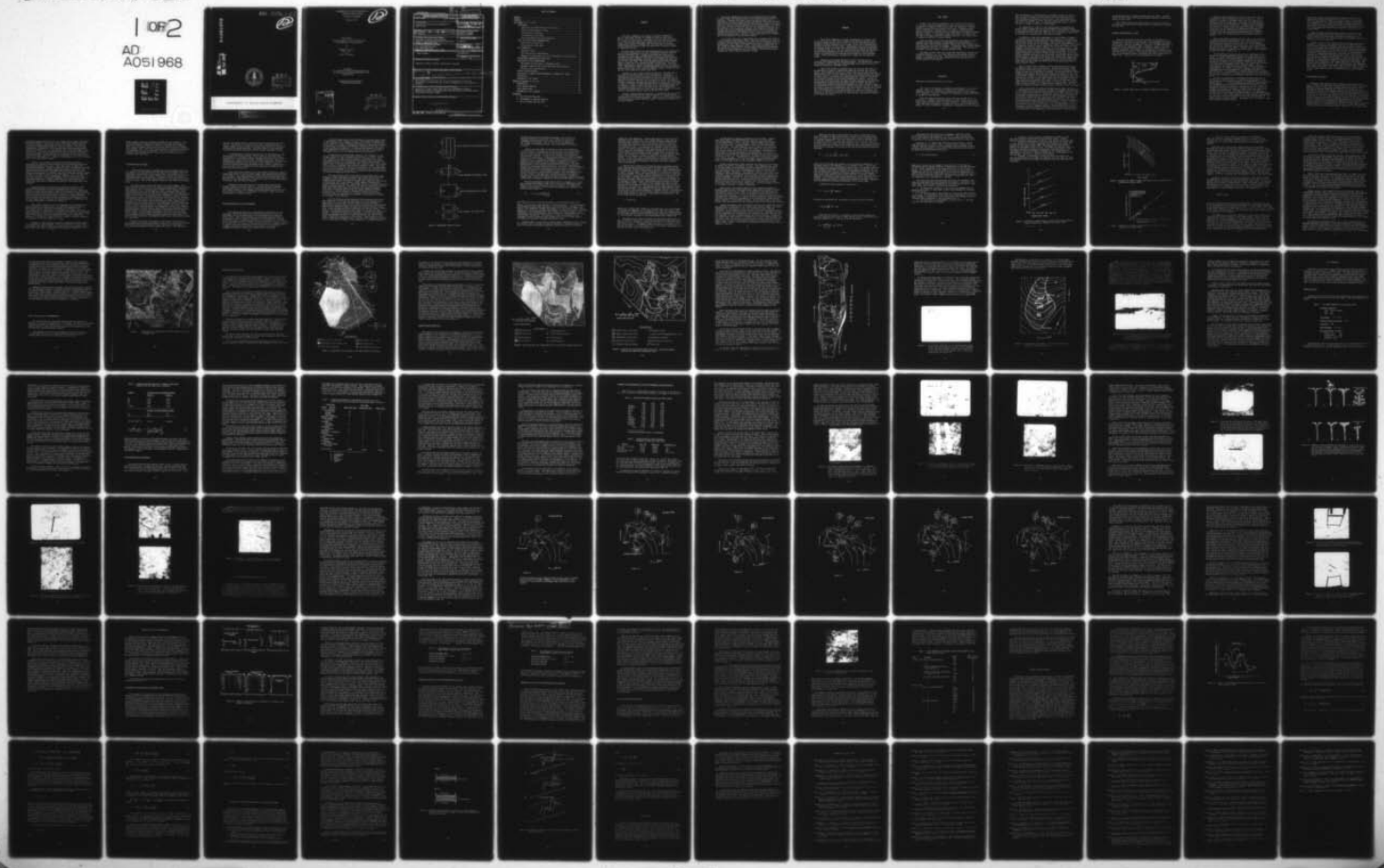

DEPARTMENT OF APPLIED EARTH SCIENCES

LABORATORY FOR RATIONAL GEOMECHANICS
SCHOOL OF EARTH SCIENCES
Stanford University, CA

December 1977

Final Report

SEASONAL CREEP OF SILTY CLAY SOIL AND The Formation of Small Gullies

by

Alejandro E. Soto
Rex Upp
and
Arvid M. Johnson

OF COURSE
THE FINDINGS IN THIS REPORT ARE NOT TO BE
CONSTRUED AS AN OFFICIAL DEPARTMENT OF THE
ARMY POSITION

APPROVED FOR PUBLIC RELEASE;
DISTRIBUTION UNLIMITED

Unclassified
SECURITY CLASSIFICATION OF THIS PAGE (When Data Entered)

(18) ARO (19) 13336.1-GS

REPORT DOCUMENTATION PAGE

READ INSTRUCTIONS BEFORE COMPLETING FORM

1. REPORT NUMBER
2. GOVT ACCESSION NO.
3. RECIPIENT'S CATALOG NUMBER

4. TITLE (and Subtitle)
Seasonal Soil Creep and the Formation of Small Gullies

(9) 5. TYPE OF REPORT & PERIOD COVERED
Final Report. June 75 - May 77

6. PERFORMING ORG. REPORT NUMBER

7. AUTHOR(s)
(10) Alejandro E. Soto, Rex Upp, Arvid M. Johnson

(15) 8. CONTRACT OR GRANT NUMBER(s)
DAAG29-75-C-0025

9. PERFORMING ORGANIZATION NAME AND ADDRESS
Department of Applied Earth Sciences
School of Earth Sciences, Stanford University
Stanford, California 94305

10. PROGRAM ELEMENT, PROJECT, TASK AREA & WORK UNIT NUMBERS
DD-1473

11. CONTROLLING OFFICE NAME AND ADDRESS
U.S. Army Research Office
Post Office Box 12211
Research Triangle Park, N.C. 27709

(11) 12. REPORT DATE
Dec 77

(12) 13. NUMBER OF PAGES
129 p.

14. MONITORING AGENCY NAME & ADDRESS (if different from Controlling Office)
Same as above

15. SECURITY CLASS. (of this report)
Unclassified

15a. DECLASSIFICATION/DOWNGRADING SCHEDULE
NA

16. DISTRIBUTION STATEMENT (of this Report)
Approved for public release; distribution unlimited.

(16) 17. DISTRIBUTION STATEMENT (of the abstract entered in Block 20, if different from Report)
Seasonal Creep of Silty Clay Soil and the Formation of Small Gullies.

18. SUPPLEMENTARY NOTES
The findings in this report are not to be construed as an official Department of the Army position, unless so designated by other authorized documents.

19. KEY WORDS (Continue on reverse side if necessary and identify by block number)
Seasonal soil creep, black silty clay soil, shrink-swell behavior, dessication cracks, self-mulching soil, wetting front, rate process theory, discontinuous gullies, piping.

20. ABSTRACT (Continue on reverse side if necessary and identify by block number)
See attached Abstract

42062

DD FORM 1 JAN 73 1473 EDITION OF 1 NOV 65 IS OBSOLETE

Unclassified
SECURITY CLASSIFICATION OF THIS PAGE (When Data Entered)

TABLE OF CONTENTS

PREFACE

This report summarizes the results of research conducted for the U.S. Army under Contract No. DAAG29-75-C-0025 for the period May 15, 1975 to May 14, 1977. The report is for the final two years of a three-year investigation of seasonal soil creep and its manifestations. The Principal Investigator during the first year of the investigation, Robert W. Fleming, left the University of Cincinnati and the study was continued under the supervision of Arvid M. Johnson of Stanford University.

The first year of the study was largely devoted to the installation of new field instrumentation at sites on Stanford University property and near Cincinnati, Ohio. During the remaining two years of the investigation, additional instrumentation sites were established at Stanford to monitor seasonal creep, and an investigation was initiated to understand the development of gullies such as those that appear in most of the study areas. The field instrumentation provided a limited amount of data, due to an untimely drought in California. The below normal precipitation virtually stopped all seasonal creep in our study areas. Nevertheless, some of the instrumentation sites will be monitored during the next year or two, provided rainfall returns to normal values and the soils resume their normal creep rates.

Alejandro E. Soto, Graduate Research Assistant, performed most of the field and laboratory work, and is continuing the research on mechanisms of soil creep as the subject of his Ph.D. dissertation. He performed engineering classification tests and swell potential tests on samples of the silty clay soil that is involved in creep. He prepared detailed topographic, geologic and soils maps for each of the study areas in order to establish the physical setting for the occurrence of the creep. In addition, he made a cursory analysis of the relationship between soil and vegetation types at one of the study sites. He has extensively reviewed the literature on soil creep, and has begun to apply rate process theory to understand seasonal creep in the silty clay soils.

Rex Upp, Graduate Research Assistant, is responsible for the section of this report dealing with the study of gullies. Dr. Bernard Hallet introduced Soto to rate-process theory. Onder Gokce, Ze'ev Reches, Richard Turnbull and Douglas Yadon, graduate students at Stanford, assisted with the field studies.

This report summarizes only part of the research into the nature of gully erosion and seasonal creep of soil being performed at Stanford University. Research into creep of soils was initiated by Alberto Lobo-Guerrero and Arvid Johnson (Johnson and Hampton, 1969), who estimated long-term creep rates by measuring and analyzing tilt of steel fence posts. Robert W. Fleming contributed much more to our understanding of the nature and timing of creep in the silty clay soils by measuring creep rates in the field and in the laboratory (Fleming, 1971; Fleming and Johnson, 1975). Fleming also discussed engineering characteristics of the creeping soil and made observations on the physical state of the soil during seasonal wetting and drying cycles. The work on creep described here by Alejandro Soto is an outgrowth of this previous research.

Our research into gully erosion began with a thorough field study of a gully system by David Keefer (1969). This was followed by the study of a series of discontinuous gullies in Foothill Park by a graduate class in geomorphology (e.g., Marsh, 1975) and by a much more thorough study for a M.S. thesis by Thomas Nicholson (1976). The research reported here by Rex Upp should be considered to be preliminary although he has abandoned the plan to study gullies for his Ph.D. research. We tentatively plan further Ph.D.-level research into gully erosion.

ABSTRACT

This report summarizes a two-year investigation of seasonal creep in a black silty clay soil that is common in the San Francisco Bay Area. Because of drought during the two years, the soil did not become entirely saturated and there apparently was no creep, so that field instrumentation provided no new data on creep rates. Nevertheless, much data was obtained on seasonal changes of the soil and on displacements produced by shrinking and swelling of the soil. The data indicate that directions and magnitudes of horizontal displacements of soil that occur between a wet and a dry season are controlled by the positions and attitudes of nearby shrinkage cracks. These displacements, averaged over a large area, are therefore random.

During the wet seasons wetting of the soil occurred along an irregular front advancing from the ground surface. The wetting front advanced more rapidly in debris that had filled shrinkage cracks than in the soil in polygons surrounded by shrinkage cracks.

Many of the features of seasonal creep of the silty clay soils can be understood in terms of a theoretical model that utilizes rate process theory. Three essential features of creep of this soil are that the creep-displacement profile is convex upwards, that creep begins shortly after initial wetting of the soil, and that creep eventually stops without obvious changes in water content. The theoretical model assumes that creep is a result of the diffusion of oxygen in and around interparticle contacts. The initial wetting and swelling decreases the number of bonds through the adsorbed water and increases the shear stress per bond, thereby increasing the rate of diffusion which manifests itself macroscopically as creep. Diffusion tends to decrease the stress concentrations, thereby decreasing the rate of diffusion and rate of creep so that eventually creep stops even at constant water content. The convex-upward shape of the creep profile is a result, according to the model, of an increase in the number of bonds per area with increasing depth, reflected in the lower decrease in the swelling and in the seasonal change of water content with depth.

SOIL CREEP

Seasonal soil creep, as defined for the purposes of this report, is the slow, downslope movement of soil under the influence of gravity in response to changes in soil water content and temperature. Terzaghi (1950) recognized two basic types of soil creep: 1) seasonal creep, which is restricted to a depth equal to or smaller than the depth of seasonal variation in conditions such as temperature, freezing and thawing and water content; 2) continuous creep, which occurs at a depth below the zone of seasonal variations in ground conditions. The latter occurs in response to gravity or surface loading.

Creep processes in soil have been extensively investigated by soils engineers and several theories or mechanisms have been proposed to describe creep. Most of these studies, however, have been concerned with continuous creep as defined by Terzaghi. In addition, many of these studies have considered creep as it is related to landsliding. Thus theories of continuous creep are unable to explain seasonal creep.

The theory of soil creep as a rate process developed by Mitchell and co-workers (Mitchell, et. al., 1968, 1969) does show promise of applicability to seasonal soil creep. Continuing research by Alex Soto will attempt to determine if the rate process theory can indeed be used to explain seasonal creep behavior.

BACKGROUND

Importance and Identification of Soil Creep

Soil creep is of interest to engineers and geologists. To the soils engineer, creep is of importance in terms of the economic life of an engineering structure, which may be shortened because of creep movements. To the geologist, creep is of interest as a geomorphic process, particularly as an agent to mass wasting.

Generally associated with soil creep, and used as evidence for its occurrence, is damage to man-made structures such as fences, roads, sidewalks, pipes, railroad tracks, and other structures. Fleming and Johnson (1975) described the damage to a residence built so that it straddled the margin of a valley filled with creeping soil. Engineers are also concerned

with the movements of retaining walls and abutments caused by creep, as well as with the changes in earth pressure exerted on such structures which accompany the creeping of the soil mass. Creep deformations produce structural changes in soils, which may lead to reduced soil strength and failure of the soil mass. On natural and man-made slopes, creep of the soil is commonly a precursor to landsliding.

The importance of creep as a mass wasting agent is exemplified by Kojan's (1967) estimate that 70% of the sediment reaching major streams in the Northern California Coast Ranges is due to soil creep and landsliding. He estimated that each year more than 750 tons of sediment per square mile in that area are transported by creep alone to streams.

In addition to the direct measurement of creep movement, a number of features have been long associated with areas subject to creep and have been used to identify slopes undergoing creep deformations. Sharpe (1938) has described several of these features. They include the formation of "stone lines" at the base of the creeping soil mass, transported joint blocks, the downslope bending or drag of bedded rock, curved tree trunks (concave upslope), and displaced surface features, such as fences and poles. Other geomorphic features associated with creep are the development of anomalous relationships between soil and bedrock (Fleming and Johnson, 1975); the apparent carving out of bedrock valleys by the creeping soil, so that the bedrock topography exhibits a sag, not evident at the ground surface, below creeping lobes of soil (Sharpe and Dosch, 1942; Fleming and Johnson, 1975); and the gradual thickening of soil towards the axes of small topographic swales, which produces the flat-bottomed valleys of the type found in the study areas and the rounded or convex crests of hillslopes described by others (Gilbert, 1909).

Many of these lines of evidence, cited as indicators of soil creep by different authors, have been disputed. Parizek and Woodruff (1956b) and Phillips (1974) have argued that the curvature of the trunks is most likely the result of normal growth processes. Parizek and Woodruff (1965a) disagreed with Sharpe's assertions concerning the occurrence of soil creep in the Georgia Piedmont, particularly as regards the evidence he used to establish its occurrence. They doubted the correlation between stone lines and slow mass wastage. Kojan (1968) argued that the downslope tilting of fence posts is not necessarily the result of creep, but may result from random vibrations because the uphill side of the fence posts is supported along a greater portion of its length than the downhill side. Once the posts are slightly inclined, further tilting is induced by their own weight.

That creep results in tilted and displaced fence lines, and that it is associated with the concentration of large rock fragments along the base of the creeping soil layer has been verified in the black silty clay which is the subject of this report. Fleming and Johnson (1975) described creep displacement measurements based on the tilt and displacement (relative to an initially straight line) of fence posts where the fence line crossed a lobe of creep soil. The calculated amounts were compativle with creep displacement measurements made by more direct means. Gravel concentrations have been observed along the base of the creeping soil layers, as shown in the log for test pit no. 8 (see Fig. 10 in following pages). The fact that most of the rock fragments consist of basalt whereas the bedrock is a weathered claystone leaves little doubt that creep has been the cause of the concentration. Such migration of coarse particles to shear surfaces

in cohesive materials is common (Trollope and Chan, 1960). Terzaghi (1953) and Kojan (1967) have described similar features in other areas subject to soil creep.

What becomes evident from this discussion is that care should be exercized in interpreting the evidence used to establish the occurrence of soil creep.

General Considerations on Creep

Creep can be defined as the slow, progressive deformation of a material with time under a constant load. This phenomenon is observed in metals, in ionic and covalent crystals, and in amorphous materials such as glass, plastics and rubbers. Creep tests in these materials can be carried out in compression, shear or bending. However, the usual method is to subject the specimen to a constant tensile stress at a constant temperature and to measure the deformation at different times since the start of the test. The data are represented in the form of a plot of the deformation versus the elapsed time (for a given stress and temperature). Such a plot is shown schematically in Figure 1.

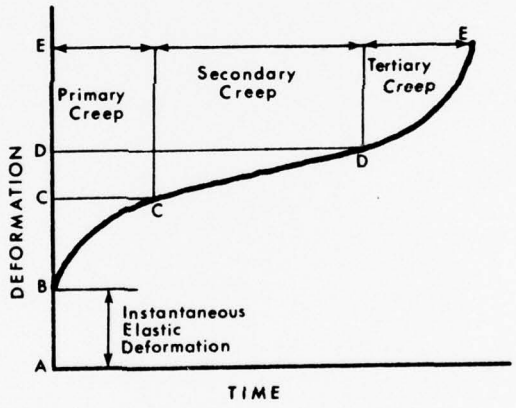

Figure 1. Typical creep curve at constant temperature and stress.

When the load is applied at the start of the creep test, an instantaneous elastic deformation, AB, occurs (Fig. 1). This is followed by a period of decreasing creep rate, BC, known as the primary or transient creep stage. This stage is characterized by work hardening, or a predominance of strengthening over weakening processes active within the material. Primary creep is followed by a period of constant strain rate known as secondary or steady-state creep, CD, during which the strengthening and weakening processes are equal. DE represents the stage of increasing rate of strain, where the weakening mechanisms predominate. Known as tertiary creep, the increasing strain rate ultimately results in failure.

These relationships generally hold for creep of all materials although, depending on the magnitude of the creep stress, the test temperature, and the duration of the test, the three stages are not necessarily evident in a given creep test. At low temperatures and stress levels secondary and tertiary creep do not always occur and the creep is said to be damped. Undamped creep is that in which deformation proceeds through the three creep stages. These generalizations also apply to most soils.

The evaluation of creep data for soils is complicated by the particulate, multiphase (mineral grains, water, air) nature of soil bodies. As Lafeber (1966) has indicated, the mechanical behavior of any material made up of different phases is generally not given by the sum of the behavior of the different components, but depends on their mutual interaction and interference. The interaction is affected by the spatial arrangement of the component phases. This is illustrated by the stress concentration which occurs around holes in solid mediums. If a number of holes are present, their geometric arrangement affects the strength and the deformation pattern of the entire material. This dependence of material behavior on the arrangement of the various phases is enhanced when the mechanical properties of the different components are significantly different, as is the case with soils.

In soils it is necessary to distinguish between creep tests in an open system (drained) and in a closed system (undrained). In an open system, creep of saturated samples is accompanied by consolidation wherein excess pore pressures arising from the applied stress are dissipated by flow of the pore fluid out of the soil. Creep in an open system involves a decrease in the volume of the soil as well as changes in the shape of the sample. Volume changes also occur during secondary consolidation in which water flows out of the sample at constant effective stress. Consolidation leads to a strengthening of the soil mass so that a normal increase of strain rate with shear stress is likely only at the initial stages of the creep process, when the soils have similar structures. Because of the increased consolidation of samples loaded to higher stresses, the strain rate of these in time will be smaller (Haefeli, 1953).

In a closed system (constant volume) the principal strain of the samples can be used as a measure of the creep rate. It is evident that true creep effects, which occur under a constant stress, have to be separated from the deformation which may accompany changes in pore pressure and, as a result, in effective stresses within a soil mass. Hirst and Mitchell (1968) have limited the definition of creep to time-dependent pure shear, which occurs under conditions of no volume change.

These statements illustrate that a number of factors must be considered in assessing the creep behavior of a given soil. One further complication arises when considering unsaturated soils, in which the interplay of the different phases in determining stress-strain behavior is not fully understood.

Studies of creep in soil have historically followed two different approaches. Studies by soil engineers have for the most part been concerned with evaluating continuous creep data obtained in the laboratory. Field studies have similarly been concerned with continuous creep. The main purpose has been to establish functional relations describing the stress-strain-time behavior of soils for use in the design and construction of engineering structures. Geologists have been primarily concerned with compiling field observations on soil creep and with establishing the geomorphic significance of various creep processes. In all, most of the previous field studies of creep have been done in areas subjected to landsliding or seasonal freezing and thawing (Sharpe, 1942, Goldstein and Ter-Stepanian, 1957, Rapp, 1960, Saito and Uezawa, 1961, Everett, 1963, Goldstein, et. al., 1965, Ter-Stepanian, 1965, Washburn, 1967, Owens, 1969, Shibata and Karube, 1969, Yen, 1969, Barr and Swanston, 1970, Hardy 1970, Harris, 1971, Ter-Stepanian, 1974). Data on creep rates in areas subjected solely to seasonal moisture content changes is scanty.

The Geologist's Approach

Geologists have recognized the occurrence of soil creep for many years. Sharpe (1938) described four mechanisms by which soil layers creep downhill. Three of these, frost heaving, temperature changes, and the dessication-expansion mechanism are variations of the process first described by Davidson (1889) whereby expansion associated with freezing of the pore water results in a movement of soil particles perpendicular to the slope; when the ice melts, the soil particles fall back under the influence of gravity in a direction approximately vertically downward, the exact path being influenced by the amount of cohesion possessed by the soil. Davidson's view is a reinterpretation of observations presented by Kerr (1881) on the "action of frost in the arrangement of superficial earthy material". Davidson supports his conclusions with experimental data, and it is generally accepted that such a mechanism results in creep in areas where periodic freezing and melting of pore water occurs (Leopold, et. al., 1964). Sharpe

and several workers before him (see, for example, Davis, 1892), generalized Davidson's concept to account for creep in areas where freezing and thawing are non-existent, even though, as noted by Fleming (1971), there is no logical or observational reason for such an extension. The so-called "shrink-swell" mechanism of soil creep persists in modern day geological literature (Leopold, et. al., 1964; Kirkby, 1967; Carson and Kirkby, 1972; Young, 1972). The latter two works deviate from the classical shrink-swell theory by allowing for some component of the total creep to occur during the swelling stage. Swelling is thus not considered to occur normal to the slope but at some angle to it. However, creep phenomena are still attributed solely to the shrink-swell process.

There are two probable reasons why the shrink-swell behavior associated with changes of water content has been interpreted as being the same mechanism which causes creep. First, the concept is simple and intuitively reasonable. Second, in most areas where creep has been observed, the soils involved have contained significant amounts of expansive clay. It has been speculated (Carson and Kirkby, 1972) that seasonal creep is in reality an acceleration of continued creep that results when seasonal changes decrease the strength of the soil (Barr and Swanston, 1970, concluded this to be so in an area of active landsliding). Whether this is the case, detectable changes in creep rates invariably occur in soils which expand to some extent when wetted. These considerations may explain why little research has been done to establish the validity of the shrink-swell creep mechanism.

Some workers have not accepted the shrink-swell theory of creep. Culling (1963) suggested on theoretical grounds that creep occurs in response to random forces acting on individual soil particles. Random movements of particles was presumed to result in a diffusion of particles from regions of high particle concentration to regions of lower concentration. The forces imparting random motions include those due to thermal expansion, surface tension and capillary effects, and expansion and freezing of water in soils, among others. Culling's theoretical analysis is complicated and the proposed mechanism is difficult to visualize.

Kojan (1965) clarified the role of expansion and contraction due to moisture changes in producing creep. He noted that seasonal changes in water content affect creep rates by reducing the strength of soil in a number of ways: expansion of the adsorbed water layer, solution of cement, reduction of friction due to increased pore pressures, and decreasing the mean viscosity of water films around particles. In a later paper, Kojan (1967) listed several microscale deformation mechanisms considered by engineers to contribute to creep, as well as a number of factors considered to contribute to the time dependence of creep.

A number of other processes have been attributed with either causing or contributing to creep movements. These are summarized by Young (1972) and include: the effect of plant roots which, upon decay, provide holes for soil to move into; forces transmitted by the swaying of vegetation in the

wind; creation of holes by burrowing organisms and the transport of soil by earth worms; and, temporary increases in load caused by animals. To these may be added the splatter of soil due to raindrop impact (Briggs, 1972), and soil material falling into vertical dessication cracks (Sharpe, 1938; Fleming, 1971). That any of these processes is singularly responsible for measurable soil creep is doubtful. There is no doubt that they contribute to mass wastage; however, most are best considered as part of processes other than creep.

A Geologist Sees the Light

A detailed field study of seasonal creep in an expansive silty clay soil common to the San Francisco Bay Area has provided valuable information on seasonal creep phenomena and has cast doubts on the validity of the shrink-swell theory of soil creep (Fleming, 1971, Fleming and Johnson, 1975). Displacement profiles were measured at different times of the year with a tiltmeter lowered down flexible pipes anchored into the bedrock which underlies soil layers. Some of the important results of this study are discussed below.

The displacement profiles were found to be convex upwards. This shape has been recognized for a long time as being characteristically produced by the various types of seasonal creep (Davidson, 1889, Sharpe, 1938, Rapp, 1960, Washburn, 1967, Barr and Swanston, 1970). Sharpe and Dosch (1942) illustrated graphically the bending and stretching of weak, horizontally bedded strata which extend into the zone of creeping soil; the convex-upwards shape is clearly seen. Ter Stepanian (1965) presented a profile based on measurements in depth-creep wells (holes lined with metal cylinder segments or filled with wood pegs or other materials). The upper part of the profile, the zone of "surface creep" has the characteristic shape. Fleming (1971) speculated that the peculiar shape of the displacement profile (displacement profiles in most other materials are concave upwards) could result from two factors. First, it may be related to the magnitude of the cyclic change in water content at different depths, the profile of which resembles the displacement profile. Second, the resistance to deformation may increase with depth. Kirkby (1967) and Carson and Kirkby (1972) account for the shape of the profile in their modified shrink-swell theory of creep by assuming that the change in water content decreases exponentially with depth in the profile and by introducing an appropriate function into their general equation for creep rates.

Fleming observed that the change in soil moisture with depth had the appearance of an advancing wetting or drying front, and that the displacement in the flexible pipes reflected this. Wetting or drying began at the surface and extended vertically through the profile. The thickness of

soil that was moving could be correlated with the depth penetrated by the "front". The entire soil thickness (up to about 2 meters) was seen to undergo changes in water content, the change being greatest at the ground surface and decreasing with depth. The water content of the stationary and underlying bedrock remained relatively constant throughout the year.

The measurements by Fleming indicate that the soil begins to creep shortly after the initial wetting. The creep rate is initially high, but diminishes to a negligible amount with time, whereas the soil remains essentially at constant water content. Movement during the drying cycle apparently was random in direction and of variable magnitude. The direction of displacement appeared to be controlled by the position of the pipe relative to adjacent developing shrinkage cracks. However, Fleming showed that the drying cycle is necessary for the recurrence of downhill creep during the next wetting cycle.

These observations dispute two of the premises on which the classical shrink-swell theory of creep is based; namely, that movement during swelling occurs normal to the ground surface, and that dessication results in movement downslope. Thus, whereas Fleming concedes that the shrink-swell theory may apply to some expansive soils, it does not account for the creep behavior of the silty clay soil which he studied.

Fleming also made observations on features associated with the seasonal changes in the silty clay soil. Of interest are his comments on dessication and on the occurence of sub-planar features, which he calls "shiny surfaces", that resemble the slick surfaces seen in serpentine and which may be related to the expansion of the soil. These topics will be discussed in a separate section.

Creep Investigations by Soils Engineers

The engineering literature on time-dependent deformation of soils is diverse. Several different models have been proposed to account for experimental and field observations of soil deformation under sustained loads (creep). These can be grouped into four broad categories based on: 1) jumping of bonds; 2) growth of fissures; 3) the interaction of various levels of structure, as exemplified by the work of Hoelzer, et. al., (1973), and 4) structural viscosity, in which the soil structure is assumed to possess an inherent viscosity, generally associated with the flow of adsorbed water. A number of rheological models have been formulated to describe soil deformation; these can generally be included in the last group.

In the following pages a brief description, presented approximately in chronological order, is given of some of the proposed mechanisms. Prior to the discussion of the engineering literature on creep, a clarification of two terms is necessary. International rheological nomenclature restricts the term creep to recoverable deformations, whereas the term flow refers to non-recoverable deformations. In studying time-dependent deformation, soils engineers have used the terms creep and flow more or less interchangeably, and it is in this context that they are used here.

As has been the case with many aspects of soil mechanics, it was Terzaghi (1929) who first recognized the importance of creep in relation to the stability of slopes and the movement of retaining walls. Since then, engineers have been concerned with the changes that time-dependent deformations produce in soil properties, particularly shear strength. As a general rule, it has been observed that soft, sensitive clays lose strength after a period of undrained creep (Hirst and Mitchell, 1968). The effect of creep on partly saturated soils is more variable; such soils may exhibit gain or loss of strength, or no change in strength at all. Engineers have also been concerned with the pattern of strains which precede creep failure or which occur during non-failure creep.

The first detailed study on the effects of sustained creep on the strength of clayey soils was by Casagrande and Wilson (1951) who studied a number of soils from around the world. They found that clay-rich saturated soils showed a decrease in strength after undrained creep relative to the strength of un-crept, normally loaded samples, whereas partly saturated soils which contained a significant fraction of granular materials showed a strength increase. For some of the tests in unsaturated materials creep would cease after short time intervals even though the applied loads were only slightly smaller than the normal compressive strength of the soils. They attributed the strength increase in the partly saturated soils to the occurrence of "internal consolidation" whereby gas in the voids was compressed and dissolved in the pore water, leading to a decrease in the void ratio.

Tests by Goldstein and Ter-Stepanian (1957) supported this notion. They showed that the strength decrease which occurred in samples tested undrained did not occur when identical samples were tested drained. These authors considered that in clay soils the interparticle bond strength depends on the distance between the particles and their relative arrangement. During deformation bonds are broken and new ones are formed. However, since it was considered that most bonds require a long rest for their renewal, a continuous deformation would result in a progressive weakening of the soil. Interparticle bonds were classified as brittle, which permit elastic deformations and fail at a given deformation, and viscous, which impart "liquid-like" properties to clayey soils. These authors also presented a simplified rheological model to describe soil deformation, apparently one of the earliest to appear in the literature. It is shown in Fig. 2-a.

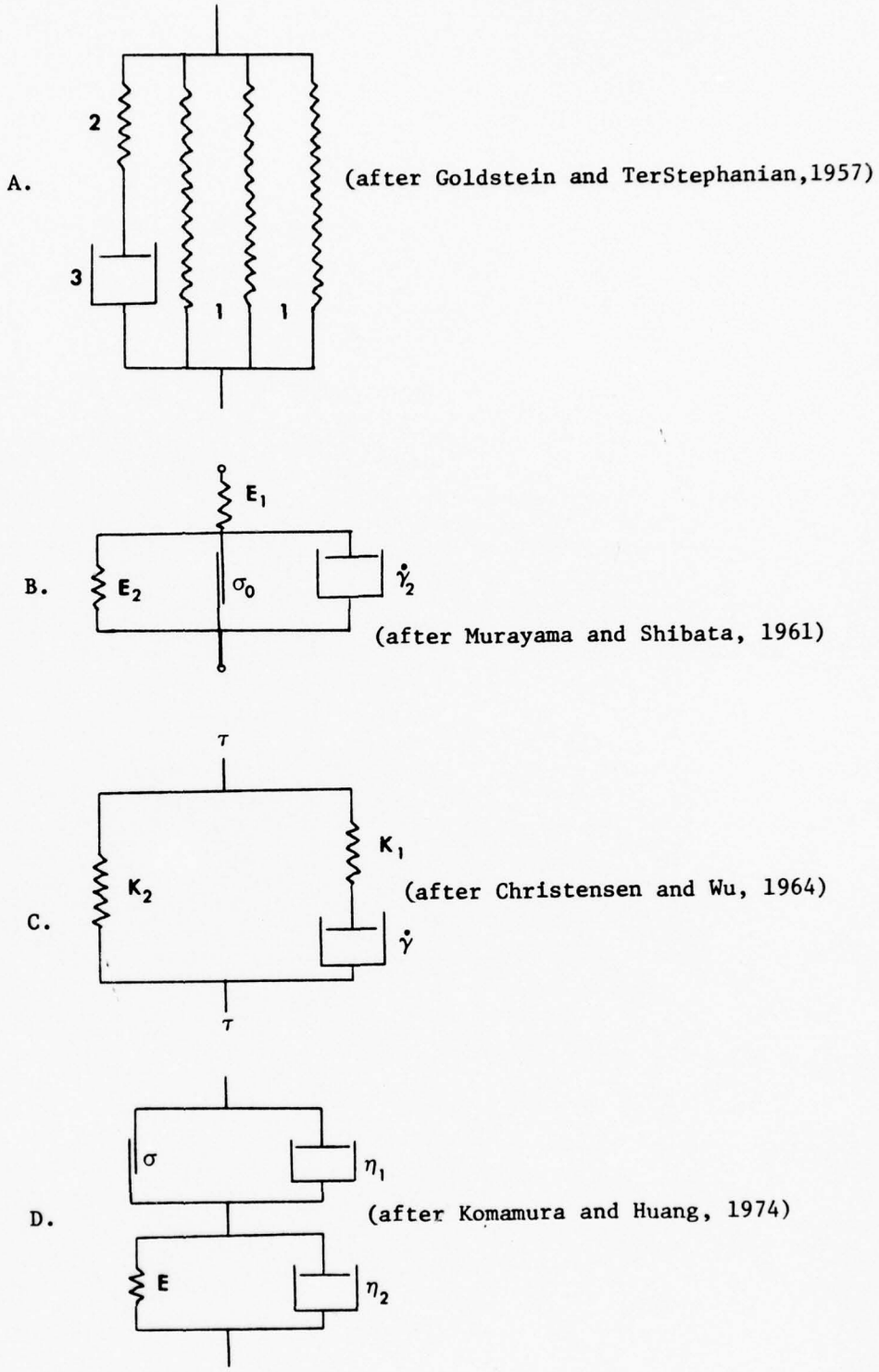

Figure 2. Rheological models of soils.

An instantaneous elastic deformation (springs 1 and 2) occurs on loading, followed by viscous flow in the dashpot (3) with a corresponding redistribution of the forces as the load taken up by the springs is increased. When all the force is transmitted to the springs, the deformation stops. Such a phenomenon was defined as creep.

Trollope and Chan (1960) attributed the step-strain phenomenon, so called because it appears as a series of steps in the stress-strain plot for a soil, to the migration of granular particles towards shear zones in clayey material. A typical soil consists of both granular and colloidal particles. For the cases considered, the granular fragments "float" in a clayey matrix. Loading leads to yielding in the clay matrix. Yielding leads to a progressive alignment of the clay particles in the direction of the potential failure surface (presumably the plane of maximum effective shear stress in unconfined compression). The coarse grains migrate to the potential failure surface and add intergranular friction to the strength along the surface. The steps in the stress-strain diagram result because, once granular particles begin to interact along the failure plane, an increased amount of energy must be supplied to overcome the effect of these "keyed-in" grains. When this happens an interval of plastic flow occurs until more granular particles migrate to the failure zone to add additional frictional contacts. Eventually, complete shear failure will take place when the maximum possible frictional contribution to strength in addition to the yield of the matrix is overcome.

The first application of rate process theory to studies of soil creep was by Murayama and Shibata (1958, 1961), who used the rheological model shown in Fig. 2-b to characterize clay soil behavior. The dashpot was assumed to be nonlinear, with the strain rate governed by a modified rate process equation given as

$$\dot{\varepsilon}_b^0 = A(\sigma - \sigma_o) \sinh\left(\frac{B\,\sigma_b}{\sigma - \sigma_o}\right) \qquad (1)$$

where $\dot{\varepsilon}_b^0$ is the rate of strain of the bonds; σ_b is the stress acting on the bonds; σ is the total stress applied to the clay skeleton; σ_o is the restraining resistance acting inside the bonds, or the yield stress (Terzaghi, 1950, called it the fundamental strength and defined it as the stress at which creep begins); and A and B are constants which depend on a variety of factors, including temperature. The rheological model shows elastic and viscous behavior, both recognized as clay soil properties, and it accounts for instantaneous as well as time-dependent deformation. The viscosity of clays was attributed to the "exchange of position between a water molecule and a void in a bond material containing soil particles" (Murayama and Shibata, 1961).

Mitchell (1964), in the first of several papers dealing with creep, utilized rate process theory to develop an equation relating the shearing resistance of soil to frictional and cohesive properties, effective stress, soil structure,

strain rate, and temperature. Because many aspects of the theory were modified in later years, only a few, salient details of this work are described here. Mitchell's use of rate process theory differed from that of previous workers in that he related the theory to processes occurring within the soil at the scale of individual particles, namely the breaking of bonds. He considered soil strength to arise from two sources: the energy required to move particles and produce spaces for them to move into (corresponds to dilatant contribution to friction of other workers), and the energy required to break bonds at particle contacts. The interparticle contacts were presumed to be effectively solid, whether they be mineral to mineral or mineral to adsorbed complex to mineral. In the latter case, he assumed that the interparticle contact zone force fields were great enough to generate a basically solid interparticle contact region through which both shear and normal stresses could be transmitted.

Shortly after publication of Mitchell's paper, Christensen and Wu (1964) utilized rate process theory and a rheological model to describe shear along well defined planes within a clay soil. They considered creep to be the result of slip at weakly bonded contacts followed by a transfer of load to stronger bonds. The bond strength at a contact was defined as the stress required to produce relative displacements of the two particles at that contact. Actual contact between particles is not necessary, as the term contact was meant to apply to the point where a bond between two particles was formed. Relative displacement at the contacts consists of the movement of "kinetic units" from one equilibrium position to another over an energy barrier. The kinetic units (termed flow units by other authors) are not defined specifically; the authors state that they may be molecules or clay particles. The magnitude of the energy barrier, called the activation energy, ΔF, depends on the adhesion and friction at the contacts, and on the dilatant component of internal friction. The magnitude of the energy barrier and of the distance between successive equilibrium positions was assumed to vary over a large range in any given soil. The rate of shear strain was given by:

$$\dot{\gamma} = A \sinh B\tau_f \qquad (2)$$

where A is a constant which depends on the temperature, the yield strength of the bond, the magnitude of the energy barrier, and other factors; B is a constant which depends on the temperature, the number of flowing contacts per unit area, and the distance between adjacent equilibrium positions; and τ_f is the stress (in excess of the yield strength) which causes flow.

Christensen and Wu (1964) presented the rheological model shown in Fig. 2-C, which is equivalent to that of Goldstein and Ter Stepanian (1957) shown in Fig. 2-a. Spring, K_2 represents the effect of the nonflow stress and elastic behavior. The Maxwell element represents the response of the particle structure to the flow stress; flow in the dashpot is governed by the equation for shear strain rate given above.

An experimental program was designed to test the model. Samples were tested under consolidated-undrained conditions with pore water pressure measurements. Most of the pore pressure changes were observed to occur during the first load increment. Both incremental and single creep loads were used. Agreement between theoretical and observed behavior was good. The model parameters, $\underline{A}$, $\underline{B}$, $\underline{K}_1$ and $\underline{K}_2$, were calculated from the test data. From these, values for several soil properties of interest were calculated for the first load increment. The distance between planes of slip was determined to be approximately 1.2×10^{-5} cm. The distance between adjacent equilibrium positions was calculated to lie between 2.3 Å and 21 Å. The magnitude of the energy barrier varied between 23 to 27 K_{cal} per mole. The authors concluded that the agreement between theory and experimental data on dry clay samples suggests that adsorbed water is not the main source of the viscoelastic behavior of the soil.

Mitchell and McConnell (1965) described the effect of soil structure on elastic and plastic deformation of soils. They suggested that, owing to the wide range of bond strengths and bond orientations that can exist in a clay soil, purely elastic deformations are likely to develop only at very low stresses, since some of the bonds may rupture at low stresses leading to plastic deformation. Nonetheless, a portion of the total strain is elastic. They also postulated that the elastic response should be nonlinear and delayed. Nonlinearity results because the stress dependence of particle deformation and that of contact area deformation probably differ, and both may occur in a soil. Delayed elasticity was ascribed to atomic diffusion within particles and at contacts, and to viscous flow of water within pore spaces, both of which require time. Creep was assumed to result in a transfer of elastic to plastic deformation.

These effects were studied using soils with dispersed (prepared by kneading compaction) and flocculated(static compaction) structures. In soils with dispersed structures the amount of recoverable strain decreased with load duration owing to creep. This effect became more pronounced with increasing stress intensity. The rate of transfer of elastic to plastic strain decreased with load duration. In soils with flocculated structures, the recoverable strain was essentially independent of the load duration, reflecting the greater rigidity of flocculated structures. A much greater part of the deformation of the flocculated soils was recoverable than for the dispersed structures.

Complex rheological models presented to describe soil deformation behavior were described by Goldstein, et. al. (1965) and by Sheriff (1966). The former considered that the strain in a clay soil consisted of three different components: an instantaneous elastic strain, a long-term viscoelastic strain, and an irrecoverable strain associated with viscous flow. Expressions for each of these components were determined by the hereditary equations and these were then combined to obtain a complex equation for the total strain. Noting that the stress-strain-time behavior of Grantham Clay at water contents greater than the plastic limit differed from that when the water content was less than the plastic limit, Sheriff (1966) presented separate rheological models for each range of water contents. From these he formulated two equations describing the behavior of the soil.

Andersland and Akili (1967) studied the creep of frozen clay soils. Tests on a number of samples showed that a linear relation existed between axial stress and the logarithm of the axial strain rate for secondary creep at different temperatures. They also observed that plots of the reciprocal of temperature versus the axial stress needed to attain a given creep rate produced a series of roughly parallel straight lines. From these observations they concluded that the creep of the frozen clay soils being studied could be described by an equation of the form of the rate process equations previously described:

$$\dot{\varepsilon} = \sum_i C_i \exp\left(-\frac{\Delta F_i}{RT}\right) \sinh\left(B_i \sigma\right) \qquad (3)$$

where R is the universal gas constant, T is the absolute temperature, σ_i is the axial stress on the specimen, C_i is a frequency factor, ΔF_i is the activation energy, and B_i represents a stress factor. The authors considered that a number of deformation mechanisms may be operating simultaneously, so that the total strain rate is the sum of i deformation mechanisms. If more than one deformation mechanism contributes significantly to deformation, the exact form of this equation would be very difficult to evaluate. However, normally one mechanism is rate controlling and the form of the equation can be obtained. A plot of activation energy versus axial stress showed that for stresses between 600-800 psi, the activation energy was constant, suggesting that one deformation mechanism predominates in this stress range.

A simplified form of equation 3 was given as:

$$\dot{\varepsilon} = C \exp\left(-\frac{\Delta F}{RT}\right) \exp(B\sigma) \qquad (4)$$

from which an expression for the strain (ε) at any time (t) is derived:

$$\varepsilon = Ct \exp\left(-\frac{\Delta F}{RT}\right) \exp\left(B\sigma\right) \qquad (5)$$

Using this last equation, the values of the activation energy (ΔF) could be calculated from a plot of strain versus time for creep tests at two different temperatures (T_1 and T_2) using the expression:

$$\Delta F = \frac{2.303 R T_1 T_2}{T_2 - T_1} \log\left(t_1/t_2\right) \qquad (6)$$

Andersland and Akili (1967) also estimated a theoretical volume for the flow units of approximately 1.1×10^{-5} Å^3. They concluded that such a value supports the notion that the creep mechanisms are restricted to particle or ice contact points and do not involve entire soil particles.

Mitchell, et. al. (1968, 1969) used rate process theory to analyze creep test data for a number of soils. They were able to develop an internally consistent picture of the relationships between bonding, effective stresses, and the strength of soils, and of how these affect soil behavior. The equation governing creep was given as:

$$\dot{\varepsilon}^{o} = AX \exp(-B\Delta F)\exp(C\sigma) \qquad (7)$$

where X is a function of the number of flow units in the direction of deformation and the average component of displacement in the same direction due to a single surmounting of the energy barrier; ΔF is the activation energy; σ is the deviatoric stress; A and B are constants which depend on temperature; and, C is a constant which is a function of temperature, the distance between adjacent equilibrium positions, and the number of bonds per unit area for a given soil structure. The value of X may vary with time; for convenience it is considered as a constant.

The theory describes laboratory data quite well for secondary creep. Using the experimental data and variations of equation 7, the authors calculated values for the various parameters in the strain rate equation. From their study, they arrived at the following conclusions:

1. The temperature dependence of the creep rate conforms with theoretical predictions, so that creep of soils can be treated as a thermally activated process.
2. For stresses greater than 20-30% of the short-term shear strength of the soils, the logarithm of axial strain rate, determined at a given time after loading, is proportional to the creep stress, the constant of proportionality being independent of time, as shown in Fig. 3.
3. The creep rate is time dependent, as seen in Fig. 4. The exact nature of the relationship is unknown.

4. Variations in water content, consolidation pressure, or void ratio had no effect on the values of the activation energy. Similar values of activation energy were obtained for sand and for wet and dry clay.

5. Values for the energy of activation were found to be in the range of 25-45 kilocalories per mole, suggesting that interparticle bonding is probably of the primary valence type. This implies that interparticle contacts are effectively solid to solid. The number of bonds per contact at any given consolidation pressure increases with increasing particle size (the number of contacts decreases); it depends on the compressive force transmitted at the contact. Individual bonds are all of approximately the same strength. Water has no effect on bond strength.

6. Strength, as determined by short-time tests, was found to be directly proportional to the number of bonds per unit area, (Fig. 5), which are themselves of the same strength for different soils and under different conditions.

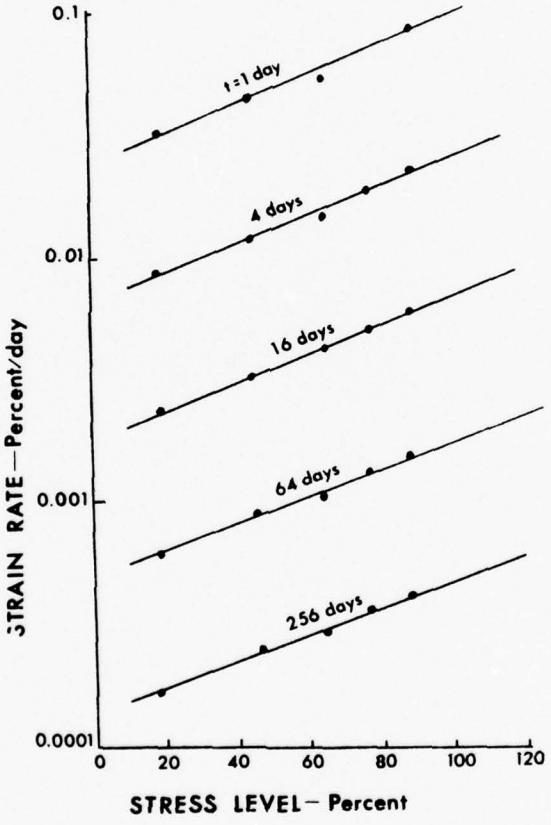

Figure 3. Influence of stress level on strain rate during undrained creep of London Clay. (Mitchell and others, 1969).

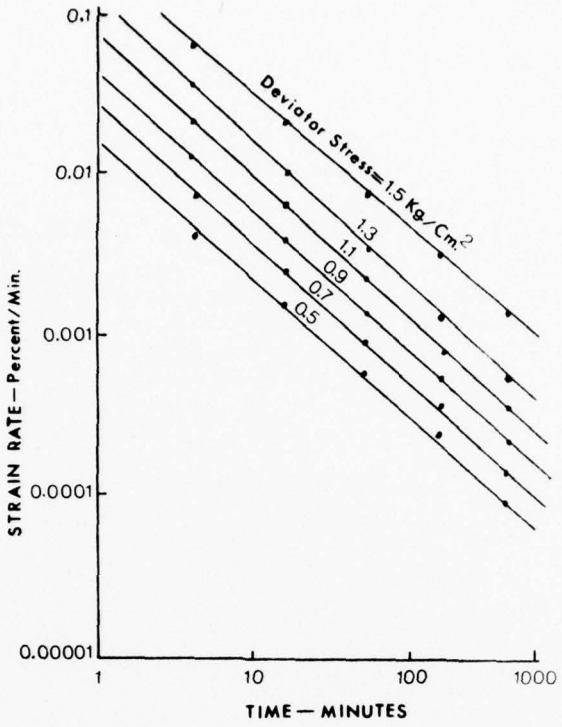

Figure 4. Influence of time on strain rate during creep of remolded illite (Mitchell and others, 1969).

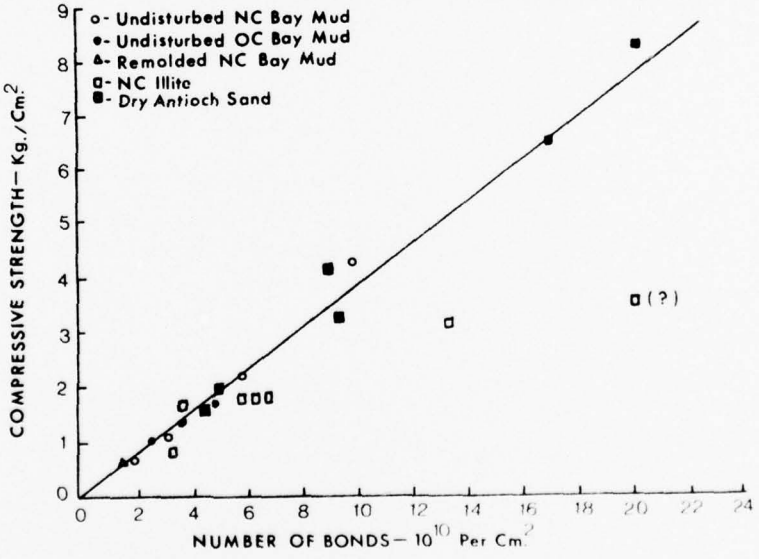

Figure 5. Compressive strength as a function of the number of bonds. (Mitchell and others, 1969).

7. Overconsolidation leads to an increase in the number of bonds over that for a normally consolidated soil as a result of nonrecoverable particle rearrangement and the formation of new contacts during compression. As a result, overconsolidated soils show a higher peak strength.

Andersland and Douglas (1970a, 1970b) reported tests performed to determine the energy of activation of homoionic samples of Sault Ste. Marie clay saturated with lithium, sodium, or potassium at varying concentration of solids. For solid particle concentrations where the particles did not form a continuous structure, the energy of activation for viscous flow was that of pure water, and they concluded that the flow mechanism involved was that of free water moving in an increasingly restricted space. For remolded samples consolidated in triaxial cells (high solids concentration), the activation energy was determined to be about 28 kcal per mole. There was no significant deviation from this value for changes in the degree of consolidation or in the nature of the adsorbed complex. On this basis, the authors concluded that the bonding mechanism is not related to the adsorbed complex, but is due to a direct mineral to mineral contact and to the formation of ionic bonds. Increasing the consolidation pressure increased the number of contacts; existing contacts were unaffected by the pressure changes. These authors also calculated the volume of a flow unit from the experimental data. The calculated volume of 1.7 $\mathring{A}^3$ is of the same order of magnitude as that of individual atoms.

An empirical equation describing the observed linear relation between the logarithm of the strain rate and the logarithm of time (Fig. 4) for a constant load was presented by Singh and Mitchell (1968, 1969). The equation applies for the range of stresses where a linear relationship exists between the logarithm of the strain rate versus the stress, whether the soils are tested disturbed or undisturbed, wet or dry, normally consolidated or overconsolidated, or tested drained or undrained. The equation is:

$$\overset{o}{\varepsilon} = A\left(\frac{t_1}{t}\right)^m \exp(\alpha D) \qquad (8)$$

where D is the deviator stress, A is the strain rate at unit time (t_1) and $D = 0$ (an imaginary value obtained by projecting the stress versus logarithm of the strain rate curve for unit time to $D = 0$); α is the slope of the linear stress versus logarithm of strain-rate plot for any time (Fig. 3); m is the slope of the linear log. strain-rate vs. log. time plot; and, t is the time at which the strain rate ($\overset{o}{\varepsilon}$) is observed.

The parameter m is relatively constant for a given soil, being little influenced by the test conditions or the loads imposed. Hence, it was considered to be a material property. It determines whether a soil is strain softening ($m < 1$), strain hardening ($m > 1$), or insensitive to strain ($m = 1$). Singh, et. al. (1971) used this relationship to determine that the settlement of a large fill mass on which several houses was built would not lead to reduced soil strength and eventual failure. The m-value for the fill was found to be, on the basis of field and laboratory measurements, approximately equal to one, indicating that creep would decrease at an ever decreasing rate.

Bishop and Lovenbury (1969) described the results of undrained, constant stress, triaxial creep tests on undisturbed samples of overconsolidated London Clay and normally consolidated Pancone Clay in which the test duration was up to 3 1/2 years. Test results illustrated the limited period of applicability of simple logarithmic or power laws which relate strain to time. For the London Clay, the strain was observed to be a linear-function of the logarithm of time up to 100 days for all stress levels, and for longer periods at lower stress levels. For the Pancone Clay, the linear relationship was evident for shorter periods, although, as with the London Clay, it persisted for longer times at lower stress levels.

No period of secondary creep was observed. (Singh and Mitchell (1968, 1969) also concluded that secondary creep in soils is generally absent, and is, at best, a useful engineering approximation). The strain rate either decreased steadily or increased. If it increased, it either led to instability and failure or was followed by a period of decreasing strain rate. The instabilities were associated with volume reductions and were interpreted to represent a modification in soil structure. The authors also noted that, for the overconsolidated London Clay, creep occurred at all stress levels, there being no apparent threshold value of stress below which the time-dependent deformations were absent.

Walker (1969) noted that undrained creep leads to a steady increase in pore water pressure, which shifts the effective stress state of the sample closer to the failure envelope. He concluded that creep strain and creep in the pore pressure are related. He considered undrained creep to consist of two parts: a primary part associated with pore pressure equalization and a secondary part which takes place under a uniform increase of pore water pressure. The basic creep mechanism proposed assumes that the structure of a clay soil has an inherent viscosity resulting from the increased viscosity of the adsorbed water relative to free water.

Hoelzer, et.al. (1973) studied the role of pore pressure during the consolidated undrained creep testing of San Francisco Bay Mud. They found that a significant, gradual increase in excess pore pressure occurred in their samples due to the arresting of secondary consolidation when drainage was inhibited. This increase was independent of the applied shear stress, so that the pore-pressure increase had two components: one due to the creep stress, and the other due to the arresting of secondary consolidation. The magnitude of this increase could be reduced by increasing the time of consolidation prior to undrained creep. They argued that the observed long-term, time dependent increase of pore water pressure, which results in a time dependent decrease in effective stress, could cause the time dependence of axial strain during undrained creep. The time-dependency of the excess pore water pressure, and hence, of the strain, was presumed to be caused by the drainage of water from a system of micropores into a system of macropores, both of which probably exist in the soil. They conclude that any mathematical model purporting to account for the stress-strain-time behavior of clayey soils should account for the increase in pore pressure during undrained creep.

In a theoretical analysis, Vyalov, et. al. (1971) considered that the long term deformation and failure of soil was accompanied by a weakening of internal bonds and the development of defects in the soil structure (weakened planes in the soil system; i.e., various voids, fissures, etc.) which eventually lead to failure. Defect formation is abetted by the reorientation of the basal plane of the clay particles in the direction of shear. The reorientation

of particles and the growth in the number of defects reduce the number of bonds and, hence, the load bearing area, resulting in increasing rates of deformation. The defect density is defined as the ratio of the area occupied by defects to the total cross-section area normal to the shear direction. At failure, it is assumed to be independent of the stress level or the time to failure for a given soil. At this value, the micro-defects begin to merge into large fractures which causes the soil to fail. The time needed for the defect density to attain this value depends on the initial stress, which will control both the number of bonds initially broken and the rate of fissure formation, and it depends on the plastic properties of the soil, which determine the ease with which soil particles are reoriented. Creep and delayed soil failure thus result from the interaction of the orientation and defect formation processes. This view was supported by Barden (1972).

Komamura and Huang (1974) presented a rheological model which describes well the deformation behavior of a number of soils under variable conditions of stress and water content. The model consists of a Bingham element in series with a Voigt element, as shown in Fig. 2-d. Mitchell (1976) suggested that an additional spring in series is needed to account for initial elastic deformations. Although the model proposed by Komamura and Huang can account for a wide range of soil rheological behavior, it is purely a descriptive tool and makes no pretense as to the mechanism of deformation.

STUDY SITES AND FIELD INSTRUMENTATION

The areas selected for the present study include two new sites in addition to the sites instrumented by R. W. Fleming. The latter are described in detail by Fleming and Johnson (1975). The location of all the sites is shown in Figure 6. Only the new study sites will be described here. Both are located on Stanford University property.

The different types of field instrumentation that were installed in the black silty clay at the study sites have been described by Fleming (1976) and will not be described in detail here.

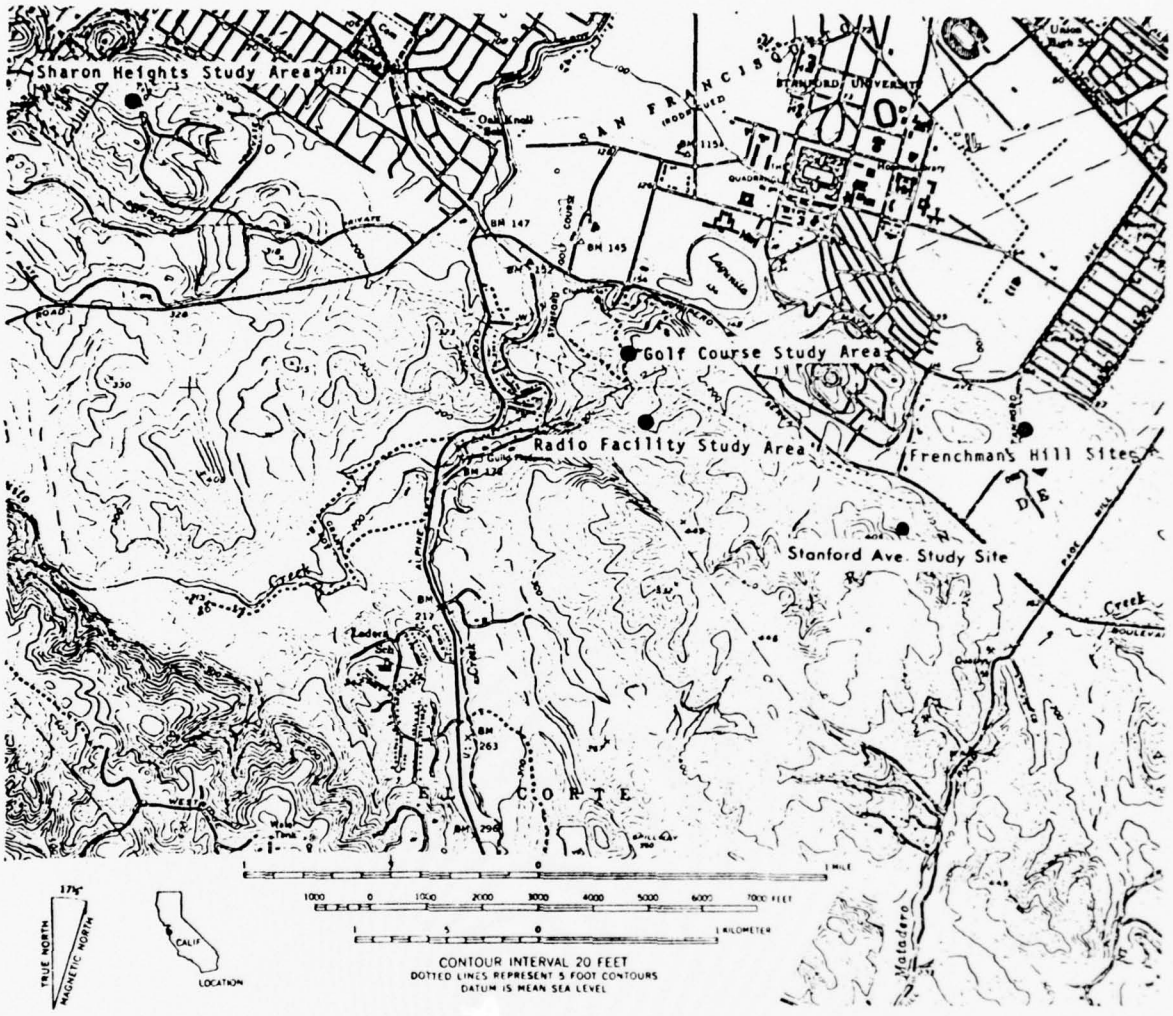

Figure 6 Topographic and road map of study area showing location of study sites.

Radio Facility Study Area

The radio Facility Study Area is approximately 0.35 km south of the Golf Course Study Area of Fleming and Johnson (1975). Figure 7 is a map of the site showing soils, man-made features, instrument sites, and borehole locations. The site is bordered on the west and northwest by minor roads, to the east by a flat-bottomed narrow valley, and to the northeast by a developing gully. A barbed wire fence crosses the area approximately in an east-west direction. The ground surface slopes about 10 degrees to the east and northeast.

Most of the site is underlain by weathered Eocene marine claystone. A moderately cemented Eocene sandstone is exposed along the paved road and on the hillside north of the site. Fleming (1971) reports a probable attitude for the bedding of N45°W strike, dipping about 30° to the southwest. Sandstone also occurs uphill (southeast) of the site. The location of the contact between the sandstone and claystone could not be accurately determined. It appears to be gradational, at least in some places. Highly weathered, clayey sandstone is exposed on the gully floor between the sandstone outcrops to the north and the claystone underlying the black silty clay. The gully itself appears to be growing headward along the contact between the sandstone and claystone. Fleming (1971) attributed some of the headward growth and lateral enlargement of the gully to underground piping and the formation of subsurface channels. Comparison of the gully today with photographs taken by him in 1971 show that the gully has widened considerably at the expense of the surrounding mass of creep soil.

There are two major soil types at the site (Figure 7). The black silty clay soil (also called the creep soil throughout this report) which is involved in seasonal creep covers much of the area south of the gully and extends to the west beyond the area shown in Figure 7. The appearance of the black silty clay changes dramatically with the seasons. During the winter the soil is black or bluish black; in the summer it has a dark gray tint. When dry, the ground surface is criss-crossed by large, gaping shrinkage cracks.

During the winter rains the soil swells noticeably and the shrinkage cracks close. The volume changes of the soil due to changes in water content are described in detail in a later section.

The contact is gradational between the black silty clay soil and a brown to dark gray, silty to clayey sand in the southeastern part of the area.

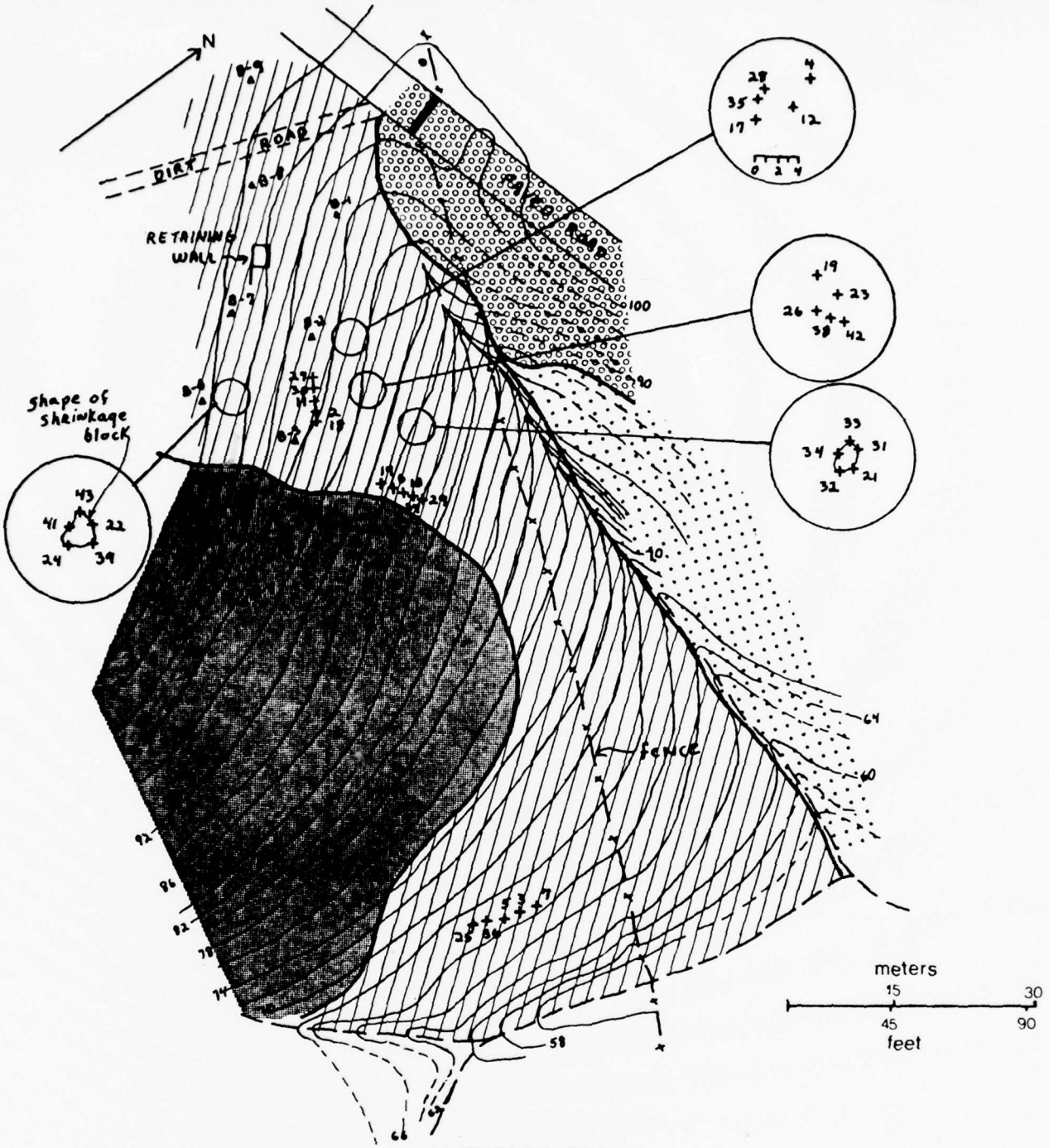

EXPLANATION

Black silty clay soil

Dark gray silty-sandy clay

+23 Steel rod location

Red-brown silty sand

Man-made fill

▲B-5 Exploratory borehole

Figure 7. Topographic and soils map of the Radio Facility Study Area.

In contrast to the creep soil, the latter is easily identified by its sandy character, by the absence of large shrinkage cracks during the dry summer months, by vegetation contrast, and by the presence of animal burrows which are absent in the creep soil.

A number of boreholes have been made at the study site, both by Fleming (1971) and as part of the present study. The boring logs are in Appendix C. These confirm that weathered claystone underlies 1 to 2 meters of black silty clay soil. The bedrock underlying the sandy soil is also weathered claystone in those locations where subsurface data was obtained. North of the gully, an area underlain by Eocene sandstone, the soil is a tan-buff colored silty sand.

Three types of instrumentation were established at the site. During the summer of 1970 Fleming installed eight flexible pipes at various places on the hillside. Of these, only two could be relocated. A retaining wall was constructed to provide a rigid surface on which to measure earth pressures exerted by the creeping soil. The retaining wall was located near the northwest corner of the study site, as far removed as possible from the other instrumentation points so as not to interfere with the soil behavior at their locations. Finally, 35 steel rods of different lengths were placed throughout the hillside. Rods were cut to lengths of 46 cm. (1.5 ft.), 76 cm. (2.5 ft.), 107 cm. (3.5 ft.), 122 cm. (4.0 ft.), 137 cm. (4.5 ft.) and 168 cm. (5.5 ft.). The rods were placed in groups of five so that, in all, seven groups of rods were installed. In three of these, rods of equal length were placed in the shrinkage cracks surrounding and defining individual shrinkage polygons or blocks, the idea being to observe the behavior of the block when it was wetted and to determine if the cracks recurred in the same location yearly. Two groups of five rods, each of different length, were placed roughly parallel to the slope countours, one group being located near the retaining wall and the other one east of it, near the base of the hill (Figure 7). Another group of five rods of different length was aligned roughly parallel to the slope direction. Finally, a group of five rods of different lengths was placed in a small, random cluster near the retaining wall.

Stanford Avenue Study Area

The Stanford Avenue study site is southwest of Junipero Serra Boulevard, roughly opposite to its intersection with Stanford Avenue (Fig. 6). It is shown in Figures 8 and 9. Figure 8 is a soils and bedrock map of the site. Figure 9 shows the distribution of soils, and the location of instrumentation sites, boreholes, and test pits. Topographically the area consists of a series of flat-bottomed, northeasterly trending valleys separated by northeasterly sloping, smoothly rounded ridges. The valleys open into a broad plain which includes the land on the west side of Junipero Serra Blvd. The slope of the valleys decreases from about 12-14 degrees in their upper reaches, to about 2-3 degrees in the vicinity of Stanford Avenue. Most of the site is underlain by Eocene sedimentary rocks, with the southwest margin being underlain

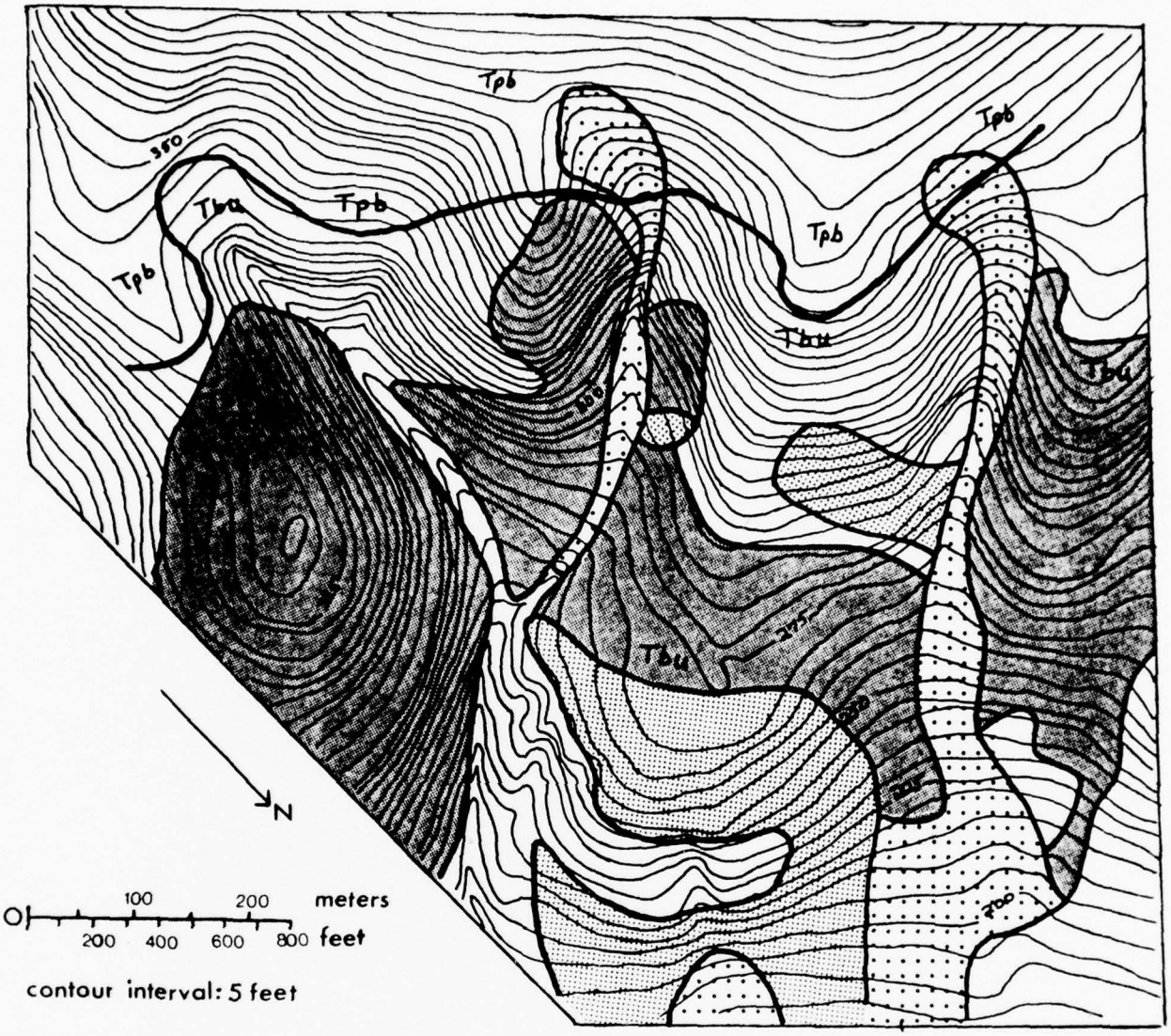

Figure 8. Soils, geologic and topographic map of the Stanford Avenue Study Area.

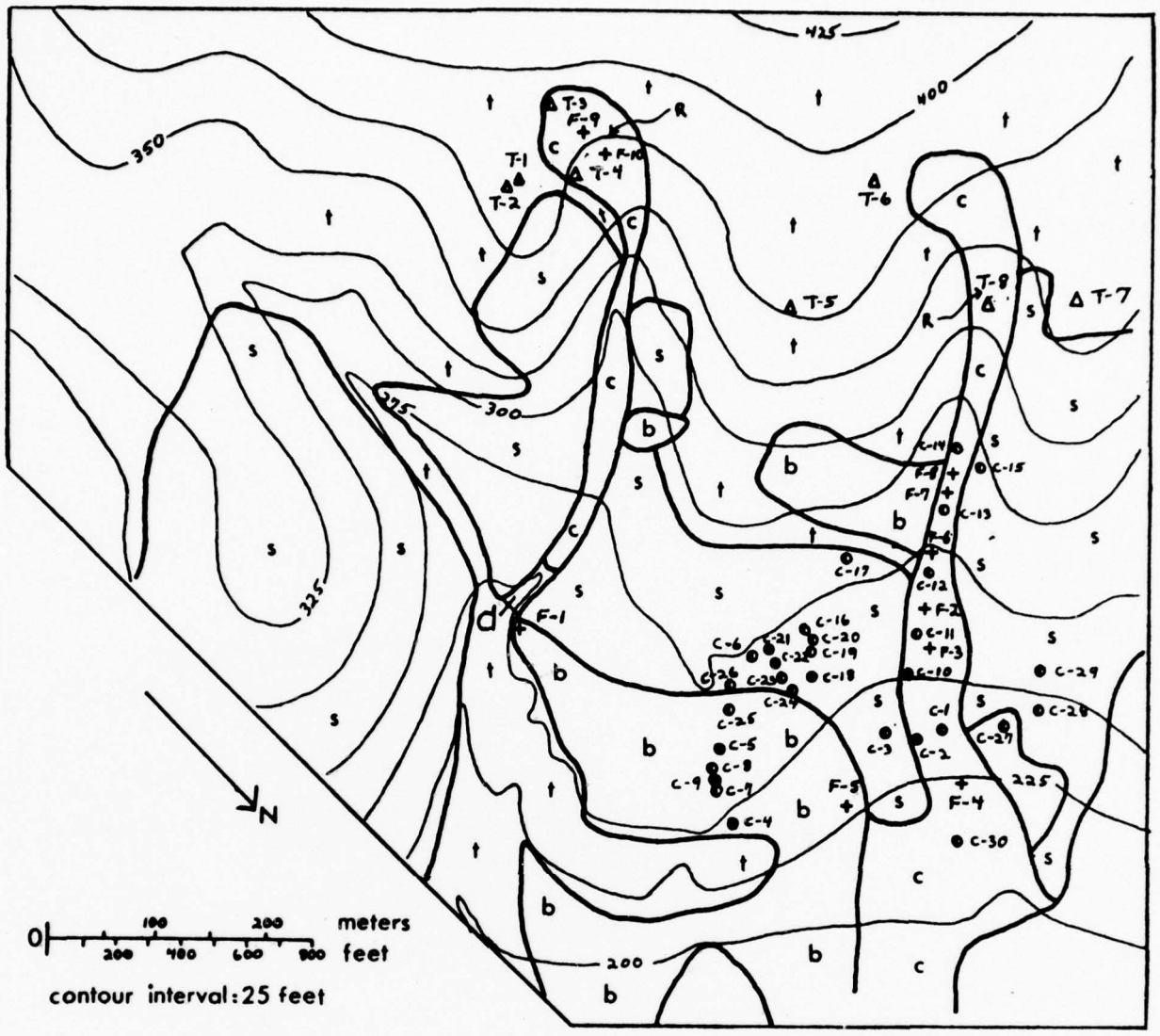

EXPLANATION

c Black silty clay soil	+F-5 Flexible pipe
b Brown silty-clay soil	R Steel rod instrumentation site
t Transition type soils	●C-7 Borehole location
s Sand or silty sand	▲T-5 Exploration test pits
/ Contact between soils	d× Dam site

Figure 9. Soils map of the Stanford Avenue Study Area, showing instrument stations and subsurface exploration sites.

by the Page Mill Basalt of middle Miocene age. The exact location of the contact between these two rock masses is known only near the ridge crests, where the contact is expressed by a step in the topography. Elsewhere the contact is drawn approximately based on subsurface data, types of soil, and surface topography.

Four major soil subdivisions are shown in Figures 8 and 9. The soils in this study area were differentiated on the basis of color, field observations on the relative percentages of clay, silt, and sand-sized particles, dry strength, and plasticity characteristics. The black, silty clay creep soil occurs in two distinct masses. The largest one extends almost entirely across the northern part of the study area in a northeasterly direction. It consists of two distinct parts. The westernmost part has a spoon-shaped or lobate form and is the area where the creep soil appears to be actively forming. It extends at least as far east as the site of test pit no. 8. The upper reaches of the source area are underlain by Page Mill Basalt; Eocene claystone underlies the remainder of the source area. East of the source area the creep soil thins out in plan view, as the soil creeps into a narrow part of the valley. Here, the creep soil does not fill the valley but rather is concentrated against the north valley wall. A narrow transition zone separates creep soil from sandy soils to the south; the contact with sandy soils along the north edge of the valley is abrupt. Still farther to the east the valley widens, and the soil appears to fan out into the broader valley. Contacts with adjacent soils are gradational, the width of the gradation zone being greater than 3 meters in most cases. The gradational contacts suggest that mixing of the creep soil with adjacent soils takes place along the soil mass boundaries, with the volume of creep soil possibly growing in this fashion.

Below the source area the soil is underlain in most places by weathered claystone. Subsurface data shows that in most places the soil grades vertically into the claystone, the gradation generally being reflected by increasingly lighter colors, stiffness, and, in some places, sand content with depth. Whether this gradational zone undergoes seasonal creep is unknown. There is no noticeable decrease in the thickness of the black creep soil as it passes from the narrow zone to the broad valley. Thus, the increase in surface extent of the creep soil is probably the result of continued influx of soil creeping down from higher, steeper areas and, possibly, the lateral growth of the creep masses.

In the source area the ground surface is littered with basalt fragments of gravel to boulder sizes. These are also found within the soil and may be concentrated near the soil-bedrock contact (Fig. 10) by creep movements. The percentages of boulders on the ground surface and within the soil decreases with distance from the source area. In the lower reaches of the creep mass there are very few basalt fragments on the surface. The fragments are derived from basalt outcrops at higher elevations and possibly from the normal weathering of basalt below the soil layers. Fragments on the surface presumably enter into the soil via open shrinkage cracks which develop in the soil when it dries out during the summer.

Six flexible pipes were installed at various places below the source area, as shown in Figure 9. The pipes were installed near the center of the

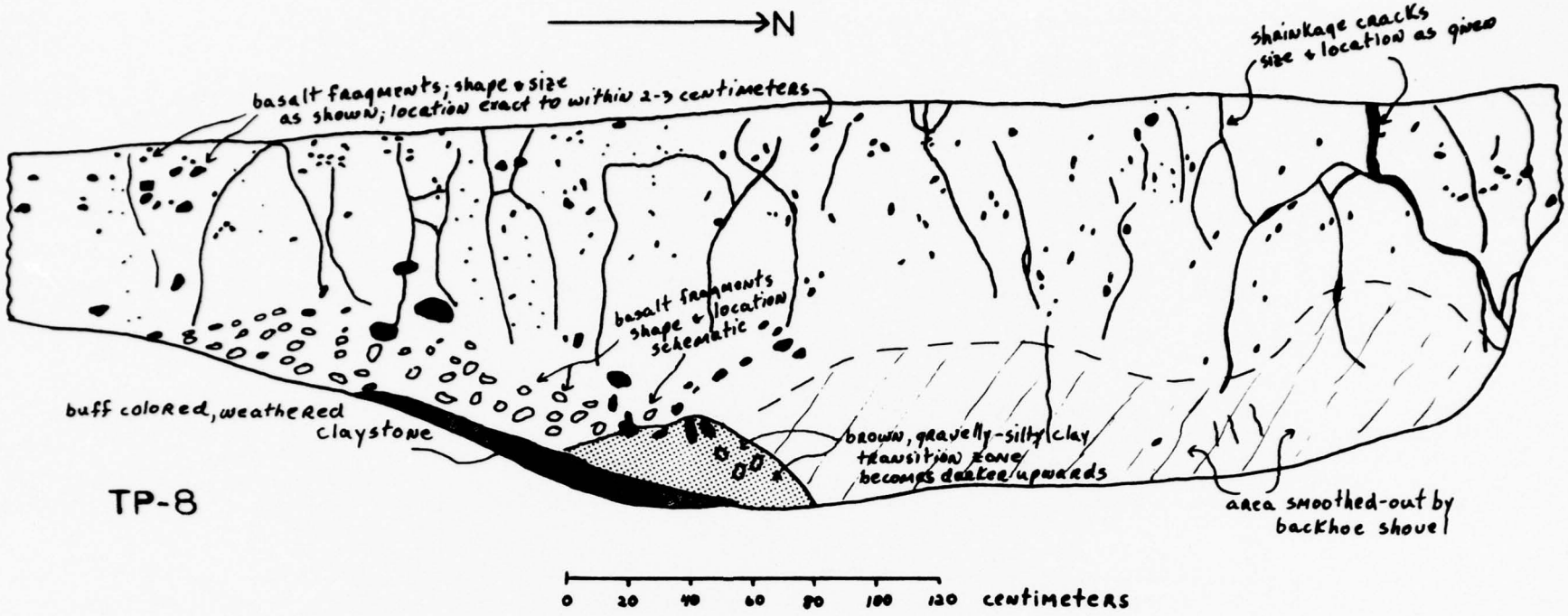

Figure 10 - Detailed Log of Test-Pit No. 8

valley and near its southern border so as to determine the relative rates of motion of the soil at different points along a cross-section through the creep mass. In the source area, test pit no. 8 was excavated and left open with the idea of observing how the soil creeps into the pit. For this reason, the trench was logged in great detail (Fig. 10). Seven steel rods, having lengths of 31 cm., 61 cm., 92 cm., or 122 cm., were installed about one meter from the uphill side of the trench to measure relative movement directly.

A second spoon-shapped mass of creep soil occurs in the next valley south of the one described above (Figs. 8, 9 and 11). This creep mass extends in a northeastern direction into a narrow valley where it is dissected by two gullies and eventually disappears. The source area is underlain by Page Mill Basalt. The thickness of the soil increases from the south and east margins of the creep lobe, being about one meter near the boundary and increasing to at least five meters near the center. The contact between the creep soil and the underlying basalt is gradational. The contact with adjacent soils is abrupt along the east edge of the creep lobe; elsewhere it is gradational. The ground surface is mantled by basalt fragments; this is also true of the adjacent soils. The volume of basalt fragments within the soil is as high as 50%.

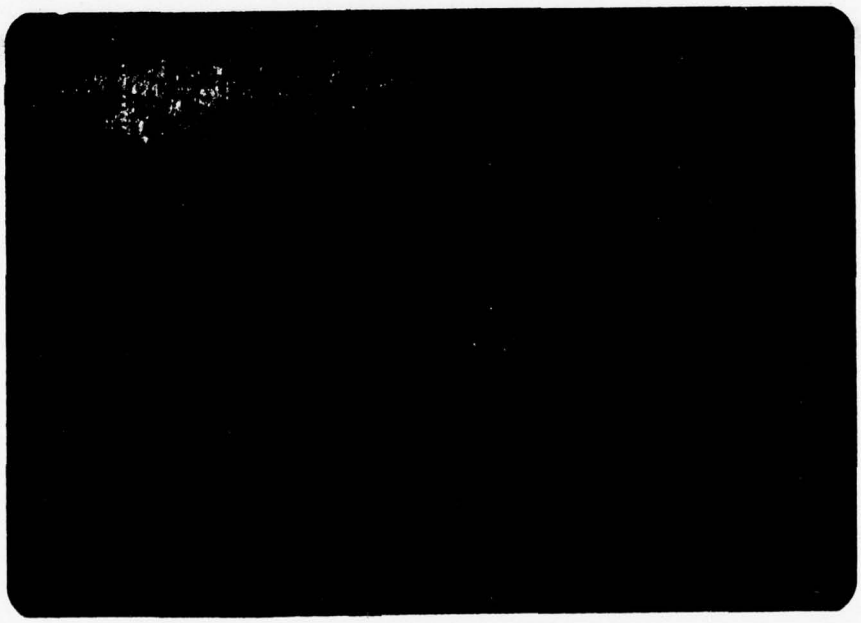

Figure 11 - Southernmost creep lobe at the Stanford Avenue Study Area. The lobate shape of the creep lobe is enhanced by the vegetation contrast which occurs between the black silty clay and the adjacent soils. Note gully eroding into the creep lobe.

Instrumentation on the creep soil consists of two flexible pipes, anchored in bedrock, placed near the axis of the lobe, and two sets of five steel rods of different lengths aligned perpendicular to the valley axis (Figs. 9 and 12). In drilling holes for the installation of the flexible pipes several attempts had to be abandoned because hard basalt fragments were encountered before reaching bedrock.

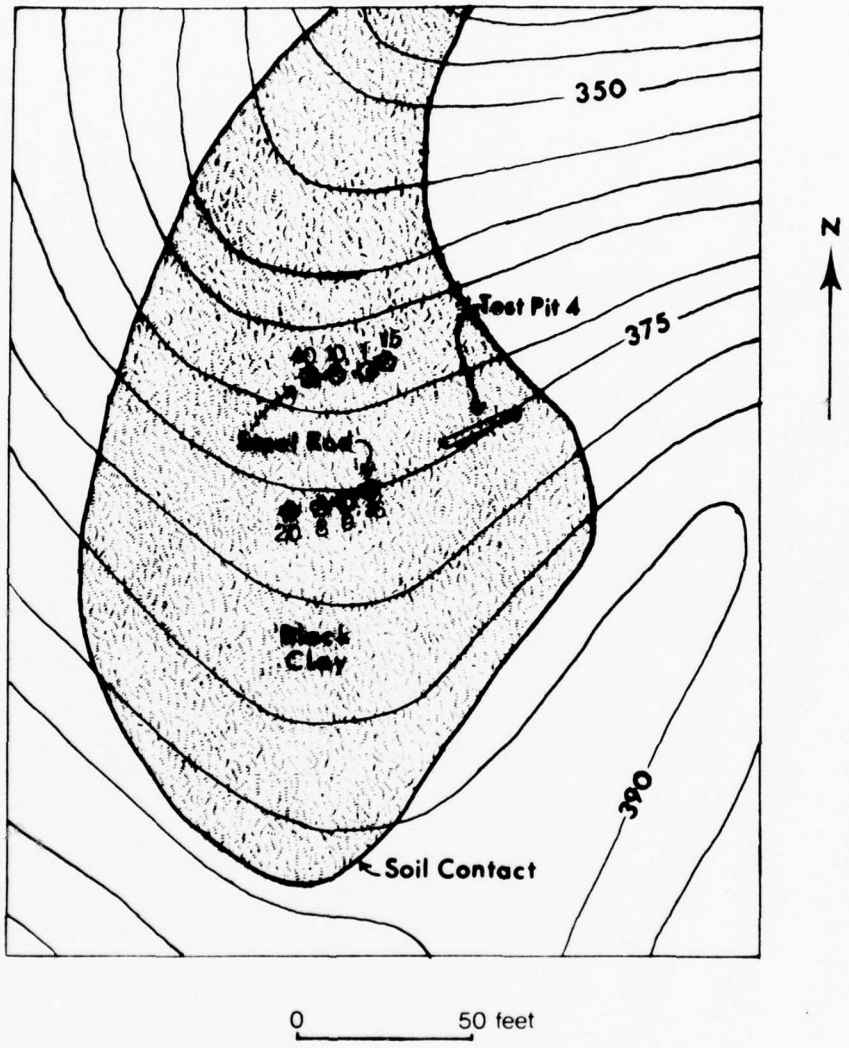

Figure 12 - Southernmost creep lobe at the Stanford Avenue site showing location of steel rods.

Unlike the larger mass of creep soil to the north, the downslope extension of this creep mass is limited. A large gully (Fig. 13) which extends uphill from the dam site (Fig. 9) to an elevation of between 280-285 feet (85-86 meters) has dissected the creep mass. The headward migration of the gully proceeds faster than the rate at which soil creeps down the valley, so that the role of creep as a mass transport agent is being diminished. Below the elevation of maximum migration of the gully the creep soil is no longer a continuous mass but consists of thin patches on either side of the gully. Gully widening is occurring through steepening and slumping of the sides with the result that the creep soil is being removed by running water. To our surprise the small dam constructed near the mouth of this valley silted up during the winter of 1974-75, a winter of below normal precipitation. Thus, it appears that the quantity of material removed by running water is substantial, as the mere presence of the gully suggests.

Figure 13 - View of large gully which has dissected the lower reaches of the southernmost creep mass at the Stanford Avenue site. The ridges and depressions seen on the gully walls are produced by slumping of the sides.

Another gully, visible in Figure 11, has migrated during the last three years (1974-1976) into the lower part of the source area, again during winters of below normal rainfall. It appears likely that the continued headward migration of this gully will eventually cut across the creep lobe so that for

creep to continue to be an important process here, the production of creep soil west of the lobe will have to be increased. Extension of the creep mass in other directions is unlikely: to the south there is a ridge-crest and to the east the bedrock is sandstone.

It is interesting to note that there appear to be gullies developing in the large creep mass to the north. In several places between elevations 300-325 feet (91-99 meters) the soil is being eroded along the downhill side of large basalt fragments or pieces of wood which rest on the ground surface producing shallow holes or steps immediately downslope of the obstacle. Whether this process can eventually lead to the formation of gullies and dissection of the creep mass remains to be seen.

A smaller mass of black silty clay exists along the northeast boundary of the site. No instrumentation was placed here, and there was no subsurface investigation of this mass.

The second major soil type is a dark to reddish brown expansive silty clay which occurs in three different places (Figs. 8 and 9). Like the black creep soil, its appearance changes markedly with the seasons. Wide, deep shrinkage cracks develop during the dry summer months. The cracks become closed during the normal, wet winter. This soil approximately has the same relative percentages of clay, silt, and sand that the black creep soil has. The composition of the clay-sized particles is unknown. No basalt fragments were observed on or within the brown silty clay. In addition, this soil lacks the relatively high percentage of organic material which presumably gives the black silty clay its color. Subsurface data from the largest of the brown silty clay soil bodies indicates that this mass, at least, is underlain by weathered claystone at depths ranging between 1.3-2.0 meters. It is not known if the brown silty clay creeps noticeably in response to changes in moisture content. One flexible pipe was installed in this soil.

A sandy or silty sand soil covers most of the ridge areas underlain by Eocene sandstone. The sandy soils are non-expansive, light colored, and generally very thin, sandstone bedrock occurring at the surface or at very shallow depths. No instrument stations were placed on these soils.

The last major soil type shown in Figures 8 and 9 includes a wide range of soils of different compositions (relative percentages of the various grain sizes), color, and plasticity characteristics. They are generally intermediate in these properties between the soil types described above and usually grade into one of these. Pockets of brown expansive clay and sand exist in places, but no such isolated occurrence of black silty clay was observed. In general, the soils mapped under this category which occur overlying Eocene sedimentary deposits are sandy with varying, though minor percentages of clay. Those which overlie Page Mill Basalt are rich in basalt fragments of cobble or larger size. These fragments may make up to as much as 80% of the soil near the sandstone-basalt contacts, and possibly elsewhere. Generally, the clay content of all transition soils increases as they approach the black silty clay soil. No instrumentation stations were established on the soils of this group.

SOIL PROPERTIES

The silty clay soil has several distinctive characteristics, both in the field and in the laboratory. A number of lab tests have been performed to determine the "index properties" of the soil. The index properties of a soil are those properties used by soils engineers to differentiate and classify different soils. They provide a means of comparing the soil with others previously encountered, because soils having similar index properties are likely to exhibit similar engineering behavior (for similar fabrics). The tests are described below. Also, a description of the gross appearance of the soil as it occurs in the field and the soil-bedrock relations are given.

Laboratory Tests

Fleming (1971) has described the index properties of silty clay soil from the Sharon Heights and the Golf Course study areas. These are summarized in Table 1.

TABLE 1. SOIL INDEX PROPERTIES (from Fleming, 1971)

Gradation (averages)

sand	30% (by weight)
silt	30%
clay	40%

Dry Density 92.7 lb/ft^3

Specific Gravity of Solids 2.56

Saturation 98%

Swell Pressure 26.3 psi

Atterburg Limits (averages)

Plastic Limit	25%
Liquid Limit	65%
Plasticity Index	40%
Activity	ca. 1

Some additional tests have been performed on soils from the Radio Facility and Stanford Avenue sites. The main purpose of these tests was to try to determine if variations in the soil index properties occur with depth in the

soil profile. No distinctive difference could be detected in the Atterberg limits for soils sampled at different depths. A comparison of results of tests on samples taken at different points on the ground surface relative to shrinkage cracks gave similar results. Average values for the liquid limit, plastic limit and plasticity index from twelve tests were 61%, 26%, and 35% respectively. The value for the plasticity index is slightly lower than those given in Table 1 for soils from the Sharon Heights and Golf Course study areas.

Swell potential tests were performed on six samples taken from different depths using the PVC Meter and method described by Lambe (1960). Again, no significant pattern was observed in the results. The average value of the swell pressure developed after two hours under an initial load of about 1.4 psi was approximately 29 psi, which is comparable with the value reported by Fleming (1971) and in Table 1.

Because the procedure used in preparing the samples for both the swell test and Atterberg limit test results in a complete breakdown of the soil fabric, and because similar fabrics result for each sample prepared, any differences in the test results would likely be due to variations in soil composition. Thus, it appears that the composition of the silty clay soil is fairly uniform with depth. This agrees with field observations. Any differences in soil behavior due to differences in soil fabric with depth, however, is not reflected in the results, as the original fabric is destroyed during sample preparation. Because of the more intense dessication which occurs near and at the ground surface, the soil fabric, and hence mechanical behavior, of in-situ material is expected to vary with depth.

It has been stated that the combination of high values of activity and plasticity index, large swell pressure, and relatively low specific gravity suggest that the predominant clay mineral is montmorillonite (Fleming, 1971, Fleming and Johnson, 1975). A competent geochemist, Kilinc (1969), analyzed the x-ray diffraction patterns of samples of the silty clay from two different sites and reported that the only identifiable clay mineral is montmorillonite.

Some idea on the nature of the adsorbed complex of the clay is obtained from two indirect lines of evidence. The presence of gypsum in the weathered claystone which underlies the creep soil suggests that calcium is abundant in the parent rock. It is possible that it is also abundant in the soil developed from it. Such a conclusion is in accord with the analysis of the saturation extract of two samples from the Sharon Heights study site done by Nick Sitar, graduate student in soil mechanics. The pore water of the samples was removed under suction and analyzed for dissolved solids. The results are shown in Table 2. Although these values may be subject to some error (due to inexperience in performing the tests) they are considered to represent the various constituents in roughly the right relative proportions.

The Gapon equation (Mitchell, 1976) can be used to estimate the relative proportions of various cations in the double layer if the cation concentration in the equilibrium solution is known. The equation is:

TABLE 2. SATURATION EXTRACT ANALYSIS OF SAMPLES FROM SHARON HEIGHTS (Data from Nick Sitar, Stanford)

Element	Concentration in milliequivalents	
	Sample 1	Sample 2
Ca	1.32	0.64
Mg	0.49	0.22
Na	0.80	0.51
K	0.02	0.01
Totals:	2.63	1.38
	Percent of total disolved solids	
Ca	50.2	46.4
Na	30.4	37
$Na^+/(Ca^{2+}+Mg^{2+})_A$	0.0143	0.01322

$$\left(\frac{Na^+}{Ca^{2+} + Mg^{2+}}\right)_A = k \left[\frac{Na^+}{\left(\frac{Ca^{2+} + Mg^{2+}}{2}\right)^{\frac{1}{2}}}\right]_E \qquad (9)$$

where the subscript A refers to the adsorbed complex, E refers to the equilibrium solution, k is a constant having a value of 0.017 for a wide range of soils, and the concentration of the different ions is given in milliequivalents per liter. This equation conforms with double-layer theory which provides that in mono-divalent cation systems, the ratio of di- to mono-valent ions is greater in the double layer than in the equilibrium solution. This relation, when applied to the data obtained by Sitar suggests that Ca^{2+} predominates in the adsorbed complex.

Field Description and Relations

The study sites were first visited in Sept. of 1974. At this time the soil was dry and hard. Although the soil had a high dry strength it broke easily along very fine fissures, most of which were invisible to the naked eye. The soil surface as a whole consisted of numerous small prisms of irregular shape the maximum dimensions of which ranged between 0.3-3.5 cm. Dark

clay soils which break up into finely aggregated polygons at the surface and which develop large shrinkage cracks are formally termed vertisols by soil scientists. The term self-mulching has been used to describe the aggregate formation. The size of the polygons appeared to be related to the amount of sand-sized particles in the soil, the larger prisms occurring in the sandier soil. The faces along which soil prisms broke had a dull, earthy luster not evident within the soil blocks. Examination of these faces with a hand lens showed the existence of numerous very fine, discontinuous fissures.

The amount of gravel and larger-sized fragments of the soils varied in the two study sites. The soils from the Stanford Avenue site may contain up to about 80% by volume of rock fragments in these size ranges. Those from the Radio Facility site have less than 5% by volume. Soils from both sites contain organic material and sand-sized particles. The soils from the Stanford Avenue site generally have less than 20% sand by volume. The sand-sized fragments are predominantly angular to subrounded basalt fragments most of which occur in the medium to coarse grained sand range. Quartz, chert, and sandstone fragments may also be present in this size range. The latter are buff in color and tend to be sub-rounded in shape. They consist of fine sand and silt. Red and white colored chert fragments were identified. Like the quartz grains they are generally sub-angular. At the Radio Facility site the soil may contain up to about 40% sand-sized grains. These are generally sub-rounded to angular, fine to medium grained quartz and dark colored rock fragments.

Near-surface soils from both sites contain up to 15% of organic material in the form of partly decomposed leaves, roots and small pieces of wood. In places these have produced casts having the dull, earthy luster evident on the sides of the fine shrinkage cracks. Similar bits of organic debris were found in samples taken from different depths in the soil profile, though in much smaller concentrations.

Numerous large shrinkage cracks separated the soil into irregularly shaped blocks. The width of these cracks varied and was greatest in the soil which had the smaller percentage of sand and gravel sized particles. The maximum width of individual shrinkage cracks was about 12 cm., although the width was as great as 20 cm. where the junction of several cracks occurred.

In the field, the black silty clay occurs as distinct masses on hillsides and filling adjacent valleys. In plan view the creep masses may be lobate, or spoon-shaped, or they may be more irregular. Lobate masses are seen where the creep soil occurs in the upper reaches of valleys (Figs. 8 and 11). Elsewhere the creep masses are more irregular in shape, although they may be roughly rectangular over all or parts of their extent (Fig. 8).

The boundary between the creep soil and adjacent soil masses is usually gradational, although it may appear to be quite sharp because of vegetation contrasts (Fig. 11). Differences in soil type are reflected by differences in vegetation. This provides a useful contrast for mapping purposes. Typically, clay soils retain water longer than sandy soils once the dry season begins so that grasses on the clay remain green for longer periods of time. In addition, certain plants such as tarweed (genus Hemizona) seem to prefer growth on the black silty clay soil. A comparison between the vegetation on the different

Throughout the wet and dry cycles the ground surface had a "hummocky"

soil types at the Stanford Avenue site was done by Bob Simons and John Vendeland, undergraduate biology students. They identified 13 different plant and root species in addition to the tarweed. Their results are summarized in Table 3. The tarweed and two species of perennial grass (of the Lolium genus) were restricted to clay-rich soils, particularly the black silty clay. It is the presence of tarweed which provides the appearance of a sharp boundary between the creep mass and adjacent soils in Figure 11.

TABLE 3. CORRELATION BETWEEN SOIL AND VEGETATION TYPES (Data from Robert Simons and John Vendeland, Biology Department, Stanford)

Plant Type		Soil Type		
Genus	Species	Black slty clay	Brown slty clay	Sandy soils
Lolium (grasses)				
	multiflorum	1*	2	3
	perenne	2	-	3
	temulentum	3	-	-
Hemizona (tarweed)		1	-	-
Bromus (grass)				
	secalinus	2	2	4
Plantago				
	hirtella	1	2	-
	lanceolata	2	-	-
Centaurea				
	calcitrapa	3	-	-
Liliaceae		3	-	-
Brassica (?) (tobacco)		-	2	-
Lepturus				
	cylindricus	-	3	-
Avena				
	barbata (oat)	-	3	2
Danthonia				
	intermedia	-	-	1
Erodium (root plant)				
	cicutarium	-	4	1
% Veg. Cover:		30-85	25-85	30-85

1. Predominant
2. Secondary
3. Minor
4. Scattered
- absent

In places where the creep soil is forming the contact with the underlying parent material may be abrupt or gradational. Fleming (1971) observed gradational contacts between the creep soil and weathered claystone at the Golf Course and Sharon Heights study sites (Fig. 6). He described the occurrence of streaks of yellow-brown clay in the lower foot of the black silty clay. It is unknown whether similar features exist in the two new study sites. At the Radio Facility site there were no test pits excavated (it was in an open trench that Fleming observed the transition zone). The subsurface exploration consisted of drilling a number of boreholes with a trailer-mounted, motor-driven auger and examining the cuttings which came to the surface. Although we were able to measure accurately the depths at which changes in the soil properties occurred, differentiating a thin horizon in which the soil is becoming mixed due to weathering processes from a sharp contact between two different materials is extremely difficult because the auger thoroughly mixes the cuttings.

What was observed at the Radio Facility site was that below a depth of 1.5-2.0 meters the color of the soil changed abruptly to dark brown. This brown soil is in effect the upper, more intensely weathered surface of the underlying claystone. With increasing depth the claystone becomes progressively lighter-colored. Gypsum chips were also observed in the cuttings originating at the depth at which the color change occurs. Thus, without the benefit of direct observation of the contact zone, it appears that an abrupt transition occurs between the black silty clay and the underlying weathered bedrock.

A sharp interface was seen in the source area of the largest creep mass at the Stanford Avenue site. The contact is shown in the log for test pit no. 8 (Fig. 10). The color of the black silty clay is uniform above the contact. Along the south part of the interface the black soil is in direct contact with a buff-colored weathered claystone. However, along the north part of the contact a dark brown transition zone separates the black soil from the claystone. This transition zone is a zone of mixing between the black soil, basalt fragments, and intensely weathered claystone. The material in the transition zone becomes lighter colored as it approaches the buff claystone. An abrupt color change occurs at the contact between these two units, suggesting that the brown weathering zone may be creeping over the buff-colored, less weathered claystone. Similarly, the transition material does not grade upwards into the black silty clay but is separated from it by a narrow zone over which the color changes abruptly.

The contact zone is also characterized by a concentration of basalt fragments. A similar increase with depth in the number of basalt fragments was seen in test pits excavated on the second creep lobe at the Stanford Avenue site (Appendix C), although there was no clear-cut concentration of these along the contact with the underlying basalt. Near the axis of this creep lobe a color change occurs at a depth of about 2 meters in which the black silty clay is replaced by a dark brown silty clay. Details of this transition are unknown. The brown silty clay becomes progressively lighter colored with depth until the bedrock surface is reached at depths in excess of 3 meters.

The observations in the creep soil outside the source areas are similar. Here, the black silty clay is present to depths ranging between 1.7-3.0 meters. At this depth an abrupt change to a brown silty clay appears to occur. This

material then becomes lighter colored with depth as it grades into claystone. Irregular patches of sandy clay or sandstone occur in this zone.

The occurrence of the creep soil in bedrock valleys was described by Fleming (1971). The black silty clay is considerably thicker than adjacent non-creeping soils so that the black soil occupies depressions on the bedrock surface. In areas where the bedrock consists of Eocene marine sedimentary deposits, these depressions usually occur in the more easily weathered claystone which underlies natural depressions such as saddles in the ridges and valleys. Fleming (1971), however, showed that, at Sharon Heights where an arm of creep soil extends over an area underlain by sandstone, the bedrock valley exists below the black silty clay, suggesting that the creep process somehow incorporates the bedrock material into the soil to produce bedrock valleys.

The question of the origin of the black silty clay remains unsolved, although some general statements may be made. The soil appears to form only on clay-rich bedrock or bedrock that weathers to clay. In the study areas it occurs on basalt and claystone, both of which fulfill this requirement. Elsewhere in the vicinity it occurs on clayey sands and gravels of the Santa Clara Formation of Pleistocene age as well as in relatively flat lying Holocene alluvial deposits of the San Francisco Bay margins.

With the possible exception of a concentration of cobble and large sized fragments near the base, the soil is uniform in composition and color with depth. The uniformity of the soil can be attributed to the combined action of dessication, expansion and creep. When the soil dries out, wide shrinkage cracks which extend through the soil profile develop. Through these, organic and soil materials (and possibly basalt fragments) fall to different depths to become mixed with the soil during swelling and creep. It is the presence of organic debris which presumably gives the soil the characteristic black color.

The field relations suggest that the formation of the creep soil involves the incorporation of bedrock material as well as the lateral growth of the creep masses. The former is suggested by the occurrence of bedrock valleys and the observations of the mixing of black silty clay with weathered claystone; the latter is inferred from the lateral gradation of the black silty clay into other soil types which was observed wherever the creep soil occurs. The occurrence of the wide shrinkage cracks extending through the soil profile is probably important in the formation of the bedrock valleys. Through these, organic debris may fall to the soil-bedrock interface where it decomposes to produce carbonic and other organic acids. The cracks also provide an avenue for oxygen, carbon dioxide and water to move directly to the interface. All of these substances act to accelerate the decomposition of the bedrock. In this respect it should be noted that on basalt the creep soil (and bedrock valleys) occur in natural topographic swales toward which both surface and groundwater flows, increasing the potential for chemical weathering.

The shrinkage cracks are also likely to be important to the lateral growth of the creep masses. Shrinkage cracks along soil unit boundaries extend into transition zones. The cracks enhance chemical weathering as described above and allow mixing of the soil which falls into the cracks.

Changes in the Appearance of the Soil Throughout the Study Period

Light rains fell intermittently during the early part of the month of Oct. 1974 followed by a three week dry period. No changes in the character

TABLE 4. PRECIPITATION AMOUNTS DURING THE STUDY PERIOD

	1974	1975	1976
January	2.84	1.42	0.25
February	1.05	3.05	1.48
March	4.07	4.66	1.15
April	1.92	1.36	0.98
May	0.06	0.01	0.04
June	0.11	0.10	0.09
July	0.34	0.15	0.01
August	0.00	0.36	1.04
September	0.00	0.00	0.54
October	1.13	1.55	0.22
November	0.77	0.45	1.01
December	2.01	0.21	0.90
Total	14.30	13.32	7.71

Precipitation amounts given in centimeters

TABLE 5. LOCATION AND ALTITUDE OF RAINFALL MEASURING STATIONS AND STUDY SITES

Station	Lat. (N)	Long. (W)	Altitude (ft.)
Palo Alto Jr. Museum	37°27'	122°08'	23
La Honda	37°19'	122°16'	750
Woodside Fire Dept.	37°26'	122°15'	380
Study Sites	37°25'	122°09'	175 to 375

of the soil were evident at this time. About 3 cm. of rain fell between Oct. 28 and Nov. 8, mostly during the last days of October. During this time the large shrinkage cracks were partly closed. The soil at the ground surface was moist but stiff, and the tendency to break up into small prisms was no longer pervasive. The first measurement of the length of the steel rods which protruded above the ground surface was made on Nov. 10.

Precipitation during the remainder of the month of November and during December and January (1975) amounted to about 10 cm. Periods of rainfall

were separated by dry spells which lasted up to two weeks. During this time the shrinkage cracks closed almost entirely at the ground surface, most being only 1-2 mm. wide and discontinuous. The depth of wetting at this time was about 30 cm. The aggregates or prisms that were at the surface during the late summer months were no longer evident. Following periods of rain the soil was sticky and plastic. During intervening dry periods the soil became stiffer as it lost moisture and small, discontinuous shrinkage cracks developed. If dessication conditions persisted these cracks grew in width and length while other small cracks were developing forming a continuous network of small polygonal blocks. These small cracks closed with renewed precipitation.

Precipitation during the first three weeks of Feb. was more or less continuous and totaled about 8 cm. The last rains of the month fell on Feb. 20 at which time the surface soil was wet and plastic. By Feb. 23, however, the soil at the ground surface was beginning to dry out once more and hairline shrinkage cracks were developing. Most of the original large shrinkage cracks had closed completely at the ground surface but their former positions were outlined by minute, discontinuous irregularities in the micro-topography of the ground surface. The former crack positions were occupied by either small ridges or valleys. Measurement of the steel rods indicated that an average vertical swelling of about 2 cm. had occurred since mid-November. The amount of swelling recorded at the different rods was irregular (Appendix B) but was generally less for the shorter rods (length = 0.5 and 0.8 m.) than for the longer ones. It thus appears that swelling occurs around the rods and that the rods are not pushed up by the swelling pressures exerted on its sides. Swelling below the depth of rod penetration is not reflected by changes in the amount that the rods stick out above the ground surface. These observations suggest that the depth of wetting had extended to about 60 cm.

March of 1975 was the wettest month of the study period. About 12 cm. of rain fell during the first four weeks of the month. Much of this precipitation is thought to have been lost as runoff. The cracks at the ground surface closed completely during this time, although the traces of some were still visible. Measurement of the steel rods in early April indicated that the ground surface rose about one centimeter during this time indicating continued swelling of the soil at depth as an increasing thickness of soil was changing in water content. Swelling of the near surface soil seemed to have ended by this time as suggested by the measurements for the shorter rods which showed little change. Some of the rods showed increases in the length they extended above the ground surface, but some of these increases are within the range of accuracy of the method of measurement. Others may reflect the fact that some dessication of the ground surface had occurred between the date of measurement and the last rains. Precipitation during April was about 3.5 cm. after which the dry cycle began.

The depth of wetting during the first wet cycle, as observed in test pits and inferred from the vertical expansion data described above, varied between 0.6 and 1.0 meter. Below this depth the soil was dry and stiff. Many of the shrinkage cracks remained open below this depth.

The dry cycle began in late April of 1975. The total precipitation during the months of March to Sept. amounted to about 1.5 cm. The first change which occurred at the onset of drying was the appearance of a large

number of hairline dessication cracks. When they first appeared these cracks were discontinuous. With time they became wider and longer; at the same time more of the cracks developed. Eventually the soil at the ground surface was broken up into small polygonal blocks having a width of between 10-15 cm. Thus, two to three weeks after the dry cycle began the ground surface consisted of a continuous network of these small polygons. This initial dessication pattern resembled that which occurred during the dry spells of the wet cycle. Figure 14 shows the appearance of the ground surface during one of these. Two sizes of small polygons can be seen. The larger polygons which develop initially are visible in the upper right half of the photograph. The breakup of these into smaller blocks is evident in the left foreground.

At some time during the first half of June 1975 the large shrinkage cracks first appeared on the ground surface, breaking up the soil into large polygons having widths of between 0.5-1.5 meters. The exact time at which these cracks appeared is unknown. They were present when the sites were visited on June 13. On this date the large cracks were well developed whereas the smaller polygons were no longer evident. Some of the large shrinkage cracks reappeared at the same place they had been prior to the wet season (Fig. 15). Others reappeared in new positions (Fig. 16). The cracks extended from the surface down to bedrock or into the weathered transition zone. In cross-section, the cracks appeared as roughly planar features generally oriented at some small angle to the vertical, some being normal to the ground surface. Many of the shrinkage cracks were slightly curved over some part of

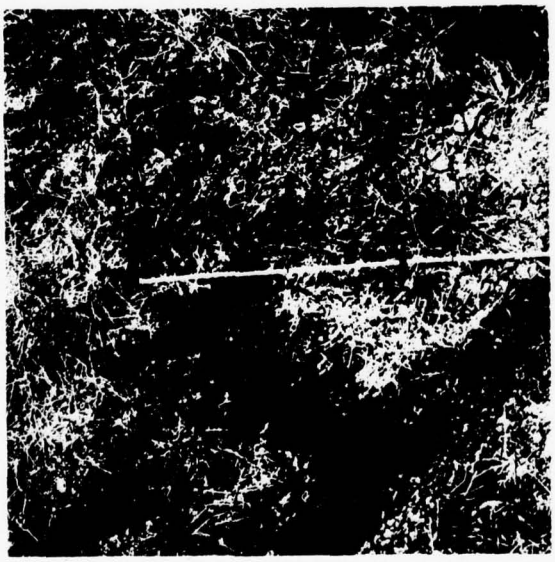

Figure 14 - Photograph illustrating the development of a network of small polygons shortly after a period of rainfall. Two sizes of polygons can be seen. In the upper right of the photo these are about 10-15 cm. wide. These larger polygons eventually break up into smaller ones as seen in the lower left hand side of the photo. The distance between rods no. 23 and 42 is about 50 cm.

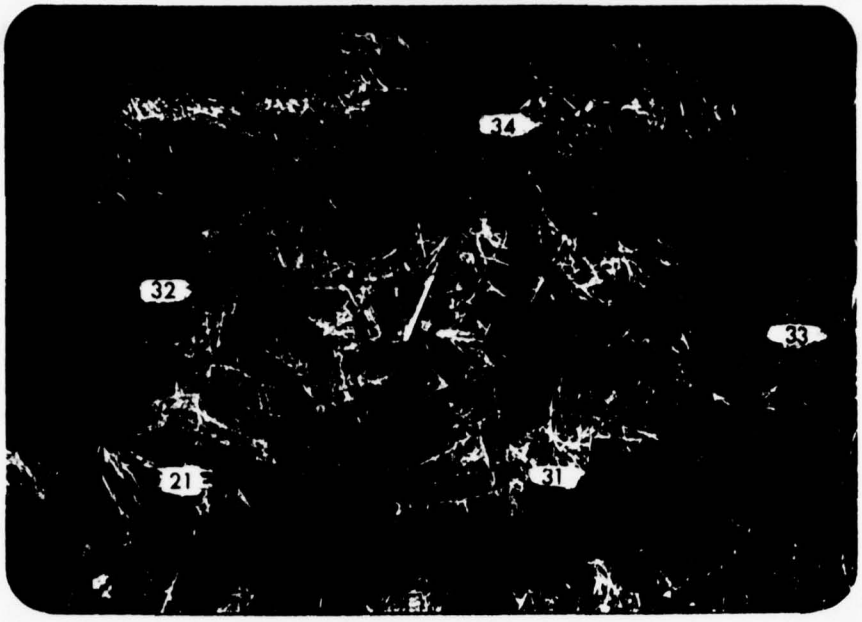

a

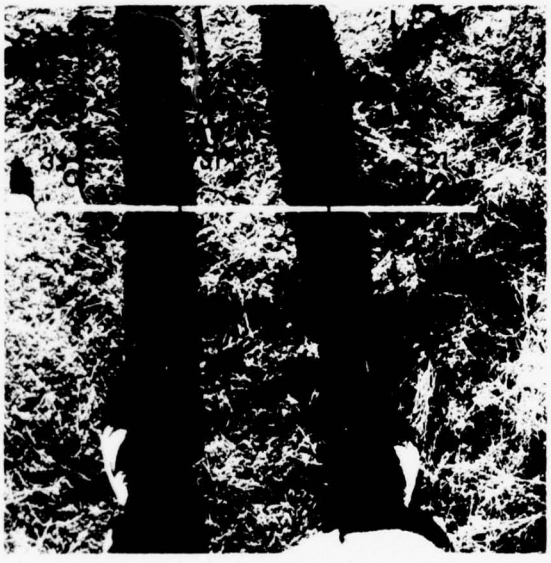

b

Figure 15 - Recurrence of shrinkage cracks. 15-a shows the position of the shrinkage block during the summer of 1974. 15-b shows the same polygon reappeared the next summer.

a

b

Figure 16 - Appearance of shrinkage cracks in a new position. During the summer of 1974 cracks passed through the 5 steel rods shown in 16-a. The relocation of some of the cracks is evident in 16-b.

their cross-sectional extent. This is well illustrated in Fig. 17 which shows several curved cracks. The curvature of the cracks denoted by the letter A is an apparent curvature. In addition, the walls of the shrinkage cracks were not smooth but were, in effect, a highly irregular surface having a maximum relief of about 3 cm.

After the large shrinkage cracks had appeared the soil continued to dessicate. The large cracks became wider. At the same time, smaller polygons bounded by fine shrinkage cracks similar to those which had first appeared early in the dry cycle developed. These polygons, or soil aggregates, became progressively smaller as fissuring increased throughout the dry period. To a lesser extent fissuring of this type also occurred along the walls of shrinkage cracks. Fissuring was more intense along the upper edges of the walls of the shrinkage cracks (Figs. 17 and 18). Small shrinkage blocks produced along the edges of the shrinkage cracks tended to fall into the cracks, in some instances possibly filling them up (Fig. 19c,g). In most cases, however, it appears that larger polygons falling into the cracks form a plug at some narrowing part of the crack (Fig. 19-f) or the falling soil prisms accumulate above a bend in the crack, as shown in Fig. 17. In either case a plug is formed so that open cracks, V, are left below a filled area, F (Fig. 17).

Many of the large shrinkage cracks eventually filled up to the ground surface and were no longer visible (Figs. 20 and 21). Elsewhere the soil also broke up into small prisms. At the Radio Facility site the ground surface on the sandier soil along the margins of the creep mass was virtually littered with small polygons (Fig. 21). In the more clayey soil, however, the soil at the surface was fragmented throughout and the soil surface consisted of a finely aggregated, loose mass of soil with few polygons resting on the ground surface.

On Oct. 4, 1975, prior to the start of the next wetting season, the length of rod which stuck out above the ground surface was measured for some rods. These measurements, along with measurements of all the rods two months later (approximately 1.7 cm. of rain fell in the interval between these two measurements, so that some expansion of the soil took place) indicated that vertical shrinkage of about 3 cm. had occurred.

During the following wet cycle precipitation amounts were only about 25% of normal. Nevertheless, many of the shrinkage cracks closed at the ground surface, especially those which had become filled with soil polygons. The depth of wetting and crack closure did not exceed about 0.5 meters. Figure 22-A illustrates an example of a crack that had swollen shut over part of its length. The outline of the original crack is still clearly visible. This crack was excavated as shown in Fig. 22-B. At a depth of about 18 cm. the crack was open. Whereas the soil above this depth was moist and plastic, that below was dry and stiff.

During this wet cycle the breakdown of the polygonal aggregates which covered or littered the surface was also observed. Following the onset of precipitation the aggregates begin to break up. The corners begin to get rounded and the size of the polygons decrease gradually (Fig. 23). The small prisms begin to acquire what can best be termed a "diffuse" appearance as they blend more and more into the parent soil. By early March 1976, the soil polygons were no longer evident.

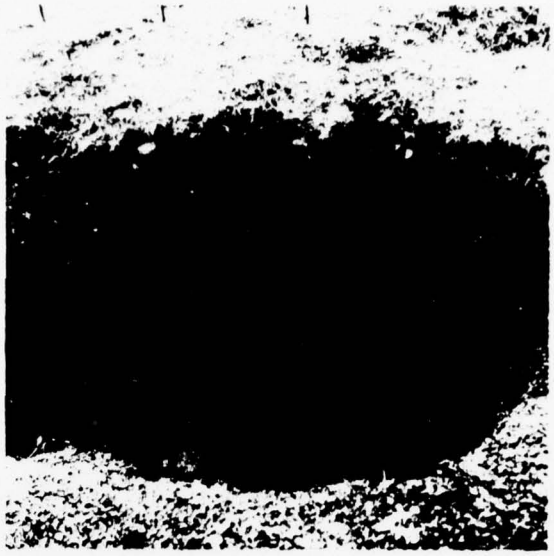

Figure 17 - Curvature and infilling of the cracks. The large, curved crack near the right margin of the photo has been partly filled (F) with falling soil polygons. Open cracks (V) can be seen above and below the filled area. Soil polygons can be seen developing along the crack near the ground surface (P). Curvature of cracks denoted by A is apparent.

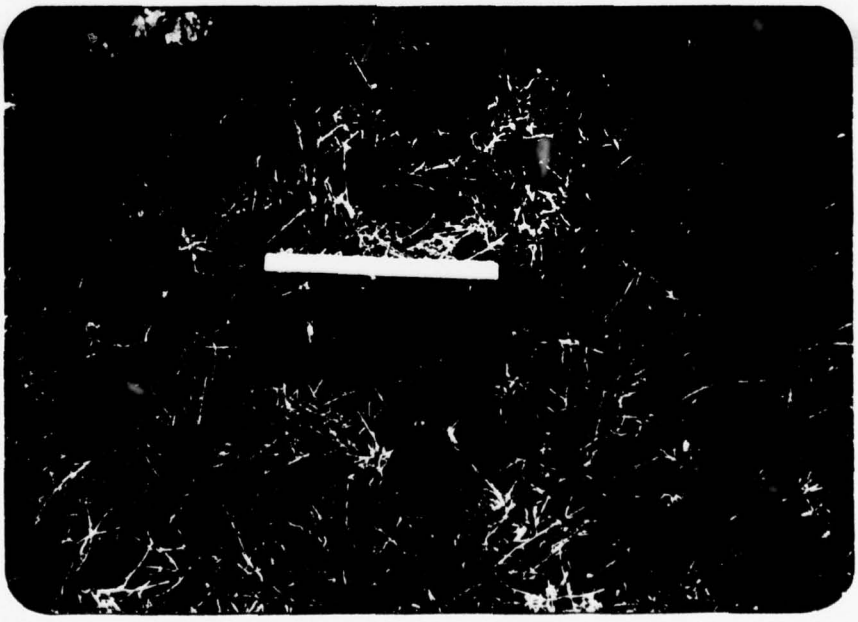

Figure 18 - Fissuring of soil along upper wall of a shrinkage crack.

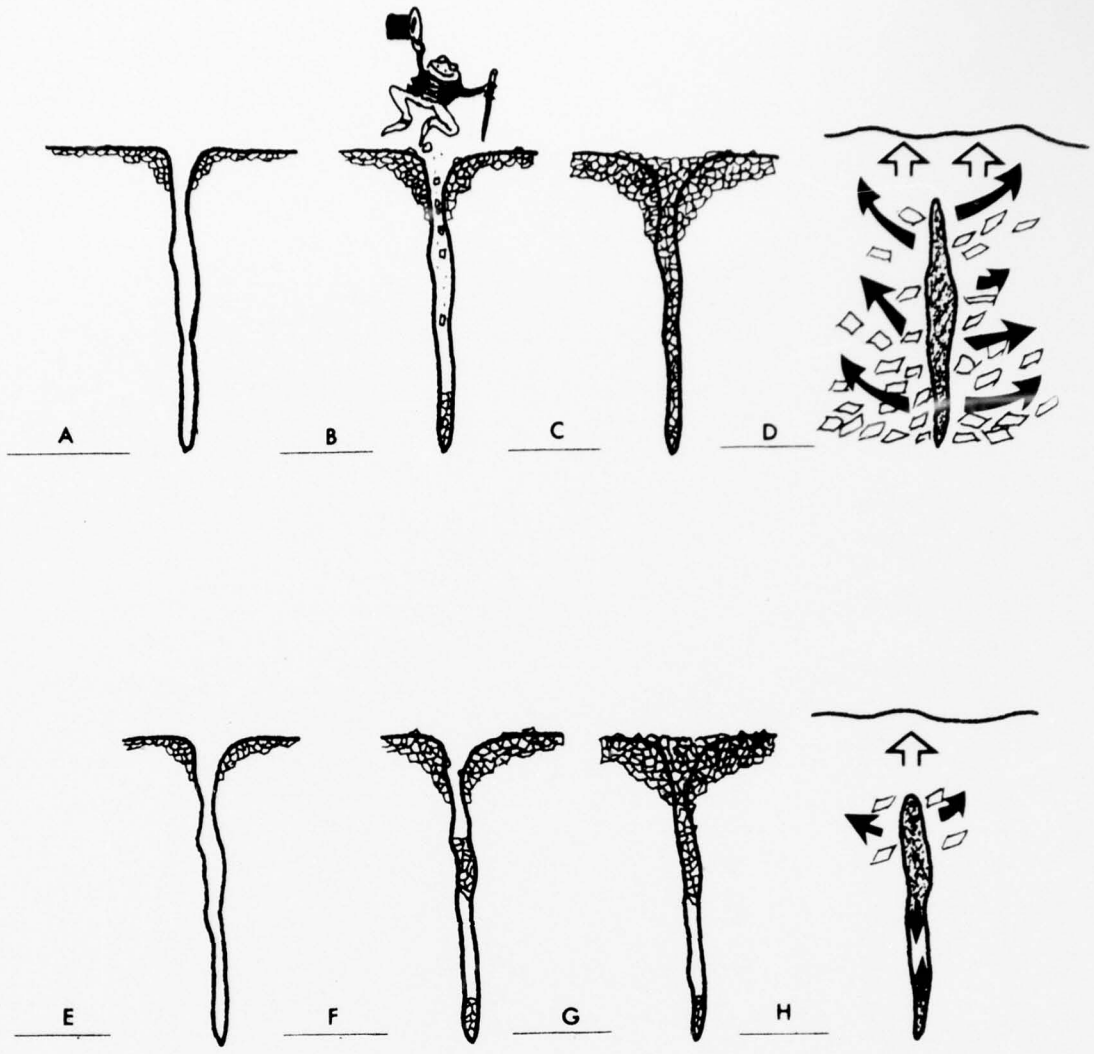

Figure 19. Schematic sequence showing the development of surface mulch and the filling of shrinkage cracks. Filling occurs from the base of the soil layer or above a constriction in the crack (G). Swell pressures developed during wetting (D and H) are responsible for the formation of shiny surfaces described by others (Fleming, 1971; Fleming and Johnson, 1975). Modified after Buol and others (1973).

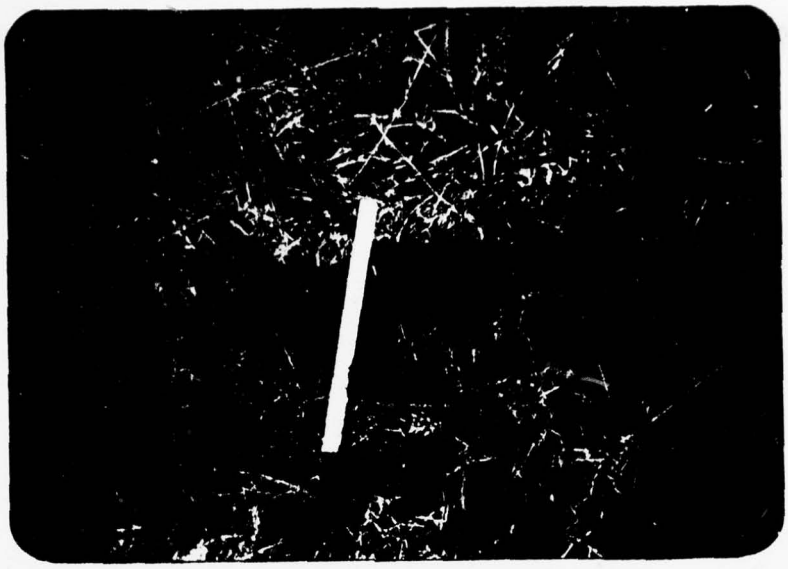

Figure 20 - Crack filled by soil polygons over part of its length.

Figure 21 - Shrinkage crack filled over part of its length by soil prisms. Note soil polygons resting on the ground surface.

a

b

Figure 22 - Photographs illustrating the closing of the large shrinkage cracks at the ground surface. The trace of the former crack is still evident in A. In B the crack has been excavated. The crack was found open at a depth of about 18 cm. Rod no. 30 can be seen just next to the pen in B.

Throughout the wet and dry cycles the ground surface had a "hummocky" appearance produced by the existence of small depressions and ridges. Maximum relief was on the order of 4-5 cm. The diameter of the depressions and ridges varied, but was generally less than about 25 cm.

Figure 23 - Breakdown of aggregates resting on the ground surface. A rounding off of initially sharp corners is evident.

DISPLACEMENTS MEASURED WITH STEEL RODS

The tilt of the steel rods was measured at different times during the wetting and drying cycles between October 1974 and February 1976. The initial tilt was measured when the rods were installed. Subsequent tilt measurements were taken on November 9, 1974, December 21, 1974, February 23, 1975, April 2, 1975, October 4, 1975, December 6, 1975, January 17, 1976 and February 7, 1976. This period of measurement covered one full wetting and drying cycle (October 1974-September 1975) and part of a second wetting cycle (October 1975-February 1976). The total estimated precipitation amounts during these two periods were

about 80% and 25% of the 50-year averages for the respective time periods (Table 4). The monthly precipitation at the study sites was estimated from the known precipitation at three nearby sites (Environmental Data Service, 1974, 1975, 1976) and a published isohyetal map of the San Francisco Bay Region (Rantz, 1971). The location and elevation of the three recording stations and the study sites are given in Table 5. Precipitation at the Radio Facility and Stanford Avenue sites was measured during the period between October 1974 to January 1975 with commercially available, plastic rain gauges placed at various points on and adjacent to the masses of creep soil. The estimated amounts show excellent agreement with the precipitation recorded at the stations during this period. Monitoring of these rain gauges was discontinued because they were regularly disturbed by hikers.

Measurements of the tilt of the steel rods provided some information about displacements associated with shrinkage and swelling of the soil. They provided no information about creep of the soil, because of insufficient precipitation. Precipitation during the study period was less than normal. Between Oct. 1974 and Apr. 1975, when the estimated rainfall was about 80% of normal amounts, about 65% of the total occurred during the months of Feb., March, and April, during which above normal amounts fell (an increase of about 50% over the 50 year monthly averages). Because of the low permeability and infiltration rate which characterizes the black silty clay once the surface soil is wetted and the dessication cracks disappear, much of this excess precipitation was probably lost as runoff and evaporation. During the previous months of the first wetting cycle (Oct. 1974 to Jan. 1975), precipitation amounted to about 40% of the average for this time period, and it fell during minor storms separated by dry intervals of up to two weeks duration during which the soil began to dry. As a result, the soil never became wet to depths greater than 0.6-1.0 meter. During the second wetting cycle (Oct. 1975-Feb. 1976) the depth of wetting did not exceed 0.5 meter.

The initial movement of the soil at any depth should correspond to swelling and the closing of the shrinkage cracks, and movement occurs in all directions. Any downhill creep, separable from movement due to expansion, that may have occurred would be restricted to the upper 0.5-1.0 meter of soil where wetting took place. Theoretically, because of the rigidity of the steel rods and the dry soil only those rods which rest entirely within, or which have most of their length in wet soil should be tilted by creep and expansion movements. Thus, only those rods of length less than or equal to about one meter should become tilted, and this only after sufficient rain has fallen for the soil to be wetted to the necessary depth. It is also evident that the tilt of the rods will not give a measure of the total displacement at the ground surface, since creep can occur near the surface before the soil is wetted to a depth corresponding to the length of the rod. Nevertheless, most of the rods became tilted shortly after the winter rains began. Most of the rods of length greater than or equal to 1.1 meters (3.5 ft.) were initially placed in shrinkage cracks. These rods were not confined by soil over a significant fraction of their length and were hence free to tilt in response to soil movements at or near the surface by becoming bent. Furthermore, the tilting of those rods not placed in shrinkage cracks suggests that even in these rods there was an open space between the rod and the soil, perhaps produced by the driving of the rods. Thus, it becomes apparent that only the relative directions of the measured tilts

are significant. As will be described below, these suggest that significant creep movements did not occur on the slopes during the study period. Because of the rainfall deficiency it appears that most of the soil movement was confined to the swelling and shrinking of the near surface soil.

The pattern of tilt of the steel rods reflects the movements associated with swelling and shrinking of the soil. Figures 24 to 29 show relative displacements of the rods at the Radio Facility site (relative to the initial zero position) at different times of the year. The solid arrows represent the relative magnitude of the displacement, calculated using the entire length of the rod, and indicate the direction of movement. Absolute values of displacement are not given since, as stated above, they have no real significance. The number next to each displacement line identifies each individual rod. The insets show the relative locations of rods placed around shrinkage blocks (the initial shape of the shrinkage polygons is shown in Fig. 25) and that of those placed in a random cluster near the retaining wall. A scale is given in one of the insets. The data for Jan. and Feb.,1976, has not been plotted as little change occurred since the previous measurement (Dec. 1975). The tilt data is tabulated in Appendix A.

From Figures 24 to 27 it is clear that the movement of rods placed around shrinkage blocks during the initial wetting cycle can be accounted for by expansion of the soil. Most of these rods moved away from the center of the shrinkage block. When initially placed, most of these rods rested against the sides of the shrinkage blocks, so that movement away from the blocks during expansion would be expected. Rods no. 33, 38, 39, and 42, however, showed movement towards the center of the block. The first three of these rested against the opposite wall of the shrinkage block, so that this direction of motion would be expected. Rod no. 42 was initially free-standing and the initial displacements were erratic. Between Dec. 1974 and April 1975 tilt of the rod was towards the shrinkage block. The crack closed during the wetting period. During the next drying period (Apr. 1975-Oct. 1975) a new crack appeared about 10 cm. west of the rod (Fig. 30), so that the rod was now situated near the edge of a new shrinkage block. The displacement direction during the drying cycle was reversed, with the tilt directed away from the original shrinkage block and towards the center of the new one. Rewetting between Oct. 1975 and Feb. 1976 caused the soil to expand and the tilt direction was again reversed, the tilt now being towards the edge of the shrinkage block as the more recently developed shrinkage cracks began to close up. This last reversal is illustrated in Figures 28 and 29 by a shortening of the displacement line.

The tilt of most of the rods initially placed in cracks around shrinkage blocks was controlled by the presence of the shrinkage cracks throughout the measuring period. During the drying period of Apr. to Oct., 1975, the shrinkage cracks surrounding the block encircled by rods no. 21, 31, 32, 33, and 34 (length = 1.4 m.) reappeared in essentially the same location they had occupied prior to the winter rains. (Fig. 15). The tilts measured in these rods reflect the opening and closing of these cracks. The shrinkage blocks around which rods no. 22, 24, 39, 41, and 43 (length = 1.2 m.) and rods 19, 23, 26, 38 and 42 (length = 1.2 m.) were placed did not develop again during the dry months of 1975. Nevertheless, large shrinkage cracks appeared at the location of all rods except for no. 23, 42, and 43. That the shrinkage cracks did not necessarily reappear at the same location during successive drying cycles is clearly illustrated in Fig. 16.

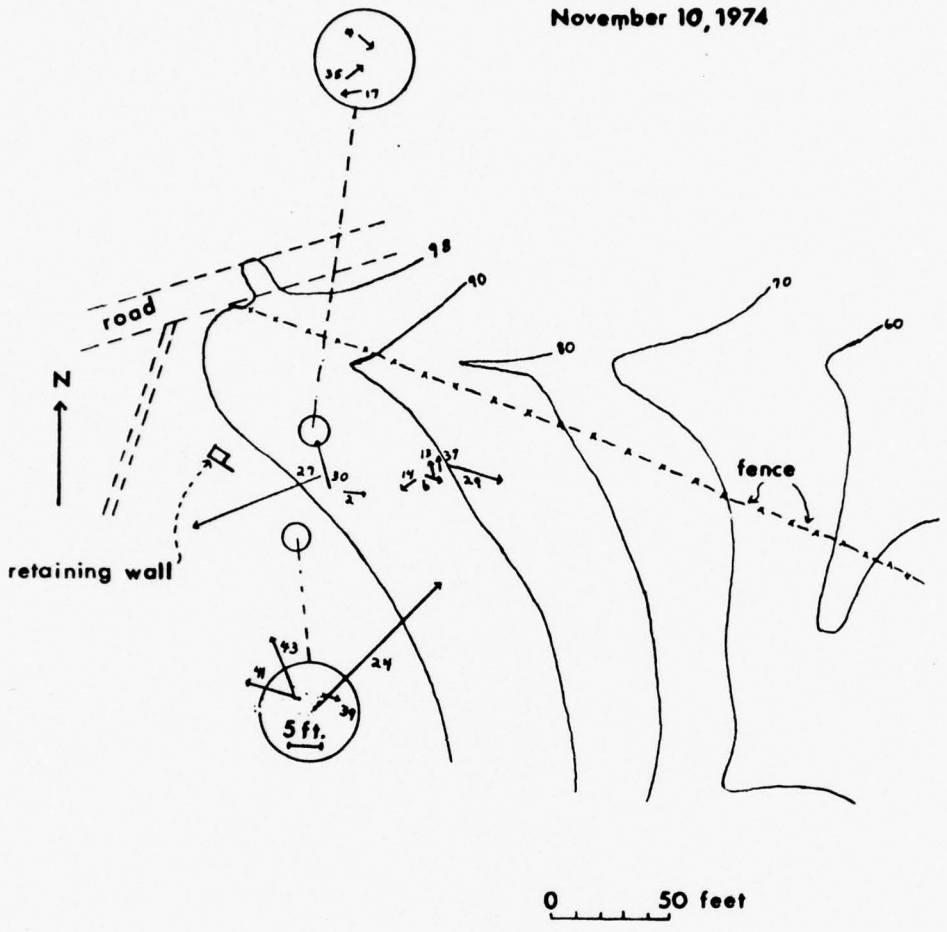

Figure 24.

Caption for Figures 24-29: Relative tilts of steel rods at the Radio Facility Study Site between November of 1974 and December of 1975. Positions of rods relative to shrinkage blocks indicated by inset figures.

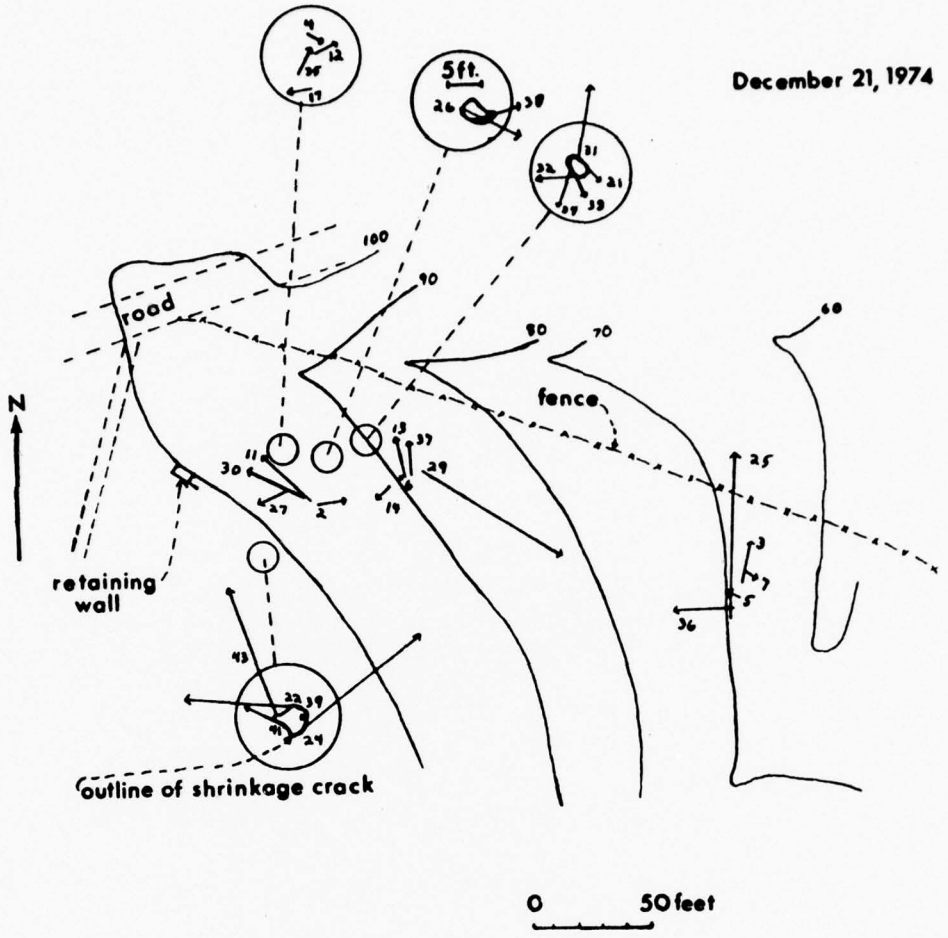
December 21, 1974
5ft.
road
fence
retaining wall
outline of shrinkage crack
N
0
50 feet

Figure 25

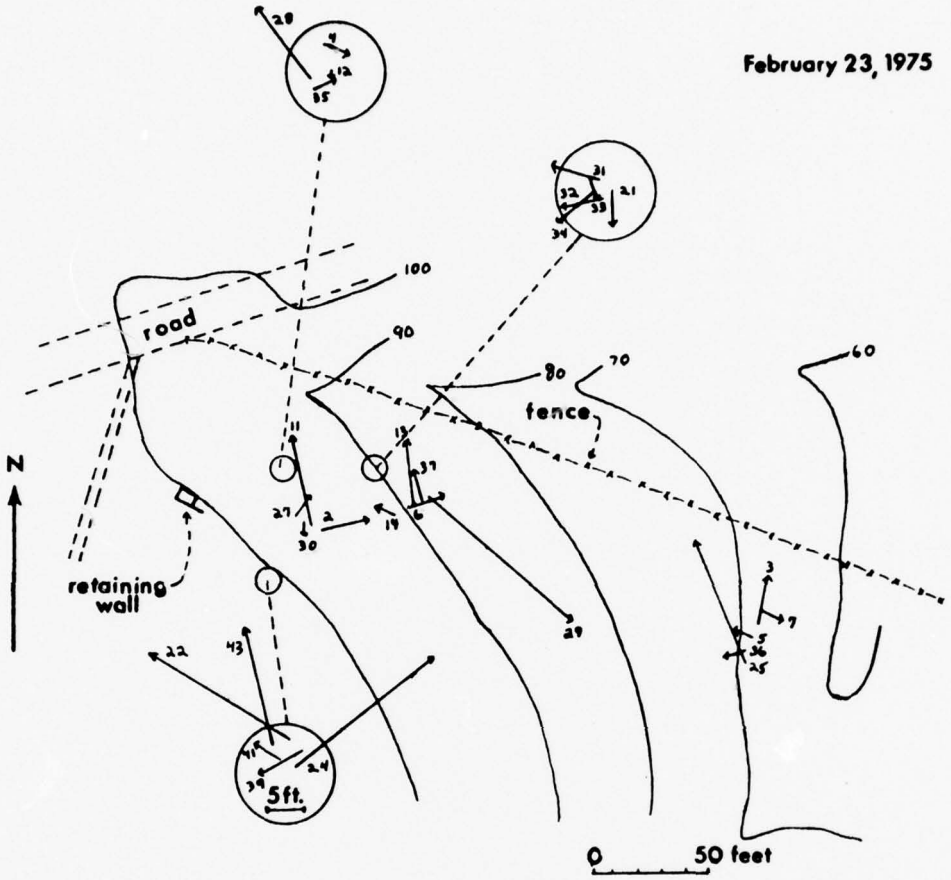
February 23, 1975
road
100
90
80
70
60
fence
retaining wall
N
5ft.
0 50 feet

Figure 26

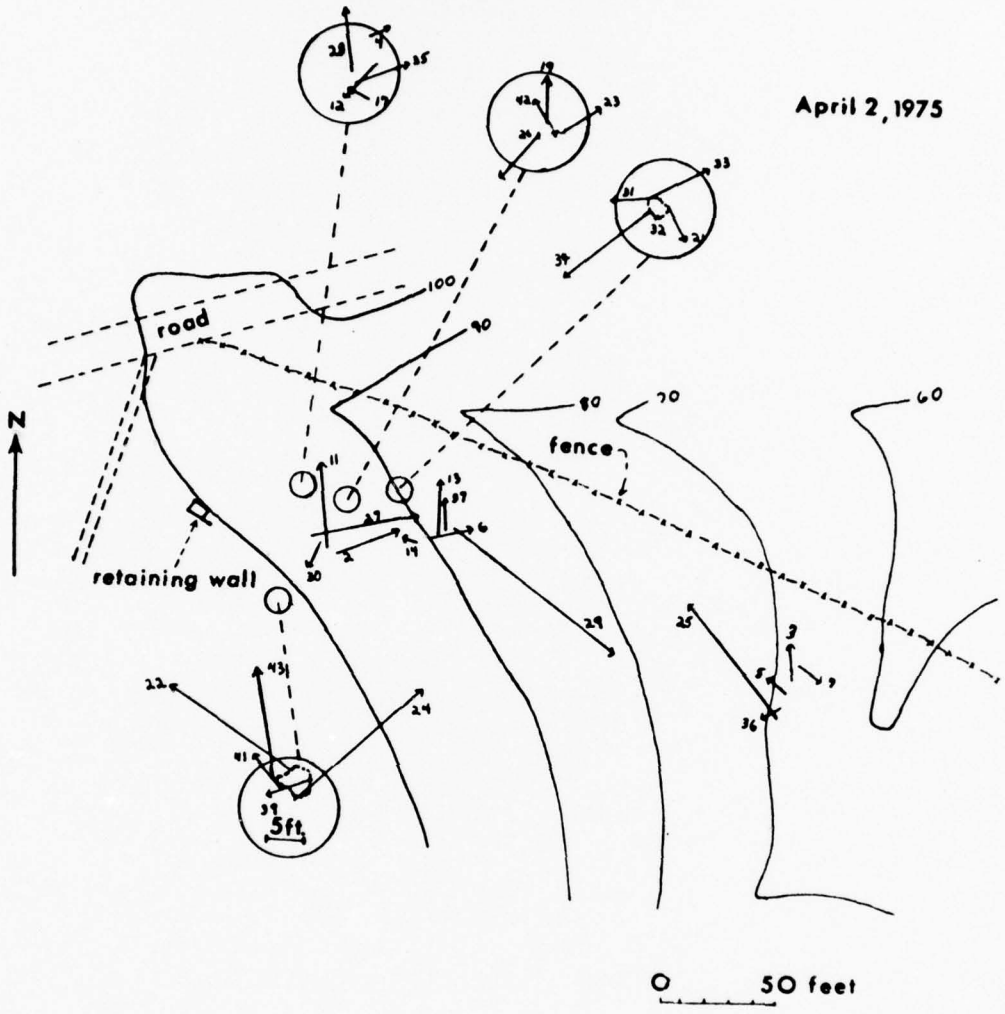
April 2, 1975
N
road
retaining wall
fence
100
90
80
70
60
5ft
0
50 feet

Figure 27

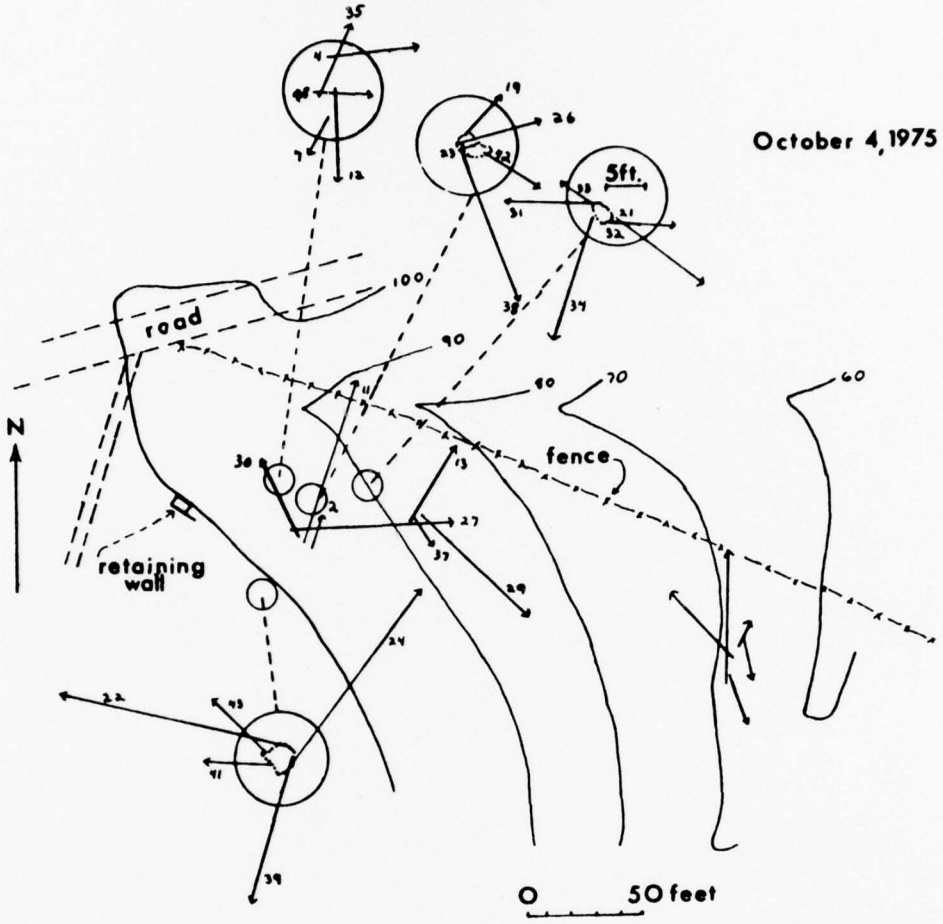

Figure 28

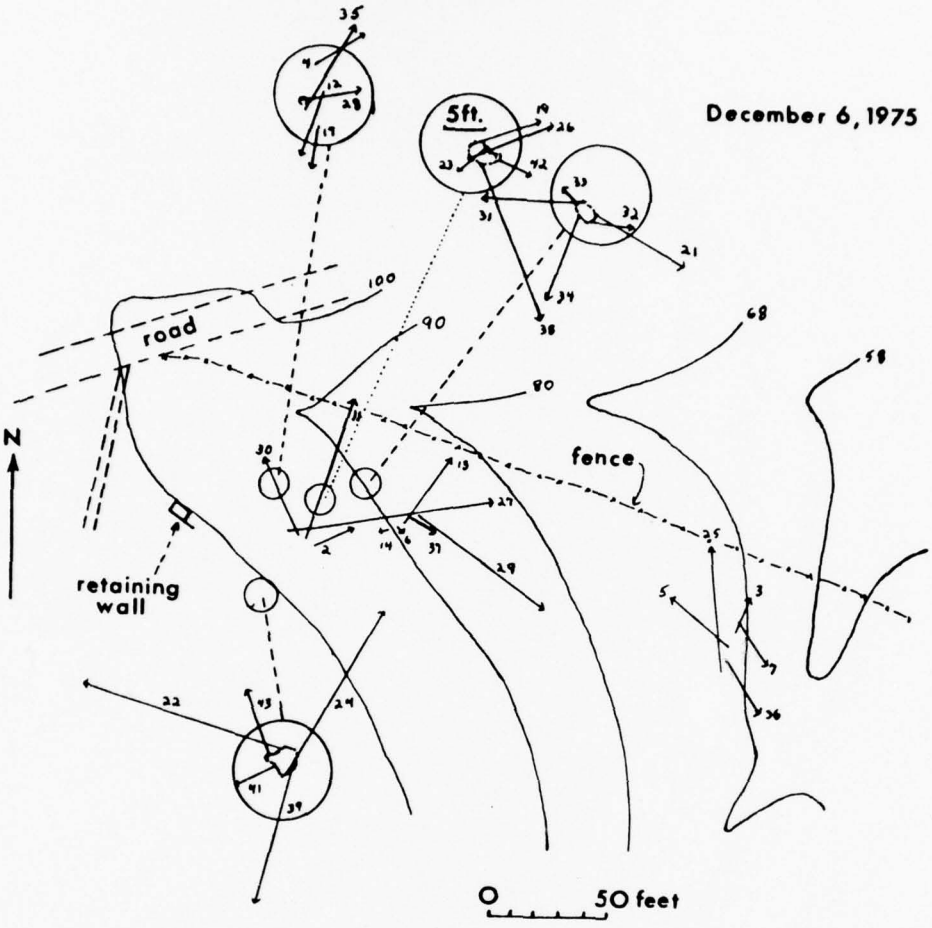
December 6, 1975
5ft.
road
fence
retaining wall
N
100
90
80
68
58
0
50 feet

Figure 29

For those rods located where new shrinkage cracks developed, the tilt of the rods during the drying and following wetting periods was normal or at an angle to the crack direction. The tilt of the three rods which no longer appeared in shrinkage cracks was controlled by the location of nearby cracks. The tilt pattern of rod no. 42 has already been described. For rod no. 23, the tilt during the drying cycle was directed away from a large shrinkage crack which developed about 15 to 20 cm. north and east of the rod. During subsequent wetting the tilt direction was erratic but was directed towards the shrinkage crack to the east. A similar relation was observed in rod no. 43. During dessication a new crack developed about 14 cm. southeast, south, and west of the rod.

Rods no. 2, 11, 18, 27, and 30 were placed so that they were aligned roughly parallel to the slope contours. Rod no. 18 (length = 0.5 m.) was removed by vandals and no data was obtained. Rod no. 2 (length = 0.8 m.) was initially placed near the center of a shrinkage polygon, where lateral movements during swelling should be small. In addition, the rod extended to a depth of about 0.6 m., a depth to which the water content of the soil was observed to have increased nearby. The magnitude of the displacement at the ground surface computed from the tilt data (about 2 cm.) is, much greater than would be expected for a thickness of creeping soil of 1.0 meter (depth of wetting). The tilt was initially directed about parallel to the slope contours, with a small component in the downslope direction (Fig. 24 and 25). By Apr., 1975, the tilt direction was roughly in the direction of maximum slope. During drying between Apr.-Oct., 1975, a shrinkage crack formed about 15 cm. east of the rod. The tilt of the rod was then directed away from the crack and towards the crack on rewetting (Oct. 1975-Feb. 1976).

Rods no. 11 (length = 1.1 m.), 30(length = 1.4 m.), and 27 (length = 1.7 m) were all placed in shrinkage cracks. The tilt of these rods during the first wetting cycle was highly irregular. During the following drying and wetting periods the tilt of rods no. 30 and 27 was controlled by shrinkage cracks. During dessication rod no. 30 was tilted away from a large crack which appeared about 15 cm. to the east and south (Fig. 22); on rewetting tilt was towards the crack. During this period rod no. 27 was moving within a northeasterly trending crack in directions approximately normal to the crack. The tilt of rod no. 11 showed no consistent direction and was actually directed towards a developing shrinkage crack located about 10 cm. east and northeast of the rod, and away from the crack during rewetting. No explanation for this behavior can be given.

The tilt of rods no. 29 (length = 1.7 m.) and 37 (length = 1.2 m.) was controlled by shrinkage cracks throughout the measuring period. Both were initially placed in shrinkage cracks that were aligned roughly parallel to the direction of maximum slope. These cracks disappeared during the first wet cycle but reappeared when the soil dried up again. The tilt of the rods was always directed roughly perpendicular to the crack. Rod no. 13 (length = 1.1 m.) was originally placed in a small crack within a shrinkage block. The tilt directions could not be correlated to any observed surface feature.

Five rods of different lengths were placed in the creep soil near the base of the hill. The tilt of rods no. 7 (length = 0.5 m.) and 3 (length = 0.8 m.) during the initial wetting cycle may be the result of creep. Both

rods, initially placed near the center of shrinkage blocks, were tilted in a downslope direction but at a relatively large angle to the maximum slope direction. Subsequent tilt was related to nearby shrinkage cracks. Rods no. 5 (length = 1.1 m.), 36 (length = 1.2 m.) and 25 (length = 1.7 m.) were placed in shrinkage cracks and the tilts associated with the initial wetting all occurred about normal to the crack direction. Both rods no. 36 and 25 showed a progressive uphill rotation of the tilt direction with time. New shrinkage cracks appeared at the three rods during the drying cycle. That at rod no. 5 appeared approximately 2 cm. east of the rod and was oriented almost due north. Tilt occurred away from the shrinkage crack during the drying cycle and towards it during the second wetting cycle. Rods no. 36 and 25 were left free standing in the new shrinkage cracks and movement after the initial wetting period was irregular.

Rods no. 4, 12, 17, 28 and 35 were placed in a small cluster near the retaining wall. Rod no. 17 (length = 0.5 m.) was placed near the intersection of three shrinkage cracks (Fig. 31). These cracks appeared in essentially the same position after the initial wetting cycle. The tilt of the rod was initially directed upslope, away from the intersection of the three cracks rather than towards it as would be expected. This anomalous behavior was also observed during the following dry period when the rod tilted towards the redeveloping crack intersection. One possible explanation for this behavior is that during the wet season the water content of the soil increased at depth faster than it did at the surface so that expansion towards the cracks at depth is greater than at the surface. This could occur because of the relatively large crack area at the intersection, which allows greater amounts of rain to enter the cracks. Similarly, a greater loss of water below the surface would produce the anomalous tilt recorded. During the second wetting cycle the tilt of the rod was directed towards the crack intersection. If the suggested method of wetting the soil through the crack occurs, this tilt towards the crack would presumably be related to the much slower rates of wetting (precipitation) which occurred during the second wetting cycle.

Rod no. 4 (length = 0.8 m.) was initially placed about 13 cm. east of a northeasterly trending crack. During the initial wetting period the tilt of the rod was first directed away from the crack and then towards it, with a net downslope tilt. During the following drying period a shrinkage crack developed in approximately the same location as the initial crack; however, the rod was now about 5 cm. from the edge of the crack. During dessication the rod was tilted away from the crack. On rewetting the tilt was initially directed towards the crack and then away from it.

Rods no. 12 (length = 1.1 m.), 35 (length = 1.2 m.) and 28 (length = 1.7 m.) were originally placed in large shrinkage cracks. The initial orientation of these cracks was not recorded. It is assumed that the tilt during the first wetting cycle occurred approximately perpendicular to the crack orientation. After the first wetting cycle the tilt of rods no. 28 and 35 was in accordance with the opening and closing of adjacent shrinkage cracks. Tilt values for rod no. 12 measured after Apr., 1975, are suspect because the rod was loose in a large (about 4.5 cm.) shrinkage crack thereafter.

Eight steel rods were placed as shown in Fig. 12 in the source area of the southernmost creep lobe of the Stanford Avenue site. The tilt of these

Figure 30 - Location of shrinkage crack which developed about 10 cm. west of rod no. 42. Also shown is rod no. 38. North is located towards the upper left corner.

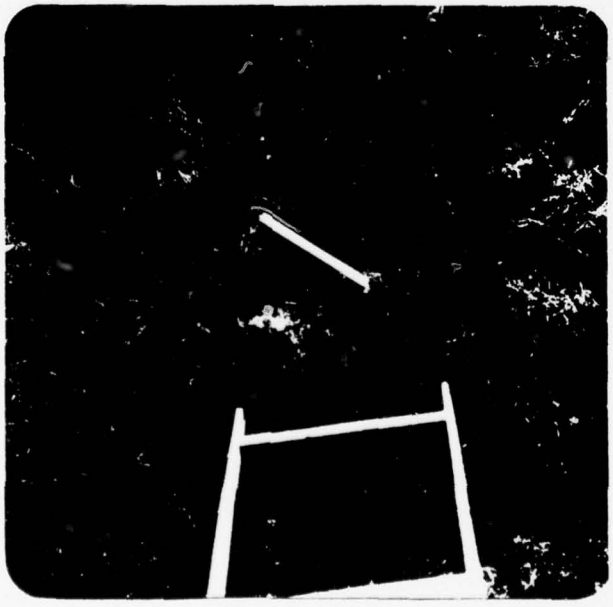

Figure 31 - Location of rod no. 17 (arrow) relative to adjacent shrinkage cracks. Scale is 0.3 meters long. The scale is aligned in a N6W direction (towards the rod).

rods was monitored at the same times as those at the Radio Facility site. Rods no. 8, 10, 20, and 40 were placed in shrinkage cracks, whereas rods no. 1, 9, 15 and 16 were placed within polygons bounded by cracks on all sides. Unfortunately, the initial location of shrinkage cracks relative to the rods was not recorded, so that it is difficult to interpret the data for the first wetting cycle. During the drying and second wetting cycles the tilt directions were highly irregular and followed no pattern in relation to adjacent cracks or the creep process. The tilt data for the rods is given in Appendix A.

Seven steel rods were installed on the upslope side of test pit no. 8, about 1.0 m. from the edge of the trench. The tilt of these rods was measured when they were installed (Oct. 4, 1975) and on Dec. 6, 1975, and Jan. 17, 1976. Six of these rods were tilted upslope by small amounts, suggesting that the soil below the surface was moving towards the trench at greater rates than that at and near the surface. The remaining rod was tilted slightly toward the trench. The tilt data for these rods is given in Appendix A.

These rather numerous data tell us nothing about creep of the soil, apparently, but they do demonstrate that most displacements can be understood in terms of locations and orientations of local shrinkage cracks. Fleming (1971) first attempted to determine magnitudes of creep displacements by comparing shapes of boreholes during a wet season with the shapes of the same boreholes during the previous and subsequent dry seasons. The results were most discouraging because the directions of movement appeared to be random. Then, however, he determined magnitudes of net creep displacements by comparing shapes of boreholes during a wet season and a subsequent wet season. The magnitudes and directions of displacement were remarkably consistent for most of the boreholes. The data reported here are similar to the first data analyzed by Fleming. We are measuring relative displacements between a net season of abnormally low rainfall with a subsequent dry season. We cannot expect the measurements to provide estimates of net displacements due to creep. However, this study, more clearly than Fleming's, indicates that the directions of displacement of markers between a wet season and a previous or a subsequent dry season are controlled almost exclusively by positions and orientations of shrinkage cracks. Fleming believed that this was true, but he did not record the positions of shrinkage cracks as carefully as we have in this study.

DISCUSSION OF FIELD OBSERVATIONS

The black silty clay soil changes significantly throughout the year. Following the wet cycle the soil begins to dry. Although there is no trace of pre-existing shrinkage cracks at the ground surface, the cracks may or may not have closed at depth. During the dry cycle the water content of the soil decreases from about 35% to less than 10% at the ground surface, and from about 25% to about 15% near the base of the soil. The soil undergoes vertical and horizontal shrinkage. Large shrinkage cracks extend through the soil profile and appear at the surface. The soil at the ground surface and along the walls of shrinkage cracks breaks up into small polygonal aggregates which litter the surface and fall into the shrinkage cracks, at times filling them up. The direction of movement of a point on the ground surface depends on its position relative to the developing shrinkage cracks.

Upon wetting the soil expands vertically and horizontally. Water enters the soil indirectly by infiltration through the ground surface and directly through open shrinkage cracks. Downhill creep apparently begins shortly after the soil begins to wet. With time an increasing thickness of soil undergoes expansion and creep movements. Below a certain depth well developed shiny surfaces develop (Fleming, 1971, Fleming and Johnson, 1975). These surfaces may be planar, undulatory, or curved. Their size is maximal, about 0.6 meters wide near the base of the soil. They are smaller and more irregular at shallower depths. Associated with them are many smaller, curved surfaces which appear to be randomly oriented, and small, discontinuous linear ridges, also randomly oriented.

In following are qualitative explanations for some of the features associated with the soil.

Development and Recurrence of Shrinkage Cracks

The development and recurrence of large shrinkage cracks during the drought of 1975-77 is intimately related to the existence of large, open cracks below a certain depth in the soil profile. As the soils lost moisture, the cracks propagated to the surface (Fig. 32). The soil to a depth of about 10 cm. below the ground surface dessicates and breaks into small polygons (maximum dimensions of about 3.5 cm.) during dry spells of duration greater than about 5 days (Fig. 32-A), presumably because of rapid heating and moisture evaporation to this depth. In the same manner, the surface breaks up into small polygons during short dry spells throughout the winter months. If the dry spell persists evaporation continues to take place near the surface but at a lesser rate. Evaporation involves the diffusion of moisture to the zone of evaporation. As the drying front penetrates the soil the moisture gradient decreases and the rate of diffusion and evaporation decreases. Thus, the net loss of moisture from near surface soil becomes small. Because of the decrease

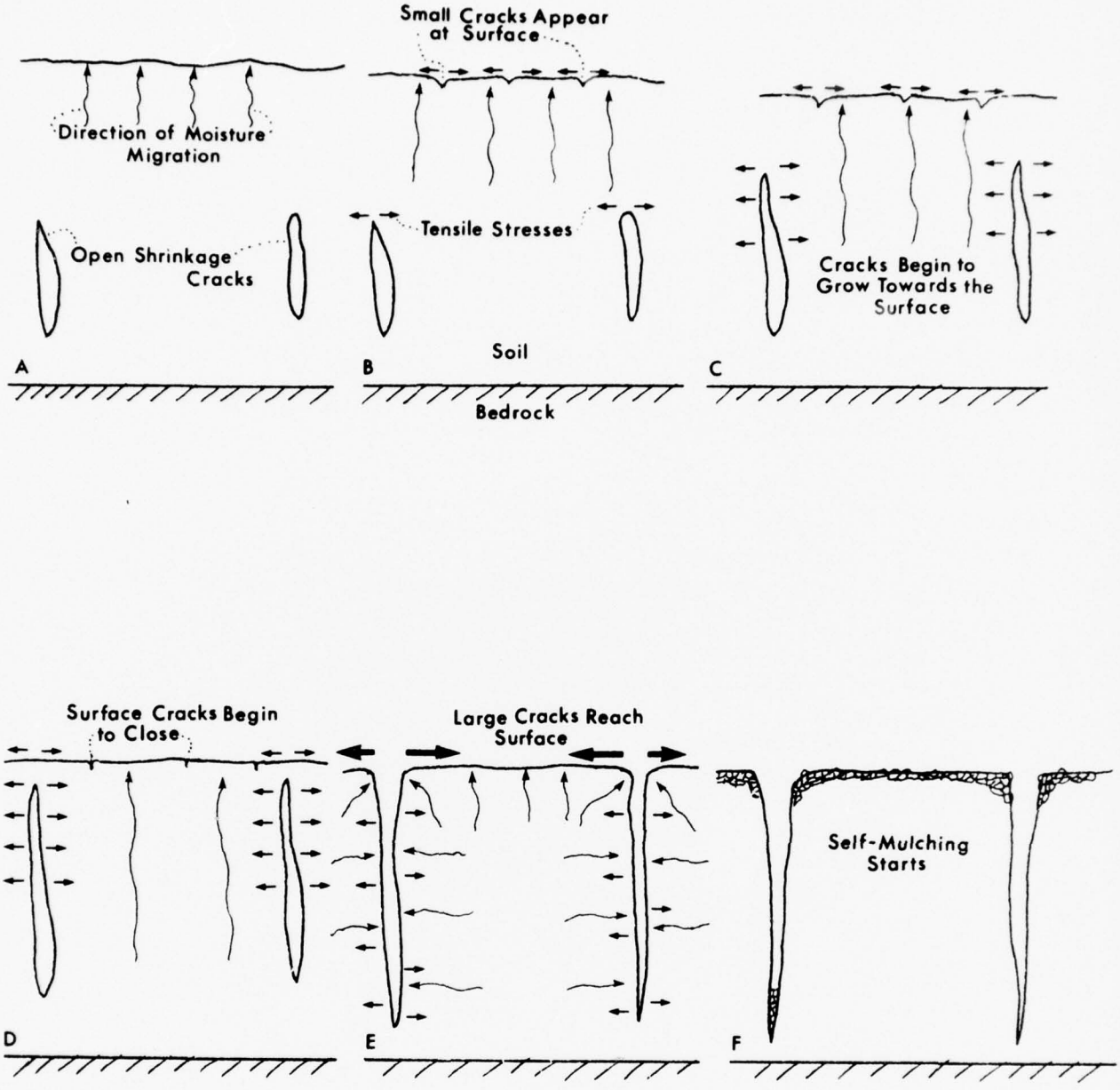

Figure 32. Schematic representation of the growth of shrinkage cracks during a dry season.

in water content the soil at depth begins to shrink. Vertical and horizontal shrinkage take place, the latter leading to the growth of the open shrinkage cracks toward the ground surface (Figs. 32C-D). The soil at depth is thus shrinking towards the center of a large block bounded by large subsoil shrinkage cracks. The small shrinkage prisms which developed at the ground surface initially are attached at their base to this larger subsoil prism. As the subsoil contracts the surface prisms are "carried" by the shrinking subsoil; the fine surface cracks eventually closing to accommodate this movement.

Eventually the large shrinkage cracks reach the ground surface at which time the moisture flow regime is altered (Fig. 32-E) as evaporation is now possible along the crack faces. Adams and Hanks (1964) have demonstrated that evaporation from shrinkage cracks in Houston Black Clay, another vertisol, may equal or exceed that occurring at the ground surface because there is a greater surface area exposed to the atmosphere along shrinkage cracks than at the ground surface. Their studies indicated that the evaporation from the side walls of shrinkage cracks varied between about 35-90% of that from a comparable area on the ground surface.

Shrinkage cracks form in response to tensile stresses which develop in a soil as a result of inhomogeneous dessication. The tensile stresses which develop and the tensile strength of most clay soils vary directionally and from place to place depending on the soil structure, which is defined by Mitchell (1976) to include the combined effects of composition, soil fabric or particle arrangement, and interparticle forces. The pattern of shrinkage cracks which develops is also affected by the rate of drying. Slow drying favors the development of few, widely spaced shrinkage cracks. With rapid dessication the soil will be broken by smaller, more numerous cracks.

It is not surprising that the large shrinkage cracks reappeared at or near the same location throughout the study period; they develop from essentially the same shrinkage cracks which did not close entirely during the wet cycles. At the study sites, most of the cracks observed reappeared at or near their original location (Figs. 15 and 16). Other factors have been credited with controlling the location of shrinkage cracks. Fox (1964) described the occurrence of shrinkage cracks in Australian vertisols where crops were planted in rows. Large cracks occur midway between the lines of plants whereas only small cracks develop across the lines. The root system appears to act as a skeleton holding the soil together. Fox considered that cracking began at the junction of the root systems and then the soil contracted towards the rows of plants. Other authors have observed how large shrinkage cracks are associated with some kind of disturbance at the ground surface, such as buried objects or areas subjected to artificial compaction by transient loading (Fleming 1971, 1976, Longworth and Tregenza, 1972, Yaalon and Kalmar, 1972).

With the exception of root systems all the factors listed above are probably important in determining the location of shrinkage cracks in the black silty clay. Undoubtedly, the fact that the shrinkage cracks remained open at some depth was the most important factor during the drought of the study period. It is likely that with sufficient precipiation the cracks will swell shut throughout the soil profile. Without open shrinkage cracks at depth, which act as zones of weakness and stress concentration along which

ranged between 5-10%. The computed values of density are shown in Table 6. With the exception of the low value for crack fill material there is no apparent pattern provided by the results. Fleming (1976) has reported that during the winter there is a marked dry density contrast between soil adjacent to or in former shrinkage cracks and soil near the interior of former shrinkage polygons. The soil has a lower density in or near the former cracks. His samples shrank when they were dried so the results reflect differences in structure in the soil. The results do not necessarily reflect true density contrasts. The values of unit weight shown in Table 6 are greater than

TABLE 6. UNIT WEIGHT OF SURFACE AND NEAR-SURFACE SAMPLES FROM THE RADIO FACILITY SITE

Within shrinkage block	1.72 to 1.82
On side of crack (5 cm. depth)	1.88
Crack fill material	1.53 to 1.74
Near edge of crack	1.77

those obtained by Fleming. Because of the slower rate of drying which takes place in the field there is more time for the rearrangement of particles in response to shrinkage stresses to take place. This leads to greater densities than the short-time drying which takes place in the laboratory.

Aggregate Formation and Self-Mulching Characteristics

We have described the tendency for the surface layer of black silty clay to shatter into small polygons which mantle or litter the surface and spill into the wide shrinkage cracks. Soil scientists have used the term self-mulching to describe soils which show this feature. The self-mulching character of the black silty clay has several important consequences. Self mulching involves a change in the macro-fabric of the soil. The soil breaks into individual polygonal aggregates of variable size which are separated from the body of the soil mass and from each other by fine dessication cracks. The surface layer of the soil is thus effectively broken into a granular mass of soil polygons which will play a significant role in establishing the rate of moisture infiltration when the soil is wetted. Soil polygons falling into shrinkage cracks produce mixing of the soil which is felt to be responsible for the uniformity of the black silty clay to depth. In addition, all dry surface material deposited at different depths within a crack effectively increase the bulk density at these depths while decreasing the average moisture content, both of which are important during the subsequent wetting and swelling cycle. Less understood is the effect on creep of the mixing of the soil aggregate with the unaggregated soil at depth. The macro-fabric of the soil in the polygons is certainly different from that of the soil as a whole,

ranged between 5-10%. The computed values of density are shown in Table 6. With the exception of the low value for crack fill material there is no apparent pattern provided by the results. Fleming (1976) has reported that during the winter there is a marked dry density contrast between soil adjacent to or in former shrinkage cracks and soil near the interior of former shrinkage polygons. The soil has a lower density in or near the former cracks. His samples shrank when they were dried so the results reflect differences in structure in the soil. The results do not necessarily reflect true density contrasts. The values of unit weight shown in Table 6 are greater than

TABLE 6. UNIT WEIGHT OF SURFACE AND NEAR-SURFACE SAMPLES FROM THE RADIO FACILITY SITE

Within shrinkage block	1.72 to 1.82
On side of crack (5 cm. depth)	1.88
Crack fill material	1.53 to 1.74
Near edge of crack	1.77

those obtained by Fleming. Because of the slower rate of drying which takes place in the field there is more time for the rearrangement of particles in response to shrinkage stresses to take place. This leads to greater densities than the short-time drying which takes place in the laboratory.

Aggregate Formation and Self-Mulching Characteristics

We have described the tendency for the surface layer of black silty clay to shatter into small polygons which mantle or litter the surface and spill into the wide shrinkage cracks. Soil scientists have used the term self-mulching to describe soils which show this feature. The self-mulching character of the black silty clay has several important consequences. Self mulching involves a change in the macro-fabric of the soil. The soil breaks into individual polygonal aggregates of variable size which are separated from the body of the soil mass and from each other by fine dessication cracks. The surface layer of the soil is thus effectively broken into a granular mass of soil polygons which will play a significant role in establishing the rate of moisture infiltration when the soil is wetted. Soil polygons falling into shrinkage cracks produce mixing of the soil which is felt to be responsible for the uniformity of the black silty clay to depth. In addition, all dry surface material deposited at different depths within a crack effectively increase the bulk density at these depths while decreasing the average moisture content, both of which are important during the subsequent wetting and swelling cycle. Less understood is the effect on creep of the mixing of the soil aggregate with the unaggregated soil at depth. The macro-fabric of the soil in the polygons is certainly different from that of the soil as a whole,

and unless the pressures and deformations associated with swelling produce a more homogeneous fabric the creep behavior of the crack fill material may be significantly different.

There is some question as to the exact cause of the formation of the self-mulching surfaces. Loveday (1972) has stated that it is a common observation that the self-mulching surface is not evident during the first drying cycle which follows a wet winter. Instead, large shrinkage cracks develop which break up the soil into large shrinkage blocks because of the homogeneous, slow drying which takes place at the ground surface before the large cracks open. The self-mulching surface develops during subsequent wetting and drying cycles, presumably because more rapid drying takes place. In the black silty clay such repeated wetting and drying cycles were absent, except for the formation of dew. Moistening by dew, however, extends to a depth of several millimeters and, in fact, does not greatly alter the water content of the soil. Field measurements by Yaalon and Kalmar (1972) support the notion that adsorption and desorption from dew has little effect on the volume change. Furthermore, there is no inherent reason for the dessication to proceed more rapidly during repeated wetting and drying cycles. Once the large shrinkage cracks open, however, more rapid drying of the surface soil is possible, because the migration of soil moisture from within the soil mass to evaporation surfaces can now occur towards crack walls.

A second possible source of the stresses responsible for the deformation of the self-mulching surface is the daily volume changes which occur due to thermal expansion and contraction of air trapped in the soil voids. Yaalon and Kalmar (1972) used a sensitive, continuous recording device to measure vertical movements associated with water content changes. Superimposed on the seasonal heave and contraction pattern they observed a daily cycle of movement having a maximum amplitude of 0.5 mm. The heaving, which started in the early morning and reached a peak at about noon, was attributed to the thermal expansion of soil air. Had dew formation or changes in the relative humidity of the air been responsible, the maximum heave would have occurred sometime during the night or early morning. The authors noted that the depth of the daily movements due to air expansion was possibly equivalent to the depth of the surface mulch. Non-uniform volume changes leading to the development of cracks could result from a non-uniform distribution of sealed, air-containing pores.

Swelling and the Wetting Front

With the onset of the rainy season the soil begins to take up moisture. The rate of infiltration, defined as the movement of water through the soil surface into the soil, is initially high and decreases with time. Data obtained by Fleming (1971), and partly supported by our own observations, suggest that water moves through the soil in the form of a wetting front which advances from the ground surface downwards. The large shrinkage cracks do not seem to play a very important role in the transmission of water to depth in the profile.

Some workers have observed how precipitation in excess of the surface infiltration capacity and water interception by plants will flow on the ground surface and enter the open crack systems. Water then flows along the base of the crack system and the soil wets from the bottom up (Berndt and Swartz, 1972; Loveday, 1972). It is possible that with rainfall of high enough intensity this would occur in the black silty clay; however, it has not been observed. Instead, Fleming (1971) reported how some of the water falling during the first winter rains was soaked up by the dry soil. Although Fleming observed raindrops falling into open shrinkage cracks and some small rivulets flowing into them, it appears that for the most part the large cracks swell shut at the surface and wetting of the soil proceeds by infiltration through the ground surface.

Water enters the soil under the influence of two potentials: the gravitational potential and the matrix, or capillary potential. The latter corresponds to the pressure head of normal hydraulic usage. For the initially dry soil it results from water adsorption forces at particle surfaces and the surface tension of the water. A third component, the osmotic or solute potential, becomes effective when continuous, interconnected water films develop on the particle surfaces.

The first winter rains fall on a soil surface in which two levels of pores exist: the relatively large macropores made up by the fine shrinkage cracks which separate the polygons of the self-mulched surface, and the capillary pores of the soil polygons themselves. The surface is more or less continuous as most of the large shrinkage cracks become filled up with small soil prisms. Water falling on this surface enters the macro-pores under the influence of gravity or is "sucked" into the surface capillary pores. Moisture entering via the macropores is distributed into the soil polygons by capillary pores on the walls of the cracks. Moisture is thus distributed throughout the surface layer relatively rapidly with the soil swelling and the shrinkage cracks closing at the ground surface. Swelling of this surface layer prevents water from entering directly into the large shrinkage cracks.

Under favorable conditions, such as during periods of normal or above normal precipitation, water does appear to accumulate and travel along the base of the crack system. It is not known, however, if this occurs at the ground surface from whence the water flows into the cracks, or if it results from the subsurface flow of water toward the cracks. Dispersion of clay particles along the walls of the cracks and their removal by flowing water results in an enlargement of the shrinkage cracks. Continued underground erosion in this way enlarges the cavities until the roof loses support and collapses. Figure 33 is a photograph of a collapsed roof near the gully which crosses the Radio Facility study site. Some of these cavities have a diameter of one meter or more. Nevertheless, they apparently occur only along drainage courses in the study sites.

Several processes decrease the initially high infiltration rate. Swelling of the surface soil destroys the network of fine shrinkage cracks (macro-pores) which enabled the rapid influx of water under the influence of gravity. A surface crust of decreased permeability may form due to the compacting action of raindrops or to the washing in of fine material into the pores. These fine

Figure 33 - View of collapsed roof due to subsurface piping. Scale is about 0.3 meters long.

particles are produced by slaking or dispersion of the surface aggregates. Once a surface crust is formed water may accumulate on the ground surface. Turbulence in this water may remove part of this skin seal (McIntyre, 1958) with some of the fine particles then being washed into the soil as the ponded water then infiltrates into the soil. Or suspended clay particles may be deposited on the surface when the ponded water evaporates, increasing the effectiveness of the skin seal.

The gradient tending to draw water into the soil is also reduced as water retention forces associated with surface adsorption, ion hydration, or double-layer formation are satisfied. The infiltration rate will decrease with time because of the continuously decreasing gradient under which water enters the soil. Much of the moisture which enters the soil is immobilized by these forces and is not free to percolate to depth. Additional moisture must be supplied from above for profile wetting to occur. Decreased infiltration rates have been measured in swelling soils in the field (Berndt and Swartz, 1972; Linsley, et al., 1975).

Displacement measurements by Fleming (1971) at different times of the wet cycle showed that with increasing time an increasing thickness of soil was creeping. This was correlated to measured water content changes as the wetting front advanced deeper into the soil. Our recent observations suggest that the wetting front is an irregular surface, the water content of the soil increasing

to greater depths at any given time along the filled up cracks. Because of the presence of macro-pores to greater depths along the filled cracks, percolation under the influence of gravity is possible and moisture migrates to greater depths. Fabric variations in the soil within shrinkage blocks also appears to affect the depth of wetting at any given time. In addition, water contents measured from specimens sampled at the Radio Facility site were greater for samples taken from the crack fill material than for samples obtained at similar depths within the shrinkage blocks. These relations are illustrated by the data in Table 7. In comparing the results, it should be

TABLE 7. WATER CONTENTS AT DIFFERENT DEPTHS AND LOCATIONS AT THE RADIO FACILITY SITE

Date	Location	Depth (cm)	Water Content (% Dry Wt.)
7 Feb. 1976	Within shrinkage block	0-4	22
	"	25	9
	"	0-4	23
	"	8-9	10
	Within shrinkage block 25 cm from crack "A"	2-4	8
	"	4-9	9
	Crack fill material (crack open to depth of 13 cm)	13-16	23
		32	8
	Crack fill material (crack "A")	0-3	25
	"	3-7	22
	"	7-13	14
	"	18	9
3 March 1976			
	Center of shrinkage block	4-6	23
	"	14-16	27
	"	29-33	25
	"	38	25
	"	40-42	22
	"	46-48	22
	"	55-57	21
	"	62-64	16
	Crack fill material	2-6	29
	"	20-21	28
	"	35	26
	"	41	22
	"	43-45	15
	"	0-4	29
	"	20	32
	"	40	32

remembered that the water content of the crack-fill material was initially between 5-10%, corresponding to air dried soil. It is also apparent from this data that water percolating through the crack fill material does not necessarily wet the walls of the large cracks to any great horizontal distance.

Wetting of the black silty clay is accompanied by vertical and horizontal swelling. Associated with the swelling of the soil is the formation of the shiny surfaces described by Fleming (1971). It is believed that these features form as a result of the infilling of the shrinkage cracks with soil. Because of the increased amount of material which results at depth, large horizontal swelling pressures will develop. If these pressures become great relative to the overburden load the soil may fail in passive compression producing the aforementioned slickensided surfaces. Once developed, these planar features may serve as conduits for the distribution of water as reported by Berndt and Swartz (1972).

THEORY OF RATE PROCESSES

The theory of rate processes has been applied by a number of researchers to the study and interpretation of the creep behavior of soils. As soil deformation (creep) involves a time-dependent rearrangement of matter (a rate process), it is amenable to study through the application of the theory of absolute reaction rates described in detail by Glasstone, et al. (1941). This theory, which is based on statistical mechanics and thermodynamics, has been used for the study of viscosity, plasticity, diffusion, friction, and lubrication (Eyring, 1936, Glasstone, et al., 1941, Eyring and Powell, 1944, Ree and Eyring, 1958). Although there is no rigorous proof of the validity of the detailed statistical mechanics formulations of the rate process theory, the theory has been successfully applied to the study of the deformation of metals (Kauzmann, 1941, Finnier and Heller, 1959), plastics and rubbers (Ree and Eyring, 1958), ceramics (Gibbs and Eyring, 1949), as well as to other materials. In soil mechanics a number of workers have used the theory or aspects of it. These include the work of Murayama and Shibata (1958, 1961) on the rheological characteristics of clay. This appears to have been the first application of the theory to aspects of soil behavior, although the concept of an activation energy needed to overcome an energy barrier which is the basic premise of rate process theory was being discussed at about the same time by Low (1959) and Mitchell (1960) in connection with the viscosity of water adsorbed on clay and the recovery of the thixotropic strength of soils. Other adaptations of the theory include the works of Christensen and Wu (1964) and of Andersland and Douglas (1970) on clay deformation, that of Wu, et al. (1966) on consolidation, and the application of the theory by Abdel-Hady and Herrin (1966) to soil-asphalt, by Andersland and Akili (1967) to frozen clay soils, and by Kojan (1967) to continuous soil creep.

The most extensive application of the theory to soil behavior phenomena has been performed by J. K. Mitchell and co-workers at the University of California at Berkeley (Mitchell, 1964, 1976, Mitchell, et al., 1968, 1969). These authors have developed a microanalytical theory of soil behavior through the application of rate process principles to creep behavior which allows the description of observed creep phenomena in terms of established physical laws. This is in contrast to the classical macroanalytical approach of describing soil phenomena which relies heavily on empirical formulations. The application of rate process theory to soil deformation studies may be questioned; however, as Mitchell, et al. (1969) point out, "it has been shown that soils behave in general conformity with the theory, provided due account is taken of soil structure variations during deformation. Perhaps the best justification for the approach used is that a consistent framework for the interpretation of soil behavior in terms of microscale phenomena has emerged that can stand independently of the validity of rate process theory."

In analyzing the flow of a liquid Eyring (1936) and Glasstone, et al. (1941) considered that the motion of one layer of the liquid past another involved the passage of a molecule from one equilibrium position in a layer to another such position in the same layer. In order for this to occur, energy must be expended to create a hole or site for the molecule to migrate into, as well as in breaking any bonds in which the molecule is involved and in moving the molecule. The jump of such molecules from one equilibrium position to an adjacent one can then be imagined as comprising the passage over a potential energy barrier, the molecules being constrained from movement relative to each other by virture of the energy barrier separating adjacent equilibrium positions. This is shown schematically by curve A in Fig. 34 which depicts the potential energy-displacement relation for a material at rest.

This concept of an energy barrier forms the basis of rate process theory. The atoms, molecules, or particles which participate in a time-dependent flow or deformation process are termed flow units. The energy that must be supplied in order for a flow unit to surmount the energy barrier (the flow unit is then said to be activated) is known as the free energy of activation, or the activation energy ΔF. The magnitude of the barrier gives a measure of the strength of the bonds holding the flow units in place. The energy which allows a flow unit to become activated is derived from the thermal energy of the material and from various applied potentials. Deformation proceeds at a rate which is dependent on the frequency with which the flow units acquire enough energy to surmount the energy barriers.

From statistical mechanics it is known that in a material at rest thermal vibrations occur with a frequency given by kT/h, and that the probability of any flow unit becoming activated, or the proportion of flow units activated during any vibration is given by $\exp\left(-\frac{\Delta F/N}{kT}\right)$. Here, k is Boltzmann's constant, T is the absolute temperature, h is Planck's constant, and N is Avogadros number. The frequency of activation k' is then given by the product of these two quantities, or:

$$k' = \frac{kT}{h} \exp\left(-\frac{\Delta F}{NkT}\right)$$

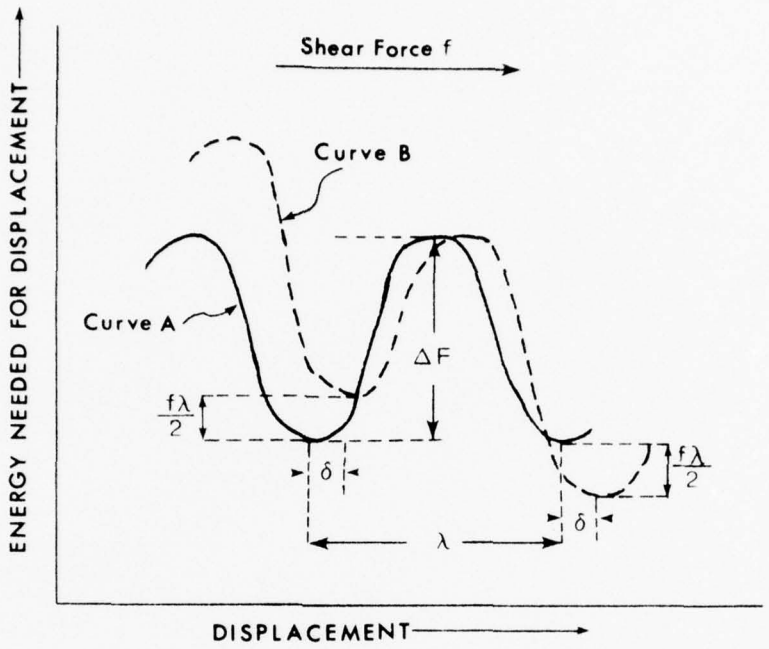

Figure 34. Change in the shape of the energy barrier by a shear force (after Mitchell, 1976).

In an equilibrium situation, i.e., in the absence of directional potentials, it is reasonable to assume that the potential energy barrier is symmetrical, as shown by curve A, Fig. 34. Hence, flow units will cross barriers with equal frequency in all directions and the system will remain unchanged.

However, if a directional potential such as a shear stress is applied to the material, the potential energy curve will be distorted as shown by curve B, Fig. 34 due to the superposition of a linear potential field and to an elastic distortion of the material. The applied stress changes the height of the energy minima, or wells, and causes an elastic distortion in which the energy wells are shifted in such a way that the distance over which the applied force must act in moving a flow unit to the activated state is smaller in the direction of the applied potential than in the reverse direction. For the moment the effect of this elastic distortion will be neglected and it will be assumed that the displacement of the energy wells is symmetrical. This is not an unreasonable assumption in view of the fact that elastic deformations can be expected to be a small percentage of the total deformation. The net result of the distortion of the potential energy curve is that the activation frequency in the direction of the applied potential will be increased whereas that in the opposite direction will be decreased.

Let $\underline{f}$ represent the force acting on a flow unit due to the applied stress and λ be equal to the distance between successive equilibrium positions (curve B, Fig. 34). Then, the energy that the flow unit acquires in moving from an energy minima to the top of the potential energy barrier is given by $f\lambda/2$, where $\lambda/2$ is the distance between energy wells and energy maxima. The effect of the force is then to reduce the height of the energy barrier in the direction of the force by an amount equal to $f\lambda/2$, and the height in the opposite direction will be raised by the same amount (curve B). Curve B also shows the energy wells displaced by a distance δ from their initial positions. This represents the elastic distorition of the material structure.

Since the barrier height is reduced by $f\lambda/2$ when the force is acting, the activation frequency in the direction of the force is now increased to:

$$k_f' = \frac{kT}{h} \exp\left[-\frac{(\Delta F/N - f\lambda/2)}{kT}\right] \tag{10}$$

The barrier height increase in the opposite direction decreases the activation frequency in that direction to:

$$k_b' = \frac{kT}{h} \exp\left[-\frac{(\Delta F/N + f\lambda/2)}{kT}\right] \tag{11}$$

The net rate of activation in the direction of the force is then given by:

$$k_f' - k_b' = \frac{kT}{h}\left[\exp\left(-\frac{\Delta F/N - f\lambda/2}{kT}\right) - \exp\left(-\frac{\Delta F/N + f\lambda/2}{kT}\right)\right]$$

$$= \frac{kT}{h}\exp\left(-\frac{\Delta F}{NkT}\right)\left[\exp\left(\frac{f\lambda/2}{kT}\right) - \exp\left(-\frac{f\lambda/2}{kT}\right)\right]$$

$$k_f' - k_b' = 2\frac{kT}{h}\exp\left(-\frac{\Delta F}{RT}\right)\operatorname{senh}\left(\frac{f\lambda}{2kT}\right) \qquad (12)$$

where $\underline{R} = \underline{Nk}$, the universal gas constant.

This equation gives the net rate of activation of each flow unit in the direction of flow under the applied potential. An expression is now desireable which can be related to a quantity measurable with conventional soil testing apparatus. Because the derived expression, the activation frequency, is an inverse time function, a strain rate has been a logical choice. The net rate of deformation in the direction of force will be the net specific rate of activation of the flow unit multiplied by some factor which will depend on the unit strain which occurs each time a flow unit changes its equilibrium position.

Christensen and Wu (1964) and Andersland and Douglas (1970) arrived at an expression for the rate of shear strain of the type

$$\dot{\gamma} = \frac{\lambda}{\lambda_1}(k_f' - k_b') \qquad (13)$$

where λ_1 is the distance between flow units perpendicular to the direction in which the shear force acts. On the other hand, Mitchell and his co-workers utilize a dimensionless parameter, $\underline{x}$, which is defined as being dependent on a unit strain (component of displacement which accompanies each jump to a new equilibrium position in a given direction expressed on a per-unit length basis) and on the proportion of flow units which actually cross the energy barrier after reaching the activated state. The latter consideration arises due to the possibility that some of the flow units may fall back to their original position after reaching the activated state. Glasstone, et al. (1941) included a transmission coefficient, $\underline{k}$, in the rate equation to account for this possibility. However, they noted that $\underline{k}$ would be close to unity in most cases. The parameter $\underline{x}$ may also be time and structure dependent.

According to Mitchell (1976) the strain rate can then be expressed as:

$$\dot{\varepsilon} = x(k_f' - k_b') \qquad (14)$$

hence

$$\dot{\varepsilon} = 2x \frac{kT}{h} \exp\left(- \frac{\Delta F}{RT} \right) \sinh\left(\frac{f\lambda}{2kT} \right) \tag{15}$$

This equation predicts two types of strain rate variation with force f, assuming λ to be constant. For the case where $\frac{f\lambda}{2kT} < 1$, then $\sinh\left(\frac{f\lambda}{2kT}\right) \simeq \frac{f\lambda}{2kT}$ and the strain rate equation can be written:

$$\dot{\varepsilon} = x \frac{f\lambda}{h} \exp\left(- \frac{\Delta F}{RT} \right) \tag{16}$$

For Newtonian flow and diffusion the transmission coefficient k is approximately unity. Then, the rate of flow (rate of change of shearing strain with time, $\dot{\gamma}$) can be expressed as

$$\frac{\tau}{\eta} = \dot{\gamma} = \frac{\lambda}{\lambda_1} \frac{f\lambda}{h} \exp\left(- \frac{\Delta F}{RT} \right) \tag{17}$$

where τ = shear stress, η = viscosity. Thus the flow rate is proportional to the force f. An expression for the viscosity derived from these solutions is identical to that derived by Eyring (1936) and Glasstone, et al. (1941).

When $\frac{f\lambda}{2kT} > 1$, $\sinh \frac{f\lambda}{2kT} \simeq \frac{1}{2} \exp\left(\frac{f\lambda}{2kT}\right)$ and the strain rate equation becomes

$$\dot{\varepsilon} = x \frac{kt}{h} \exp\left(- \frac{\Delta F}{RT} \right) \exp\left(\frac{f\lambda}{2kT} \right) \tag{18}$$

This approximation is more exact for values of $\frac{f\lambda}{2kT} > 2$. When $\frac{f\lambda}{2kT}$ lies between 1 and 2, the approximation results in values of the sinh term being 86 to 98 percent of the values obtained with the exponential substitution. It is for the range of stresses for which this approximation is justified that most of the existing data on creep of soils is given.

The term f represents the shear force acting on a flow unit. If it is assumed that the number of flow units and the number of bonds are equal, an expression can be derived for the number of bonds in a soil at a given water content or effective stress from creep test data. From these relationships the relation between the number of bonds and the strength of the soil can be established. This has been done by Mitchell, et al. (1969). The value of f will depend on the shear stress τ acting on the material and on the number of flow units (or bonds) per unit area, s:

$$f = \frac{\lambda}{s} \tag{19}$$

Under triaxial test conditions the maximum shear stress is given by $D/2$, where D is the deviator stress. Then,

$$f = \frac{D}{2s} \tag{20}$$

and equation (18) becomes

$$\dot{\varepsilon} = x \frac{kT}{h} \exp\left(-\frac{\Delta F}{RT}\right) \exp\left(\frac{D\lambda}{4skT}\right) \tag{21}$$

which can be solved to obtain a measure of s, the number of bonds per unit area.

APPLICATION OF RATE PROCESS THEORY TO SEASONAL SOIL CREEP

The rate process equations presented in the previous section describe processes occurring on a micro-scale within the soil which are manifested macroscopically as the observed continuous creep behavior of a large number of soils. It appears that these relations can also be applied to describe seasonal creep in the black silty clay, although this has not yet been verified experimentally. Nevertheless, a theoretical picture of how the theory may be applicable to seasonal creep is being developed and will eventually be tested in the lab. Because the theoretical model is not yet complete, only those details necessary to illustrate the applicability of rate process theory to seasonal creep will be discussed.

Any model purporting to describe seasonal creep of the black silty clay soil must account for several well documented features of the creep process:

1. The importance of wetting and swelling of the soil in initiating creep.
2. The reason why creep stops while the soil is at essentially the same water content as it was at the start of creep.
3. The peculiar convex upwards shape of the displacement profile.

The theoretical model assumes that at particle contacts effectively solid bonds develop. These bonds occur through the layers of adsorbed water which

are always present on soil particle surfaces under normal conditions of pressure and temperature. Mitchell (1976) pointed out that the surface layers of most soil minerals consist of oxygen atoms held together by silicon atoms and that the structure of the adsorbed water was not too different from that of the silicate layer in minerals so that a distinct boundary between the two phases may not be discernible. This ordering of the water phase near the surface of silicate minerals is supported by the experimental results of a number of workers, although the nature and extent of the ordering is still being debated (Rosenqvist, 1959, Martin, 1960).

Although more research is needed to establish its validity, the theoretical model envisions the existence of a more or less solid structure which includes interparticle water as forming the contact between soil particles. The degree of ordering in the water phase is known to decrease with distance from the soil particle surface. Hence, the number of effectively solid bonds can also be expected to decrease with increasing distance from the particle surface. This concept is shown schematically in Figure 35. Thus, swelling due to moisture intake is presumed to reduce the number of bonds effective between soil particles.

The activation energy measured for creep of a large number of soils is in the range of 25-45 kcal/mole. These values are comparable to those for the solid-state diffusion of oxygen in silicate minerals (Mitchell, 1976) and lends support to the notion expressed by Rosenqvist (1965, quoted in Mitchell, 1976) that creep in soils is the result of the slow diffusion of oxygen ions in and around interparticle contacts. This view is further strengthened by calculations of the volume of the flow units by Andersland and Douglas (1970) who obtained a volume of about 1.7Å^3, which is of the same order of magnitude as that of individual atoms.

Seasonal soil creep is envisioned as possibly occurring as shown in Fig. 36. Figure 36-A shows the soil at the end of the dry season. The water films surrounding particles are thin and highly structured allowing a large number of interparticle bonds to develop. Figure 36-B shows the situation after the soil has swollen. The number of interparticle bonds has been greatly reduced. For illite, the logarithm of the number of bonds has been shown to decrease linearly with increasing water content (Mitchell, et al., 1969). Diffusion of oxygen atoms begins to take place at a rate controlled by the rate process equation from zones of high to low pressure, as shown schematically in Fig. 36-B. As oxygen moves out of the high pressure zones the particles move closer together under the influence of gravity with a corresponding increase in the number of bonds as more ordered layers of water are brought into contact. This motion is reflected as the macroscopically measured creep. When the number of bonds between the approaching particles becomes large enough the excess pressures are reduced and diffusion and creep stop (Fig. 36-C). The soil is at essentially the same water content as it was when creep began.

The convex upwards shape of the displacement profile can be obtained from an equation in which the strain or the strain rate decreases as some negative exponential of depth. Equation 21 can be rewritten as

$$\dot{\varepsilon} = c \exp(-KS) \qquad (22)$$

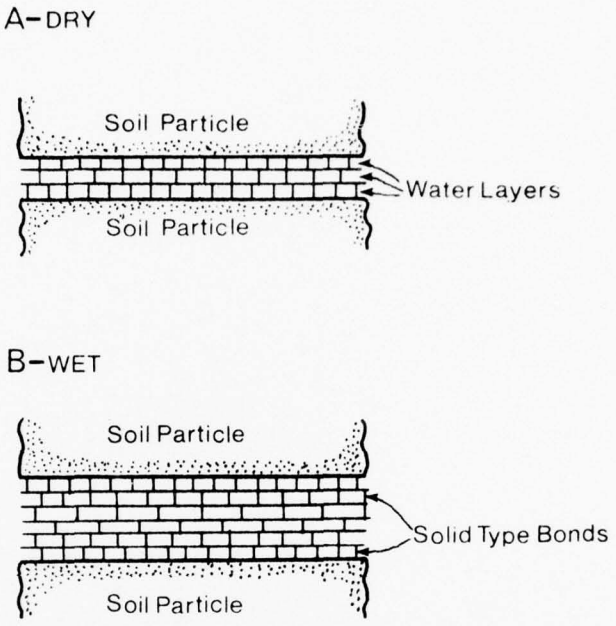

Figure 35. Schematic illustration of the decrease in the structure of adsorbed water and of the number of bonds with distance from the particle surface.

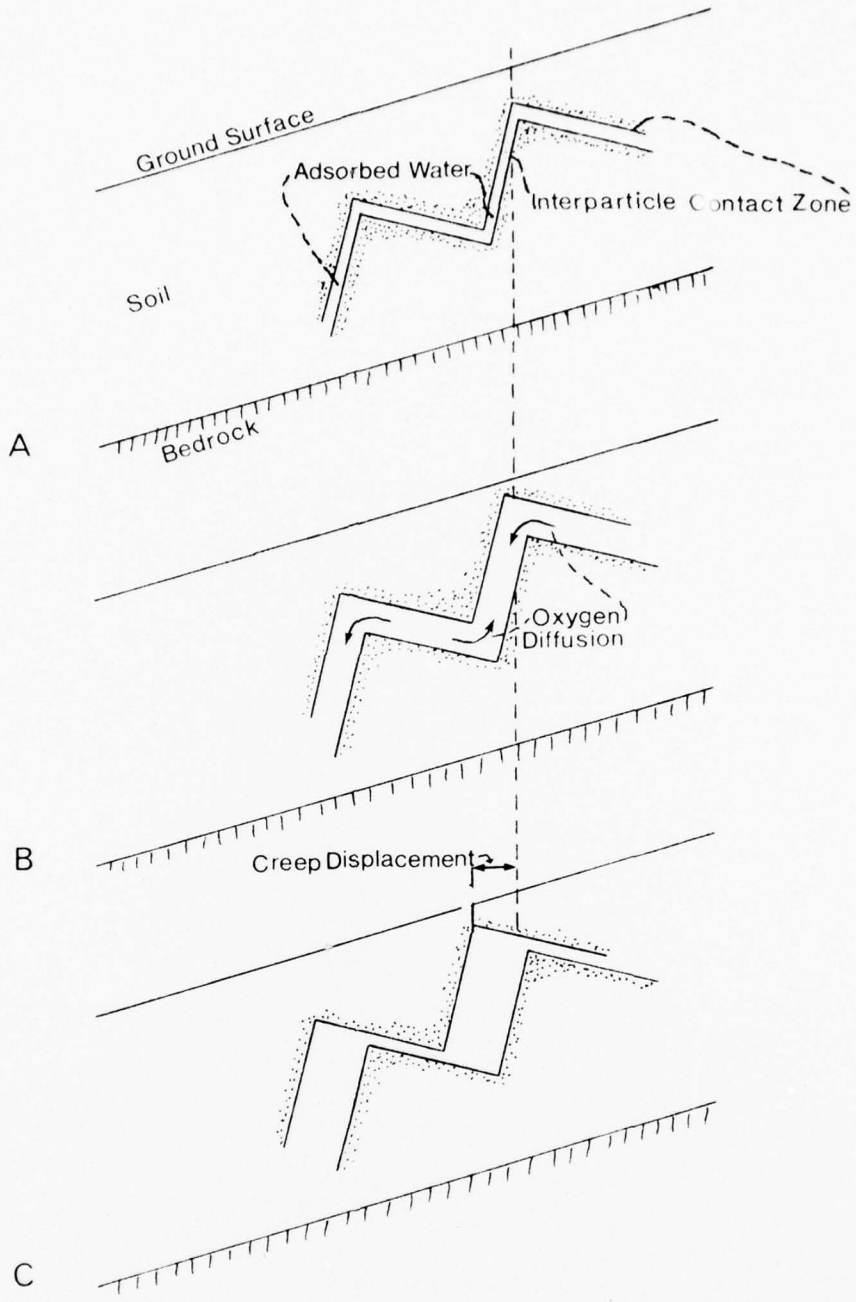

Figure 36. Schematic illustration of the theoretical model of creep of silty clay soil.

where

$$c = x \frac{kT}{h} \exp\left(-\frac{\Delta F}{RT}\right) \tag{23}$$

is assumed to be constant, and

$$K = \frac{4kT}{D\lambda} \tag{24}$$

is constant throughout the soil profile.

The number of bonds, s, increase with increasing depth due to the increasing overburden load. In addition, the water content change, and hence the change in the number of bonds, due to wetting and swelling of the soil decreases with depth. Thus, the term containing the number of bonds which appears as a negative exponential can be used to explain the shape of the displacement profile.

Rate process theory is thus seen to account for three peculiar aspects of seasonal creep in the black silty clay. It is interesting to note that in this theoretical model it is the swelling of the soil which acts as the "resetting" mechanism responsible for the recurrence of creep year after year and not the dessication process as has been previously assumed (Fleming and Johnson, 1975, Fleming, 1976).

CONCLUSIONS

The field observations made during the study period provide a greater knowledge of the properties of the black silty clay soil and how they change with the seasons. The amount of creep which occurred during the wet periods is unknown but appears to have been less than the average amount observed previously (Fleming and Johnson, 1975). This is explained by the fact that the soils did not become wet to depths greater than about 1.0 meter and that some dessication generally occurred following periods of precipitation. Measurement of the tilt of the steel rods, although ineffective in determining creep rates and the displacement profile, provided data on the shrink-swell behavior of the soil. Surface heave and shrinkage of about 3 cm. was measured for a soil thickness of about 1.0 meter.

Shrinkage cracks remained open below the depth of wetting. These cracks then grew towards the surface during the subsequent drying cycle. Infilling of the cracks by soil polygons falling from the ground surface and the edge of cracks was observed. The increase in the bulk volume of soil at depth due to this process is supposed to result in large lateral swelling pressures which lead to failure of the soil in passive compression and the production of shiny, slickensided surfaces.

Wetting of the soil occurs in the form of an advancing wetting front. The shape of the wetting front is irregular, the depth of wetting at any point being dependent on details of the soil micro- and macro-fabric.

Migrating gullies tend to destroy the creep masses thus reducing the effectiveness of creep as a geomorphic agent. Growth of the creep masses is supposed to involve the incorporation of material from below and adjacent to the creep soil into the creep mass. The vertical growth of the creep mass is supported by the formation of bedrock valleys and other observations. The lateral growth of the creep masses is inferred by the gradational contacts which occur between the black silty clay and adjacent soil masses. Gully migration rates exceed those of soil formation, so that once a gully develops on the creep soil, the creep mass is doomed.

A theoretical model to explain seasonal soil creep which makes use of rate process theory is being developed. The model accounts for features of the seasonal creep behavior of the black silty clay which have been observed and measured in the field. One aspect of the theoretical model which is of immediate interest is that the swelling process is seen as the "resetting" mechanism responsible for the recurrence of creep year after year.

REFERENCES ON SOIL CREEP

Abdel-Hady, M. and Herrin, M. (1966); Characteristics of Soil-Asphalt as a Rate Process: Jour. Highway Div., ASCE, v. 94, no. HW-1, p. 49-69.

Adams, J. E. and Hanks, R. J. (1964); Evaporation from Soil Shrinkage Cracks: Proc. Soil Sci. Soc. Am., v. 28, p. 281-84.

Andersland, D. B. and Akili, W. (1967); Stress Effect on Creep Rates of a Frozen Clay Soil: Geotechnique, v. 17, no. 1, p. 27-39.

Andersland, D. B. and Douglas, A. G. (1970-a); Discussion: Bonding, Effective Stresses and Strength of Soils: Jour. Soil Mech. Found. Div., ASCE, v. 96, no. SM-3, p. 1073-4.

_____ (1970-b); Soil Deformation Rates and Activation Energies: Geotechnique, v. 20, no. 1, p. 1-16.

Barden, L. (1972); The Influence of Structure on Deformation and Failure in Clay Soil: Geotechnique, v. 22, no. 1, p. 159-63.

Barr, D. J. and Swanston, D. N. (1970); Measurement of Creep in a Shallow, Slide-prone Till Soil: Am. Jour. Sci., v. 269, p. 467-80.

Berndt, R. D. and Swartz, G. L. (1973); Surface Hydrology: Symp. on Physical Aspects of Swelling Clay Soils, Armindale, Australia, 1972; Univ. New England, Armindale, p. 125-38.

Bishop, A. W. and Lovenbury, H. T. (1969); Creep Characteristics of Two Undisturbed Clays: Internat. Conference Soil Mech. Found. Eng., 7, Mexico City, Proceedings, v. 1, p. 29-37.

Briggs, H. S. (1973); The Erosion Process of Swelling Clay Soils: Symp. Physical Aspects of Swelling Clay Soils; Armindale, Australia, 1972; Univ. New England, Armindale, p. 149-60.

Buol, S. W. Hale, F. D., and McCracken, R. J. (1973); Soil Genesis and Classification: The Iowa State Univ. Press, Ames, 360 p.

Campanella, R. G. and Vaid, Y. P. (1974); Triaxial and Plane Strain Creep Rupture of an Undisturbed Clay: Canad. Geotech. J., v. 11, no. 1.

Carson, M. A. and Kirkby, M. J. (1972); Hillslope Form and Process: Cambridge Univ. Press, p. 272-300.

Casagrande, A. and Wilson, S. (1951); Effect of Rate of Loading on Strength of Clays and Shales at Constant Water Content: Geotechnique, v. 2, no. 3, p. 251-63.

Christensen, R. W. and Wu, T. H. (1964); Analysis of Clay Deformation as a Rate Process: J. Soil Mech. Found. Div., ASCE, v. 90, no. SM-6, p. 125-57.

Culling, W.E.H. (1963); Soil Creep and the Development of Hillside Slopes: Jour. Geol., v. 71, no. 2, p. 127-62.

Davis, W. M. (1892); The Convex Profile of Bad-land Divides: Science, 2d. Sec., v. 20, p. 245.

Davison, C. (1899); On the Creeping of the Soil Cap Through the Action of Frost: Geol. Mag., v. 6, p. 255.

Denisov, N. J. and Retlov, B. F. (1957); Elastic and Structural Deformations of Clayey Soils: Internat. Conf. Soil Mech. Found. Eng., 4, London, Proc., v. 1, p. 17-21.

Environmental Data Service (1974, 1975, 1976); Climatological Data: California: NOAA.

Everett, K. R. (1963); Slope Movement, Neotoma Valley, Southern Ohio: The Ohio State Univ., Institute of Polar Studies, Report No. 6.

Eyring, H. (1936); Viscosity, Diffusion, and Plasticity as Examples of Absolute Reaction Rates: Jour. Chem. Phys., v. 4, p. 283-91.

Eyring, H. and Powell, R. (1944); Rheological Properties of Simple and Colloidal Systems: Alexanders Colloid Chem., v. 5, p. 236-52.

Finnie, I. and Heller, W. R. (1959); Creep of Engineering Materials: McGraw-Hill, N.Y., 341 p.

Fleming, R. W. (1971); Soil Creep in the Vicinity of Stanford University: Ph.D. Thesis, Stanford Univ., 148 p.

_____ (1973); Instrument for Measuring Seasonal Soil Creep: Assoc. Eng. Geol. Bull., v. 10, no. 2, p. 83-93.

_____ (1976); Seasonal Soil Creep: Final Report: U.S. Army Research Office, N.C., Grant No. DA-HC-04-74-G0156, 31 p.

Fleming, R. W. and Johnson, A. M. (1975); Rates of Seasonal Creep of Silty Clay Soil: Q. Jour. Eng. Geol., v. 8, p. 1-29.

Fox, W. E. (1964); Cracking Characteristics and Field Capacity in Swelling Soil: Soil Sci., v. 98, p. 413.

Gibbs, P. and Eyring, H. (1949); A theory for Creep of Ceramic Bodies Under Constant Coad: Canad. J. Sci., v. 27, Sec. B, p. 374-86.

Gilbert, G. K. (1909); The Convexity of Hillslopes: J. Geol., v. 17, p. 344-50.

Glasstone, S., Laidler, K. J., and Eyring, H. (1941); The Theory of Rate Processes, McGraw-Hill Book Co., Inc., N.Y., 611 p.

Goldstein, M., Lapidus, L. and Misumsky, V. (1965); Rheological Investigation of Clays and Slope Stability: Internat. Conf. Soil Mech. Found. Eng., 6, Proc., v. 2, p. 482-5.

Goldstein, M. N. and Ter-Stepanian, G. (1957); The Long-Term Strength of Clays and Depth Creep of Slopes: Internat. Conf. Soil Mech. Found. Eng., 4, London, Proc., v. 2, p. 311-4.

Haefeli, R. (1953); Creep Problems in Soils, Snow, and Ice: Internat. Conf. Soil Mech. Found. Eng., 3, Zurich, Proc., v. 3, p. 238-51.

Hirst, T. J. and Mitchell, J. K (1968); Compositional and Environmental Influences on the Stress-Strain-Time Behavior of Soils: Rept. No. TE68-4, U. Cal.-Berkeley, Dept. Civ. Eng., Inst. Transp. Traffic Eng.; 242p.

Hoelzer, T. L., Hoeg, K., and Arulandan, K.(1973); Excess Pore Pressures During Undrained Clay Creep: Canad. Geotech. J., v. 10, no. 1, p. 12-24.

Kauzmann, W. (1941); Flow of Solid Metals from the Standpoint of the Chemical-Rate Theory: Trans. Am. Inst. Min. Metal. Engs., v. 143, p. 57-83.

Kerr, J. (1881); On the Action of Frost in the Arrangement of Superficial Earthly Material: Am. J. Sci., 3rd ser., v. 21, p. 345-58.

Kilinc, I. A. (1969); Report on Identification of Clay-Sized Particles from Rock and Soil Samples of Eagle Crest Town Houses Site, Sharon Heights: Unpub. Rpt., School of Earth Sci., Stanford Univ.; 11p.

Kirkby, M. J. (1967); Measurement and Theory of Soil Creep: J. Geol., v. 75, p. 359-78.

Kojan, E. (1965); Analytical Approach to Natural Soil Creep: Geol. Soc. Am. Spec. Paper 82; p. 335.

_____ (1967); Mechanics and Rates of Natural Soil Creep: 5th Annual Eng. Geol. Soils Eng. Symp., Pocatello, Idaho, Proc.; Idaho Dept. Hwys., Boise, Idaho; p. 233-53.

Komamura, F. and Huang, R. J. (1974); New Rheological Model for Soil Behavior: J. Geotech. Div., ASCE, v. 100, No. GT-7, p. 807-24.

Lafeber, D. (1966); Soil Structural Concepts: Eng. Geol., v. 1, p. 261-90.

Lambe, W. T. (1960); The Character and Identification of Expansive Soils: A Tech. Studies Rpt., Fed. Housing Adm., Pub. No. 701, Wash., D.C.; 51p.

Leopold, L. B., Wolman, M. G., and Miller, J. P. (1964); Fluvial Processes in Geomorphology: W. H. Freeman and Co., San Francisco; 522p.

Linsley, R. K., Kohler, M. A., and Paulhus, J.L.H. (1975); Hydrology for Engineers: McGraw-Hill Book Co., N.Y., 2 ed.; 482 p.

Longworth, L. D. and Tregenza, G. A. (1973); A Method for the Quantitative Description of Soil Cracking Patterns: Symp. Physical Aspects of Swelling Clay Soils; Armidale, Australia, 1972; Univ. New England, Armidale, p. 187-89.

Loveday, J. (1973); Field Aspects of Swelling and Shrinking: Symp. Physical Aspects of Swelling Clay Soils; Armidale, Australia, 1972; Univ. New England, Armidale, p. 45-52.

Low, P. F. (1959); Discussion: Physico-Chemical Properties of Soils: Ion Exchange Phenomena: J. Soil Mech. Found. Div., ASCE, v. 85, no. SM-2, p. 79-89.

Martin, R. T. (1960); Adsorbed Water on Clay: A Review: Clays and Clay Mins., v. 9, p. 28-70.

McIntyre, D. S. (1958); Soil Splash and the Formation of Surface Crusts by Raindrop Impact: Soil Sci., v. 85, p. 261-6.

Mitchell, J. K. (1960); Fundamental Aspects of Thixotropy in Soils: J. Soil Mech. Found. Div., ASCE, v. 86, no. SM-3, p. 19-52.

_____ (1964); Shearing Resistance of Soil as a Rate Process: J. Soil Mech. Found. Div., ASCE, v. 90, no. SM-1, p. 29-61.

_____ (1976); Fundamentals of Soil Behavior; John Wiley and Sons, Inc., N.Y.; 422 p.

Mitchell, J. K., Campanella, R. G., and Singh, A. (1968); Soil Creep as a Rate Process; J. Soil Mech. Found. Div., ASCE, v. 94, no. SM-1, p. 231-53.

Mitchell, J. K. and McConnell, J. R. (1965); Some Characteristics of the Elastic and Plastic Deformation of Clay on Initial Loading: Internat. Conf. Soil Mech. Found. Eng., 6, Montreal, Quebec, Proc., v. 1, Toronto Univ. Press, p. 313-17.

Mitchell, J. K., Singh, A., and Campanella, R. G. (1969); Bonding, Effective Stresses and Strength of Soils: J. Soil Mech. Found. Eng., ASCE, v. 95, no. SM-5, p. 1219-45.

Murayama, S. and Shibata, T. (1958); On the Rheological Characteristic of Clay: Part 1, Bull. No. 26, Disaster Prevention Research Inst., Kyoto Univ., Japan, 43p.

_____ (1961); Rheological Properties of Clays: Internat. Conf. Soil Mech. Found. Eng., 5, Paris, Proc., v. 1, p. 269-73.

Owens, I. F. (1969); Causes and Rates of Soil Creep in the Chilton Valley, Cass, New Zealand: Artic and Alpine Res., v. 1, p. 213-20.

Parizek, E. J. and Woodruff, J. F. (1956-a); Apparent Absence of Soil Creep in the East Georgia Piedmont: Geol. Soc. Am. Bull., v. 67, no. 8, p. 111-15.

_____ (1956-b); Tree Curvature Related to Slow Mass Wastage: Geol. Soc. Am. Bull., v. 67, no. 12, pt. 2, p. 1756.

Rantz, S. E. (1971); Isohyetal Map of San Francisco Bay Region, California, Showing Mean Annual Precipitation: in Mean Annual Precipitation and Precipitation Depth-Duration-Frequency Data for the San Francisco Bay Region, California; S.F. Bay Region Env. Resources Planning Study, Basic Data Contribution 32; U.S.G.S. Open File Rept. 30192-12; scale 1:125,000.

Rapp, A. (1960); Recent Developments of Mountain Slopes in Karkevagge and Surroundings, Northern Scandinavia: Geografisca Annaler, v. 42, no. 2-3.

Ree, T. and Eyring, H. (1958); The Relaxation Theory of Transport Phenomena: in Eirich, F. R., ed., Rheology, v. 2, Chpt. 3; Academic Press Inc., N.Y., p. 83-144.

Rosenqvist, I. Th. (1959); Physico-Chemical Properties of Soils: Soil-Water Systems: J. Soil Mech. Found. Eng., ASCE, v. 85, no. SM-2, p. 31-53.

Saito, M. and Uezawa, H. (1961); Failure of Soil Due to Creep: Internat. Conf. Soil Mech. Found. Eng., 5, Proc., v. 1, p. 315-8.

Sharpe, C.F.S. (1938); Landslides and Related Phenomena; Columbia Univ. Press, N.Y., 137p.

Sharpe, C.F.S., and Dosch, E. F. (1942); Relation of Soil Creep to Earth Flow in the Appalachian Plateaus: Jour. Geomorph., v. 5, p. 312-24.

Sherif, M. A. (1966); Deformation and Flow Properties of Clay Soils from the Viewpoint of Modern Material Science: Physical and Physico-Chemical Properties of Soil, Processed Soil, and Rock; Highway Research Record No. 119; Highway Research Board; p. 24-49.

Shibata, T. and Karube, D. (1969); Creep Rate and Creep Strength of Clays, Internat. Conf. Soil Mech. Found. Div., 7, Mexico City, Proc., v. 2, p. 361-7.

Singh, A., Cousineau, R. P. and Lockwood, R. (1971); Creep Movements of an Urbanized Hillside: Assoc. Eng. Geols. Bull., v. 8, no. 2, p. 103-20.

Singh, A., and Mitchell, J. K. (1968); General Stress-Strain-Time Function for Soils: J. Soil Mech. Found. Div., ASCE, v. 94, no. SM-1, p. 21-46.

_____ (1969); Creep Potential and Creep Rupture of Soils: Internat. Conf. Soil Mech. Found Eng., 7, Proc., v. 1, p. 379-84.

Taylor, A. W. (1959); Physico-Chemical Properties of Soils: Ion Exchange Phenomena: J. Soil Mech. Found. Div., ASCE, v. 85, no. SM-2, p. 19-30.

Ter-Stepanian, G. (1965); In-situ Determination of the Rheological Characteristics of Soil on Slopes: Internat. Conf. Soil Mech. Found. Eng., 6, Proc., v. 2, p. 575-7.

_____ (1974); Depth Creep of Slopes: Bull. Internat. Assoc. Eng. Geol., no. 9, p. 97-102.

Terzaghi, C. (1929); The Mechanics of Shear Failures on Clay Slopes and the Creep of Retaining Walls: Public Roads, v. 10, no. 10, p. 177-92.

Terzaghi, K. (1950); Mechanism of Landslides: in Application of Geology to Engineering Practice, Geol. Soc. Am., Berkeley Vol., p. 83-123.

_____ (1953); Some Miscellaneous Notes on Creep: Internat. Conf. Soil Mech. Found. Eng., 3, Proc., v. 3, p. 205-6.

Trollope, D. H. and Chan, C. K. (1960); Soil Structure and the Step-Strain Phenomenon: J. Soil Mech. Found. Div., ASCE, v. 86, no. SM-2, p. 1-39.

Vyalov, S. S., Pekarskaya, N. K. and Maximyak, R. V. (1971); On the Failure Process in Clayey Soils: Asian Regional Conf. Soil Mech. Found. Eng., 4, Proc., v. 1; Asian Inst. Tech., Bangkok; p. 95-7.

Walker, L. K. (1969); Undrained Creep in a Sensitive Clay: Geotechnique, v. 19, no. 4, p. 515-29.

Washburn, A. L. (1967); Instrumental Observations of the Mesters Vig District, Northeast Greenland: Meddelelser om Gronland, v. 166, Nr. 4.

Wu, T. H., Resendiz, D., and Neukirchner, R. J. (1966); Analysis of Consolidation by Rate Process Theory: J. Soil Mech. Found. Div., ASCE, v. 92, no. SM-6, p. 229-48.

Yaalon, D. H. and Kalmar, D. (1972); Vertical Movement in an Undisturbed Soil: Continuous Measurement of Swelling and Shrinkage with a Sensitive Apparatus: Geoderma, v. 8, no. 4, p. 231-40.

Yong, R. N. and Warkentin, B. P. (1975); Soil Properties and Behavior: Elsevier Sci. Pub. Co., Amsterdam; 449p.

Young, A. (1972); Slopes: Oliver and Boyd, Edinburgh; p. 48-59.

AD-A051 968 STANFORD UNIV CA LAB FOR RATIONAL GEOMECHANICS F/G 8/13
SEASONAL CREEP OF SILTY CLAY SOIL AND THE FORMATION OF SMALL GU--ETC(U)
DEC 77 A E SOTO, R UPP, A M JOHNSON DAA629-75-C-0025

UNCLASSIFIED ARO-13336.1-GS NL

2 OF 2
AD
A051968

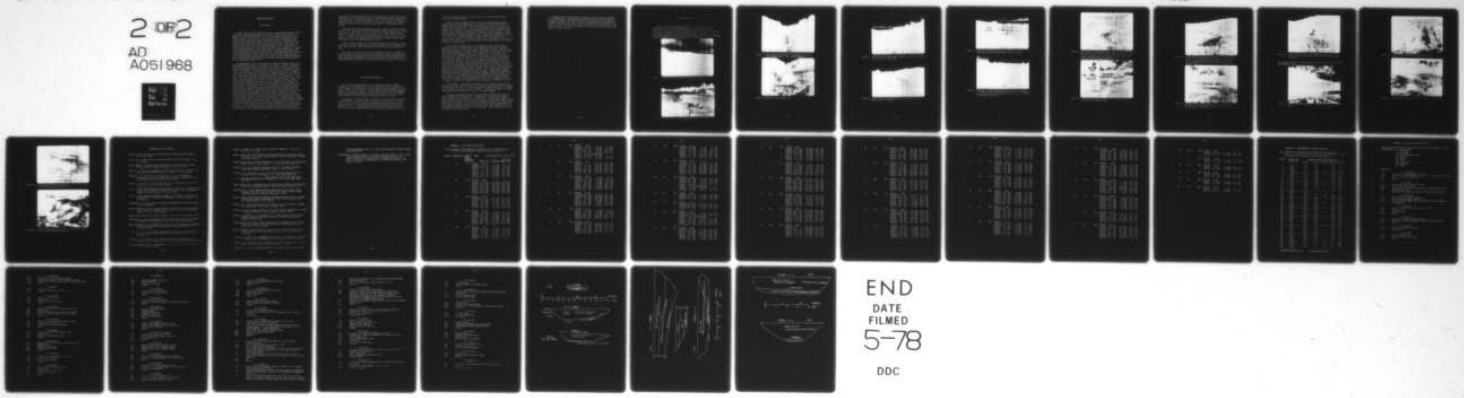

END
DATE
FILMED
5-78
DDC

EROSION OF GULLIES

INTRODUCTION

Gully erosion has long been recognized as an important process in geomorphology, engineering geology and agronomy. Dodge (1902) described a gully as a steep sided narrow gulch cut into previously filled gravel and adobe valleys in the arid west. Over the years other terms such as draw and arroyo have been used to describe similar features (Fenneman, 1922; Anteves, 1952; Leopold and Miller, 1956; Patton, 1973). In addition, gullies have been classed as either continuous or discontinuous (Leopold and Miller, 1956; Heede, 1974; and Schumm and Hadley, 1957). Those with an essentially uniform depth over long reaches and with a gradient of the channel bed almost parallel to the valley floor are continuous gullies. These gullies begin high up on the watershed divide with many small coalescing rills and continue to the main valley floor. Discontinuous gullies may start at any point along the valley slope with abrupt, nearly vertical headcuts. Their depths decrease rapidly down stream; and they have gradients less than that of the valley floor, such that the gullies intersect the valley floor and are terminated (Heede, 1974).

Although gullies form in all sectors of the United States, their most dense distribution occurs in the semi-arid southwest. Records indicate that the present gullies began to form there in the latter third of the 1800's (Bryan, 1925; Bailey, 1935; and Judson, 1952, 1952). It is generally agreed that the initiation of a period of gully erosion resulted from a change in climate, the destruction or modification of vegetative cover, or a combination of the two. Most early investigators (Dodge, 1902; Rich, 1911; and Leopold, 1921) have attributed the gully formation to the introduction of vast herds of livestock and the consequent decrease in vegetational cover. Bryan (1925, 1928) attributed gully initiation to a change to a dryer climate resulting in a depletion of vegetative cover. His views are supported by evidence which indicates that there have been several cycles of gully erosion prior to the introduction of livestock (Bryon, 1926; Bailey, 1935; and Judson, 1952). Other writers agree that past periods of erosion may have been caused by periods of drought (Antevs, 1941, 1942; Leopold, 1951; and Judson, 1952) or by irregular occurrences of heavy storms (Bailey, 1935; and Thornthwaite and others, 1942), but disagree that these are the causes of present erosion. Thornthwaite and others (1942) suggested that the erosion effects from the depletion of vegetative cover due to drought could be less than the erosion effects of decreased precipitation, and the proposed climatic change could actually produce less erosion. They also pointed out that changes in amount and timing of the winter rains and the intensity of summer rains could have varying effects on erosion without changing the total annual precipitation. Happ (1948) pointed out that gully erosion has become prominent throughout the United States since agricultural development and must have similar causes in all regions; either climatic change or decreased vegetative

cover with increased erosional runoff. He believed the latter theory more reasonable, as the vegetation in the more humid regions has not been severely depleted because of climatic changes. Antevs (1952) showed that primeval vegetation still remains or has recovered in areas protected from livestock, so that vegetative cover depletion was the result of overgrazing and not drought.

After studying rainfall records covering a period of almost 100 years, Leopold (1951) noted that although there were no significant trends in annual precipitation, the later half of the 1800's had a lesser number of small rains and a greater number of larger storms than did the first half of the 1900's. He pointed out that the decreased number of small rains would have adversely effected the vegetative cover, while the increased large storms would have led to both gully and sheet erosion.

Denevan (1967) weakened the overgrazing argument by pointing out that there were extremely large herds of cattle and sheep in the southwest in the late 1700's and early 1800's, and that during this time gully erosion was major.

The debate continues as to whether overgrazing or climatic change was the major cause of the initiation of current gully erosion. The three factors, overgrazing, drought, and increased frequency of high intensity storms, were probably all responsible to some extent, with one factor serving as triggering mechanism after the others had reduced the resistance to erosion.

GULLY FORMING PROCESSES

Very little has been written on the initiation of gully erosion. Dellenbach (1912) suggested that a gully forms when a master stream erodes its bed faster than a tributary. The tributary is then a hanging valley, and during the next runoff the water cascades over and undercuts this precipice, causing it to progress upstream. Rubey (1928), Keefer (1971) and Nicholson (1976) reported gullies which clearly were formed as the result of ground sinking and were probably caused by subsurface erosion or piping.

Thornthwaite and others (1942) described three ways of gully initiation in the Southwest: 1) whenever there is sufficient acceleration of runoff, denuded spots may form in vegetated drainageways and spread up and down the valley as a gully. 2) Where an intense storm is centered on an area with inadequate protection from vegetative cover rapid gully erosion results. This process is more common and far more rapid in arid areas than the first.

3) Finally, tributary gullies may be initiated by cutting into the side wall of an existing channel.

Schumm and Hadley (1959) theorized that the immediate cause of gully initiation is the oversteepening of the valley floor during alluviation. Sediment load from upstream erosion is deposited on a more level reach and forms a small alluvial fan. As the fan increases in size, its downstream gradient also increases. This increased gradient produces increased stream velocity until erosion is initiated, presumably by tractive forces. Following initiation, the gully may propagate both upstream and downstream. Patten and Schumm (1975) surveyed a number of gully systems and reported that there is a critical or threshold inclination beyond which entrainment of the alluvium should occur. In contrast, however, Piest and others (1975) collected evidence from a loess soil area indicating that tractive forces do not play a major role in gully erosion.

More interest has been shown in the process of gully growth than in gully initiation. Fenneman (1922) first suggested that in arid regions, sapping at the base of the scarp is the cause of gully growth. His view has been largely supported by later writers. Thornthwaite and others (1942) wrote that abrasion by water flowing over the headwall has a relatively minor affect on gully enlargement, and that the main cause is the caving of the upper walls as a result of undercutting. This caving is aided by formation of desiccation cracks and a blocky or columnar soil structure on the gully wall during dry periods. They further suggested that gully-head erosion is most effective when water that has soaked into the wall during a high stage seeps back out and carries many fine soil particles in suspension. The soil banks are thus weakened and caving could continue for hours or days after flow has ceased. Piest and others (1975) reported that similar wetting and drying cycles, and also creeping and thawing cycles, cause a decrease in shearing strength of the soil and leads to eventual collapse. Heede (1970) reported that during periods of gully flow, headcuts progressed mainly by undercutting at the face. But Leopold and Miller (1956) reported that undercutting and bank caving were not observed during high velocity flow, but were observed after the flow ceased. Schumm (1961) noticed that the propagation of a headcut seems to require some resistant material capping the erodable alluvium.

Parker (1964), Jones (1968), and Heede (1974) reported on gully growth directly to piping. Runoff first enters the ground through desiccation cracks on the surface. As the water flows underground towards the gully, it removes soil particles and creates a tunnel or pipe. Continued enlargement eventually causes the pipe to collapse and creates a new gully segment.

Gully wall propagation involves two processes; blockfall and talus formation (Blong, 1970). Blockfall acts rapidly and soon after flow ceases. Talus formation is effective over a longer period. There debris remains in the gully bottom until runoff is again sufficient to remove them. Keefer (1971), Marsh (1975) and Nicholson (1976) observed similar processes in gullies on the San Francisco Peninsula. Bradford and others (1973) studied the stability of gully walls by analyzing the forces acting on them. They found that the controlling factors are the height of the groundwater table, cohesion of the soil, and rate of water infiltration.

Thompson (1964) concluded from a study that the rate of gully advance is best correlated to the drainage area above the gully head, the slope of the approach channel, the sum of rainfall from twenty four hour rains equal or greater than 0.5 inch, and a soil factor expressing the approximate clay content. Piest and others (1975) noted that gully-erosion rates did not correlate well with soil-moisture content, well levels, storm antecedent conditions, or seasonal trends.

FIELD OBSERVATIONS

During September of 1976 Rex Upp, one of the Graduate Research Assistants, made a reconnaissance field trip to examine results of gully erosion in semi-arid areas near Winston, New Mexico, Benton, Arizona, and Earthquake Canyon, San Diego County, California. Following is a pictoral summary of his most general observations and his preliminary interpretations of these observations. Unless stated otherwise, the photographs are of areas near Winston, New Mexico.

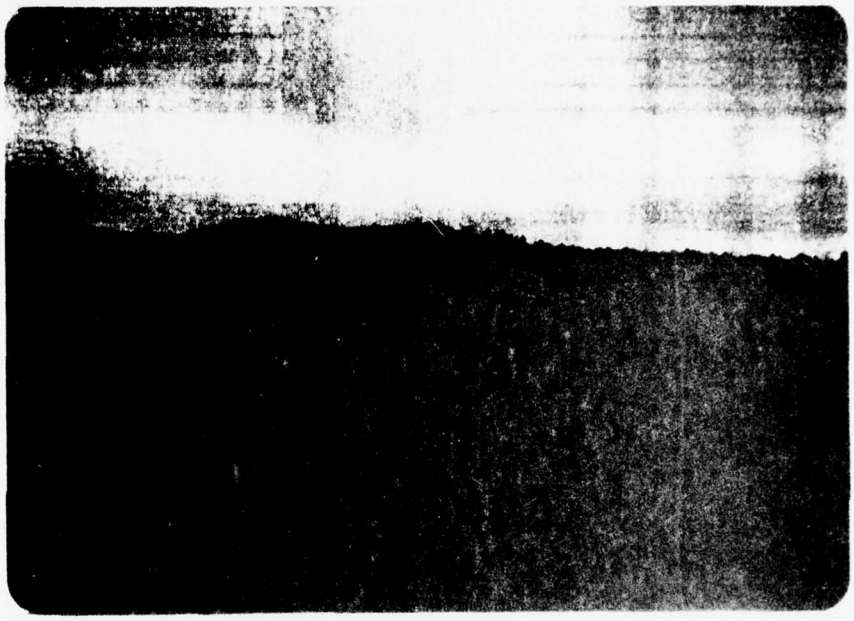

Figure 1. General view of gullies on an east-facing slope.

Figure 2. Headcut of a typical discontinuous gully.

Figure 3. Flat bottom and vertical or overhanging sides of a disontinuous gully. View toward headwall.

Figure 4. Headwall of gully shown in 3.

Figure 5. View down discontinuous gully shown in 3. Height of gully walls decreases down slope.

Figure 6. Terminal area of discontinous gully shown in 3. View toward headwall from fan.

Figure 7. Fan area of discontinuous gully shown in 3. End of discontinuous gully in upper left. View sourceward.

Figure 8. Headscarp of small discontinuous gully above that shown in 3. View upstream. This is merely one of tens of examples of incipient discontinuous gullies in the valley containing the large one shown in 3.

Figure 9. Small headcut and incipient gully. These headcuts form along the thalweg of the valley. Water flowing over the cut has created a plunge pool by removing finer grained materials. Coarser materials form a lag deposit in the pool or near the lip of the downstream edge of the pool.

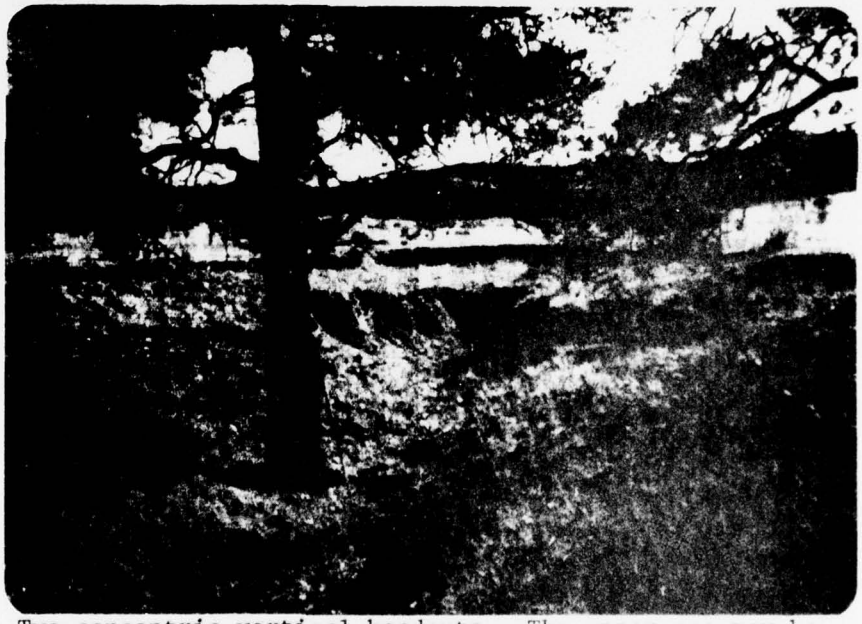

Figure 10. Two concentric vertical headcuts. The upper one may be a result of subsurface piping.

Figure 11. Large, short gully that is tributary to a larger gully system. The large volume of this gully and the small area of the watershed it drains suggest that the gully is contributing a relatively large load of debris to the main gully.

Figure 12. View upstream of debris-choked reach of main gully system. Presumably the large amount of debris is a result of contributions of tributary gullies such as that shown in 11.

Figure 13. Gully capture. The small degrading gully on the left has captured the flow from the relatively overloaded gully to the right.

The following figures show features of gullies clearly related to piping near Benson, Arizona.

Figure 14. Flat bottom and vertical to overhanging sidewall of a large gully.

Figure 15. Tunnel developed by piping towards major gully.

Figure 16. Hole and gully formed by collapse of roof of piped tunnel.

Figure 17. Nearly continuous gully system connected by short tunnels. All apparently formed by piping.

Figure 18. Collapsed pipe system with vertical chimneys to a lower system of piped tunnels and channels.

REFERENCES ON GULLY EROSION

Anteves, Ernst, 1941, Age of the Cochise Culture Stages, Medallion Papers, no. 29, pp. 31-56.

———————— 1952, Arroyo Cutting and Filling, Journal of Geology, v. 60, pp. 375-385.

Bailey, Reed W., 1935, Epicycles of Erosion in the Valleys of the Colorado Plateau Province, Journal of Geology, v. 43, pp. 337-355.

Blong, R. J., 1970, The Development of Discontinuous Gullies in a Pumice Catchment, American Journal of Science, v. 268, no. 4, pp. 369-383.

Bradford, J. M.; Farrell, D. A.; and Larson, W. E., 1973, Mathematical Evaluation of Factors Affecting Gully Stability, Proceedings of the Soil Science Society of America 37(1): 103-107.

Bryan, K., 1925, Date of Channel Trenching (arroyo cutting) in the Arid Southwest, Science n.s., v. 62, pp. 338-344.

———————— 1926, Recent Deposits of Chaco Canyon, New Mexico, in relation to the Life of the Pre-historic Peoples of Pueblo Benito (abs.), Washington Academy of Science Journal, v. 16, pp. 75-76.

———————— 1928, Historic Evidence on Changes in the Channel of Rio Puerco, a Tributary of the Rio Grande in New Mexico, Journal of Geology, v. 36, pp. 265-282.

Dellenbach, F. S., 1912, Cross-cutting and Retrograding of Stream Beds, Science, v. 35, pp. 656-658.

Denevan, William M., 1967, Livestock Numbers in Nineteenth-century New Mexico, and the Problem of Gullying in the Southwest, Assoc. Am. Geographers Annals, v. 57, no. 4, pp. 691-703.

Dodge, Richard Elwood, 1902, Arroyo Formation (abs.), American Geologist 29:322.

Fenneman, N. M., 1922, Physiographic Province and Sections in Western Oklahoma and Adjacent Parts of Texas, U.S.G.S. Bull. 730, 126-129, 1922.

Heede, Burchard H., 1970, Morphology of Gullies in the Colorado Rocky Mountains, International Association of Scientific Hydrology Bulletin, v. 15, no. 2, pp. 79-89.

———————— 1974, Stages of Development of Gullies in Western United States of America, Zeitschrift fuer Geomorphologie, v. 18, no. 3, pp. 260-271.

Johnson, A. M., and Hampton, M. A., 1969, Subaerial and subaqueous flow of slurries. Final report to U.S.G.S., Branner Library, Stanford University.

Jones, Neil Owen, 1968, The Development of Piping Erosion, Ph.D. Dissertation, Univ. of Arizona, 219 pp.

Judson, S. Sheldon, Jr., 1952, Arroyos, Scientific American, v. 187, no. 6, pp. 71-74, Dec. 1952.

Keefer, David, 1971, Gully Formation at Gravantz-Beffa Hill, San Mateo County, California, M.S. Report, Branner Library, Stanford University, Stanford, California, 104 pp.

Leopold, Arno, 1921, A Plea for Recognition of Artificial Works in Forest Erosion Control Policy, Journal Forestry, v. 19, pp. 269-270, March, 1921.

Leopold, L. B., 1951, Rainfall Frequency: An Aspect of Climatic Variation, Transactions American Geophysical Union, v. 32, pp. 347-357.

Leopold, L. B., and Miller, J. P., 1954, A Post Glacial Chronology for some Alluvial Valleys in Wyoming, U.S.G.S. Water Supply Paper 1261.

_____ 1956, Ephemeral Streams--Hydraulic Factors and their Relation to the Drainage Net, U.S.G.S. Prof. Paper 282-A pp. 1-37.

Marsh, Stuart, 1975, Preliminary Study of Gully Erosion Foothill Park--Palo Alto, California, Unpublished Report, Stanford University, March 18, 1975.

Nicholson, T. J., 1976, Geomorphology and Hydrogeology of Wild Horse Valley, Foothills Park, Palo Alto, California, M.S. Thesis, Branner Library, Stanford University, Stanford, California, 106 pp.

Parker, Garald, 1964, Piping, a Geomorphic Landform Development of the Drylands, in Assemblée Générale de Berkeley de l'UGGI, 1963: Internat. Assoc. Sci. Hydrology, pub. 65, pp. 103-113.

Patton, P. C., 1973, Gully Erosion in the Semiarid west (M.S. Thesis), Colorado State University, Fort Collins, Colorado, 129 pp.

Patton, P. C., and Schumm, Stanley A., 1975, Gully Erosion, Northwestern Colorado; A Treshold Phenomenon, Geology, February, 1975, pp. 88-90.

Piest, R.F.; Bradford, J.M.; and Spomer, R.G., 1975, Mechanisms of Erosion and Sediment Movement form Gullies, Publication ARS-S-40, Agricultural Research Service, USDA.

Rich,John Lyon, 1911, Recent Stream Trenching in the Semiarid Portion of Southwestern New Mexico, as a result of Removal of Vegetative Cover, Am. Jour. Sci. v. 32, pp. 237-245.

Rubey, William W., 1928, Gullies in the Great Plains formed by Sinking of the Ground, American Journal of Science, 5th sec., v. 15, pp. 417-422, May, 1928.

Schumm, S. A., 1961, Effect of Sediment Characteristics on Erosion and Deposition in Ephemeral-stream Channels, U.S.G.S. Prof. Paper 352-C, pp. 31-70.

Schumm, S. A., and Hadley, R. F., 1957, Arroyos and the Semiarid Cycle of Erosion, Amer. Jour. of Science, v. 255, March 1957, pp. 161-173.

Thompson, J. R., 1964, Quantitative Effect of Watershed Variables on the Rate

of Head Advancement, Amer. Soc. Agricultural Engineers Meeting, Chicago, 1962, Paper 62-713.

Thornthwaite, C. Warren; Sharpe, C. F. Stewart; and Dosch, Earl F., 1942, Climate and Accelerated Erosion in the Arid and Semiarid Southwest with special reference to the Polacca Wash Drainage Basin, Arizona, U.S. Dept. of Agriculture, Washington, D.C., Technical Bulletin no. 808, May 1942, 134 pp.

APPENDIX A. TILT DATA FOR STEEL RODS

Note: Locations of rods indicated in Figures 7 and 9, except that rods 51, 55, 56, 58, 61 and 62 are above test pit no. 8, Fig. 9.

Rod No.	Length (cm)	Maximum Slope Direction (aximuth)	Date	Tilt (Magnitude in radians X10^3) I Mag.	I Dir.	II Mag.	II Dir.	Resultant Mag.	Resultant Dir.
1	76	357	10/8/74	base					
			11/10/74	3.8	168	0.6	258	4.0	178
			12/21/74	0.9	173	4.1	083	4.3	097
			2/23/75	5.5	358	23.6	088	24.3	076
			4/2/75	1.5	180	32.6	090	32.7	091
			10/4/75	13.4	179	37.2	089	39.7	109
			12/6/75	11.6	180	42.3	090	43.7	104
			1/17/76	12.5	177	41.9	087	43.7	106
2	76	055	10/5/74	base					
			11/9/74	1.8	017	6.4	107	6.7	092
			12/21/74	7.9	038	11.6	128	14.0	084
			2/23/75	16.0	040	13.4	130	21.0	078
			4/2/75	23.6	037	13.1	127	27.0	067
			10/4/75	11.6	037	5.0	307	12.3	015
			12/6/75	16.9	040	10.5	130	20.0	069
			1/17/76	14.8	038	2.6	128	15.0	048
3	76	065	10/8/74	base					
			12/21/74	11.1	055	14.3	325	18.0	015
			2/23/75	11.1	068	15.1	338	18.7	014
			4/2/75	6.4	055	11.9	325	13.7	353
			10/4/75	9.9	054	6.7	324	12.0	021
			12/6/75	12.5	056	8.1	326	15.0	023
			1/17/76	10.8	056	8.7	326	14.0	016
4	76	065	10/8/74	base					
			11/9/74	7.0	099	3.8	189	8.9	130
			12/21/74	8.4	102	3.8	192	9.3	126
			2/23/75	12.2	104	2.3	194	12.3	113
			4/2/75	7.9	104	5.8	014	9.7	065
			10/4/75	36.9	101	13.7	011	39.3	082
			12/6/75	18.3	103	17.7	013	25.7	058
			1/17/76	38.7	102	16.6	012	42.0	079
5	107	065	10/8/74	base					
			12/21/74	1.8	232	3.9	322	4.3	298
			2/23/75	2.3	233	4.4	323	5.0	293
			4/2/75	2.0	232	7.0	322	7.4	305
			10/4/75	3.2	231	27.3	321	27.6	316
			12/6/75	5.0	232	23.6	322	24.1	310
			1/17/75	5.0	232	23.0	322	23.6	310

6	76	065	10/5/74	base					
			11/10/74	4.7	072	3.2	162	5.7	109
			12/21/74	2.3	073	1.8	343	3.0	037
			2/23/75	17.5	074	0.3	344	17.3	072
			4/2/75	18.0	074	0.6	164	18.0	075
			10/4/75	base reestablished					
			12/6/75	0.3	043	2.6	133	2.7	125
			1/17/76	0.9	220	0.6	130	1.0	188
7	50	072	10/8/74	base					
			12/21/74	0		11.3	131	11.3	131
			2/23/75	3.5	040	16.6	130	17.2	120
			4/2/75	2.9	041	17.2	131	17.2	122
			10/4/75	18.9	221	26.5	131	32.8	166
			12/6/75	10.5	221	35.5	131	37.2	147
			1/17/76	9.3	221	35.5	131	36.7	146
8	107	360	10/8/74	base					
			11/10/74	1.8	174	1.2	264	2.1	211
			12/21/74	2.3	175	4.4	085	5.0	114
			2/23/75	5.0	014	3.8	104	6.2	032
			4/2/75	8.4	356	2.3	086	8.8	011
			10/4/75	18.3	356	8.4	266	20.2	331
			12/6/75	20.4	355	2.0	256	20.5	349
			1/17/76	19.2	355	0.3	256	19.3	354
9	76	350	10/8/74	base					
			11/10/74	10.0	187	8.1	097	12.7	149
			12/21/74	16.9	188	10.8	098	20.0	156
			2/23/75	0.3	008	10.2	098	10.3	096
			4/2/75	2.3	008	10.8	098	11.0	086
			10/4/75	20.7	007	5.8	097	21.3	023
			12/6/75	18.0	007	5.0	097	.8.7	024
			1/17/76	16.6	009	5.2	099	17.7	026
10	107	350	12/21/74	base					
			2/23/75	0.9	192	0.3	282	1.0	206
			4/2/75	5.5	191	4.4	281	7.1	230
			10/4/75	23.3	011	22.1	281	32.1	328
			12/6/75	20.9	012	16.6	282	26.7	333
			1/17/76	21.5	013	16.6	283	27.1	334
11	107	065	11/9/74	base					
			12/21/74	12.8	269	14.3	359	19.3	317
			2/23/75	5.2	270	26.7	000	27.4	348
			4/2/75	2.6	268	23.9	358	24.1	353
			10/4/75	16.3	089	48.0	359	50.7	018
			12/6/75	17.5	090	43.3	360	46.7	021
			1/17/76	18.9	089	43.3	359	47.4	022

12	107	065	11/9/74	base				
			12/21/76	6.7	084	2.9	354	7.4	061
			2/23/75	0.3	082	2.3	172	2.4	168
			4/2/75	9.6	264	8.7	174	13.1	221
			10/4/75	2.0	264	29.7	174	29.8	178
			12/6/75	9.3	263	18.9	173	21.2	200
			1/17/76	4.7	263	26.5	173	26.9	184
13	107	065	10/5/74	base				
			11/10/74	2.0	296	0.9	026	2.1	319
			12/21/74	7.9	295	9.6	025	13.1	348
			2/23/75	9.6	298	16.3	028	18.8	355
			4/2/75	5.8	296	11.6	026	13.1	359
			10/4/75	3.2	114	26.2	024	26.4	032
			12/6/75	4.7	116	23.0	026	23.6	037
			1/17/76	6.4	113	22.1	023	23.1	041
14	46	065	10/5/74	base				
			11/10/74	11.1	266	7.9	176	13.3	231
			12/21/74	7.6	266	5.8	176	9.4	228
			2/23/75	14.3	265	8.1	355	16.7	244
			4/2/75	10.5	267	3.4	177	11.1	251
			10/4/75	base reestablished					
			12/6/75	4.4	265	0.6	175	4.4	257
			1/17/76	5.0	263	0.6	173	5.0	258
15	46	357	10/8/74	base					
			11/10/74	0.6	011	5.2	101	5.6	096
			12/21/74	0.9	192	14.0	102	13.9	106
			2/23/75	3.2	012	2.3	102	3.9	046
16	46	350	10/8/74	base					
			11/10/74	42.8	003	3.8	273	42.9	357
			12/21/74	46.3	002	15.7	272	48.9	343
			2/23/75	44.2	001	9.6	271	45.0	350
17	46	065	10/8/74	base					
			11/9/74	12.2	269	2.3	179	12.2	259
			12/21/74	16.6	269	2.3	179	16.7	261
			2/23/75	base reestablished					
			4/2/75	11.6	266	7.6	356	13.9	298
			10/4/75	17.5	265	26.2	175	31.7	207
			12/6/75	8.4	264	32.6	174	32.8	189
			1/17/76	11.3	264	31.4	174	33.3	193
19	122	055	11/10/74	base					
			12/21/74	1.5	066	3.5	336	3.8	358
			2/23/75	18.3	065	9.9	335	20.8	037
			4/2/75	5.0	067	10.8	337	11.9	001
			10/4/75	12.8	065	5.8	335	14.2	041
			12/6/75	17.5	066	1.2	156	17.5	070
			1/17/76	13.7	066	2.0	336	13.8	057

20	122	357	10/8/74	base				
			11/10/74	6.7	195	10.5	105	12.5	138
			12/21/74	9.3	191	9.0	101	12.9	147
			2/23/75	12.8	188	0.3	278	12.9	189
			4/2/75	5.8	188	6.1	278	8.5	234
			10/4/75	7.0	189	12.5	099	14.4	127
			12/6/75	5.5	189	1.2	099	5.6	175
			1/17/76	7.3	186	0.6	276	7.3	193
21	137	035	11/10/74	base					
			12/21/74	2.0	084	3.2	174	3.9	141
			2/23/75	0.6	266	8.7	176	8.7	178
			4/2/75	3.2	085	7.0	175	7.6	150
			10/4/75	19.5	082	17.7	172	26.3	136
			12/6/75	18.9	084	15.1	174	24.3	133
			1/17/76	19.2	083	15.1	173	24.4	132
22	122	045	10/8/74	base					
			11/9/74	14.3	301	92.2	211	93.1	222
			12/21/74	25.0	303	12.8	213	28.1	276
			2/23/75	41.6	305	0.0		41.6	305
			4/2/75	36.9	306	0.3	216	36.9	303
			10/4/75	56.4	302	21.5	212	60.4	282
			12/6/75	52.9	303	12.8	213	54.4	289
			1/17/76	52.4	303	15.1	213	54.6	287
23	122	055	11/10/74	base					
			12/21/74	3.8	053	16.0	143	16.5	130
			2/23/75	4.7	053	7.6	323	9.0	112
			4/2/75	10.8	053	0.6	323	10.9	056
			10/4/75	5.2	233	1.5	323	5.4	249
			12/6/75	9.0	233	0.9	143	9.2	228
			1/17/76	3.5	232	2.6	142	4.4	196
24	122	045	10/8/74	base					
			11/9/74	14.3	116	48.0	026	50.0	044
			12/21/74	19.2	117	37.5	027	42.1	054
			2/23/75	20.1	120	41.3	030	45.8	053
			4/2/75	14.0	119	39.0	029	41.5	047
			10/4/75	9.0	116	53.5	026	54.2	036
			12/6/75	4.7	117	49.7	027	50.0	032
			1/17/76	3.2	295	54.4	025	54.4	024
25	168	060	10/8/74	base					
			12/21/74	0.0		32.2	004	32.2	004
			2/23/75	10.2	274	21.5	004	23.8	339
			4/2/75	17.5	274	18.0	004	25.2	320
			10/4/75	2.0	273	25.6	003	25.8	000
			12/6/75	3.5	275	24.1	005	24.4	356
			1/17/76	4.4	273	22.7	003	23.2	353

26	122	055	11/10/74	base				
			12/21/74	17.2	091	8.4	181	19.2	118
			2/23/75	3.8	272	18.9	182	19.4	192
			4/2/75	9.0	272	10.5	182	13.8	222
			10/4/75	21.8	090	6.4	000	22.7	074
			12/6/75	21.2	091	9.3	001	23.1	067
			1/17/76	19.2	090	11.3	000	22.2	060
27	168	045	10/5/74	base				
			11/9/74	27.1	237	3.8	327	27.3	247
			12/21/74	7.0	239	0.9	329	7.0	247
			2/23/75	4.9	060	1.5	330	5.2	042
			4/2/75	18.0	061	5.8	151	18.9	077
			10/4/75	27.6	056	14.5	146	31.2	087
			12/6/75	36.4	059	16.0	149	39.7	083
			1/17/76	43.9	059	16.6	149	47.0	080
28	168	065	11/9/74	base				
			12/21/74	11.6	234	18.0	324	21.5	291
			2/23/75	0.9	233	15.7	323	15.8	321
			4/2/75	4.9	055	10.2	325	11.4	350
			10/4/75	8.7	055	7.3	145	11.4	132
			12/6/75	10.5	053	5.5	143	11.8	082
			1/17/76	10.2	054	5.2	144	11.5	082
29	168	065	10/5/74	base				
			11/10/74	11.1	123	3.5	033	11.7	106
			12/21/74	31.7	124	0.0		31.7	124
			2/23/75	34.6	125	4.9	215	35.0	132
			4/2/75	35.8	125	1.2	215	35.9	126
			10/4/75	26.5	122	4.4	212	26.8	133
			12/6/75	32.6	124	2.9	214	32.7	129
			1/17/76	31.1	124	0.9	214	31.2	126
30	137	045	10/5/74	base				
			11/9/74	0.6	258	10.8	348	10.9	346
			12/21/74	10.8	259	8.1	349	13.5	298
			2/23/75	0.6	260	3.2	170	3.3	179
			4/2/75	3.2	260	4.7	170	5.7	203
			10/4/75	5.5	259	18.9	249	19.6	333
			12/6/75	3.5	261	20.1	351	20.4	339
			1/17/76	2.6	256	22.7	346	22.8	343
31	137	035	11/10/74	base				
			12/21/74	2.6	093	17.5	009	17.6	011
			2/23/75	11.3	279	2.0	009	11.5	289
			4/2/75	9.6	279	2.0	189	9.8	267
			10/4/75	22.4	278	3.5	188	22.6	270
			12/6/75	24.4	280	2.3	190	24.6	273
			1/17/76	26.2	281	2.9	191	26.3	272

32	137	035	11/10/74	base				
			12/21/74	11.1	256	2.6	346	11.3	269
			2/23/75	9.9	257	0.3	347	10.0	258
			4/2/75	1.7	256	1.2	346	2.0	290
			10/4/75	15.4	076	4.1	166	15.9	091
			12/6/75	9.9	077	4.4	167	10.7	100
			1/17/76	8.4	075	5.5	165	10.2	109
33	137	035	11/10/74	base				
			12/21/74	2.6	085	9.6	175	10.0	160
			2/23/75	0.9	086	5.2	176	5.4	165
			4/2/75	15.1	085	6.4	355	16.5	062
			10/4/75	7.0	264	5.5	354	8.9	303
			12/6/75	3.2	264	4.1	354	5.2	317
			1/17/76	4.7	264	1.2	174	4.8	251
34	137	035	11/10/74	base				
			12/21/74	0.3	290	9.0	200	9.1	202
			2/23/75	6.1	292	9.3	202	11.1	233
			4/2/75	11.6	291	20.1	201	23.1	230
			10/4/75	1.5	109	30.3	199	30.4	197
			12/6/75	0.9	290	21.5	200	21.6	202
			1/17/76	0		20.9	196	20.9	196
35	122	065	10/8/74	base				
			11/9/74	3.5	093	3.8	003	5.2	049
			12/21/74	3.2	096	7.6	006	8.1	029
			2/23/75	5.8	097	2.9	007	6.5	069
			4/2/75	11.3	098	6.7	008	13.1	066
			10/4/75	6.1	095	22.1	005	22.9	021
			12/6/75	11.3	097	23.6	007	26.3	032
			1/17/76	10.2	095	23.0	007	25.2	030
36	122	060	10/8/74	base				
			12/21/74	10.2	220	11.9	310	15.6	269
			2/23/75	6.1	222	4.1	312	7.3	255
			4/2/75	4.9	219	1.7	309	5.2	238
			10/4/75	7.6	219	12.2	129	14.4	161
			12/6/75	6.1	221	15.4	131	16.7	151
			1/17/76	6.4	221	13.7	131	15.2	155
37	122	065	10/5/74	base				
			11/10/74	1.7	056	3.2	326	3.8	354
			12/21/74	4.4	056	7.0	326	8.3	358
			2/23/75	3.2	056	7.6	326	8.1	349
			4/2/75	3.8	056	6.4	326	7.5	356
			10/4/75	0		9.0	146	9.0	146
			12/6/75	3.2	056	6.4	146	7.1	120
			1/17/76	2.3	057	5.5	147	6.0	124

38	122	055	11/10/74	base				
			12/21/74	11.3	101	5.8	011	12.7	074
			2/23/75	33.7	102	18.0	192	38.3	129
			4/2/75	48.0	102	34.9	192	59.4	137
			10/4/75	22.7	100	36.9	190	43.3	159
			12/6/75	23.3	101	36.1	191	42.9	158
			1/17/76	24.1	100	36.7	190	44.0	158
39	122	045	10/5/74	base				
			11/9/74	3.2	095	0.6	185	3.3	106
			12/21/74	1.2	284	1.2	194	1.7	239
			2/23/75	8.4	292	9.9	202	12.9	241
			4/2/75	7.0	291	5.8	201	9.2	251
			10/4/75	3.8	110	41.0	200	41.3	196
			12/6/75	2.6	110	39.0	200	39.2	197
			1/17/76	1.7	110	37.5	200	37.6	199
40	122	337	10/8/74	base				
			11/10/74	29.1	188	1.2	278	29.2	193
			12/21/74	20.7	010	1.7	280	20.8	005
			2/23/75	7.6	012	0.3	282	7.7	008
			4/2/75	19.8	011	10.8	281	22.5	341
			10/5/75	31.4	008	19.5	098	36.9	042
			12/6/75	24.7	010	6.4	100	25.6	025
			1/17/76	25.0	010	7.0	100	26.0	026
41	122	045	10/5/74	base				
			11/9/74	16.3	287	0.3	197	16.3	287
			12/21/74	11.6	288	2.0	018	11.9	298
			2/23/75	8.1	289	1.7	019	8.3	300
			4/2/75	9.3	289	5.5	019	10.8	319
			10/4/74	17.2	288	4.7	198	17.7	273
			12/6/75	9.3	289	7.9	199	12.3	248
			1/17/76	14.5	288	5.8	198	15.6	266
42	122	055	12/21/74	base				
			2/23/75	6.1	269	10.8	179	12.3	207
			4/2/74	4.7	269	7.9	359	9.2	328
			10/4/75	17.2	085	11.6	175	20.8	122
			12/6/75	4.9	090	5.5	180	13.1	113
			1/17/76	16.9	089	14.0	179	21.9	128
43	122	045	10/5/74	base				
			11/9/74	9.9	284	12.5	014	16.0	338
			12/21/74	20.7	287	28.8	017	35.4	341
			2/23/75	15.7	287	26.5	017	30.8	346
			4/2/75	13.1	287	23.3	017	26.7	348
			10/4/75	17.5	290	8.7	020	19.6	314
			12/6/75	10.5	286	14.5	016	17.9	342
			1/17/76	13.1	290	14.5	020	19.6	335

51	30.5	090	10/4/75	base				
			12/6/75	18.0	177	11.9	267	21.7	211
			1/17/76	16.9	177	11.3	267	20.0	213
55	61	090	10/4/75	base				
			12/6/75	5.2	180	6.1	090	7.9	130
			1/17/76	5.8	178	6.4	088	8.8	134
56	61	090	10/4/75	base				
			12/6/75	17.7	170	6.1	080	18.8	151
			1/17/76	5.2	170	6.1	080	7.9	121
58	91	090	10/4/75	base				
			12/6/75	11.9	355	4.9	085	13.1	018
			1/17/76	10.5	353	3.8	083	11.1	015
61	122	090	10/4/75	base				
			12/6/75	3.3	162	0.6	252	3.3	173
			1/17/76	3.8	162	1.5	072	4.0	141
62	122	090	10/4/75	base				
			12/6/75	2.6	173	0.3	083	2.7	173
			1/17/76	4.9	175	4.9	085	7.1	129

APPENDIX B. MEASUREMENTS OF VERTICAL SWELLING

Note: Locations of rods indicated in Figures 7 and 9, except for rods 51, 55, 56, 58, 61 and 62, which are above test pit no. 8, Fig. 9. Unless indicated otherwise, rods installed 11/10/74.

Rod No.	Length above ground (cm)	Change in length above ground (cm)				
		2/23/75	4/2/75	10/4/75	12/6/75	1/17/76
1	17.8	-2.0	0.2		1.5	0.5
2	19.3	-2.3	0		2.1	0
3	16.8*	----	0.2		2.1	0
4	21.3	-1.7	-1.1	3.1	-0.7	-0.9
5	14.0*	----	0.2		5.1	1.5
6	18.5	-1.5	1.5		-2.7	0
7	17.8*	----	0.5		1.0	-0.2
8	19.1	-2.6	-1.0		2.8	-0.5
9	17.0	-1.2	-0.3		3.3	-0.3
10	18.5	-3.5	-1.0		2.0	-0.2
11	18.8	-2.8	-0.2		2.2	0.5
12	19.1	-1.8	-2.5	6.8	0	-0.5
13	17.5	-2.5	0.5		2.3	4.0
14	16.8	0	0		1.0	-0.3
15	16.0	-0.5				
16	18.0	-1.2				
17	17.5	1.6	-1.3	2.0	0.3	-0.5
19	16.5	-2.3	-1.5	6.1	-0.8	0.3
20	19.3	-2.5	-0.8		7.1	-0.7
21	18.5	-4.3	-0.2		5.6	-0.5
22	12.7	-3.0	-31.		3.8	0
23	17.8	-2.3	-1.8	5.1	-0.5	-1.5
24	16.0	-1.8	-2.8		8.4	-2.5
25	12.2*	----	1.8		5.3	0.5
26	17.8	-3.8	-1.5		3.8	0.2
27	20.8	-2.8	-1.5		9.7	-4.6
28	15.2	-2.7	0.7	3.8	0.3	-0.5
29	16.5	-1.8	1.8		2.6	4.8
30	21.8	-1.2	-1.8		0.8	0
31	18.5	-2.0	-2.5		4.3	0.8
32	19.8	-2.3	-1.7		5.3	0.7
33	21.1	-4.3	-1.0		7.3	-3.8
34	21.1	-2.0	-0.3		0.8	-0.3
35	18.3	-1.3	-2.8	4.3	-0.5	-0.5
36	16.0*	----	-2.3		4.6	0.2
37	17.0	-2.5	2.0		3.6	2.3
38	19.1	-2.6	-3.8		4.3	0.3
39	13.7	-2.0	-1.8		2.8	0.3
40	21.6	-4.1	-2.8		6.1	
41	17.3	-3.3	-1.0		1.7	0.3
43	18.0	-2.8	-2.2		2.5	0
51	13.2#	----	----	----	----	-0.5
55	18.8#	----	----	----	----	-1.3
56	15.7#	----	----	----	----	-0.5
58	16.5#	----	----	----	----	-0.8
61	19.8#	----	----	----	----	-1.3

* Rods installed 2/23/75 # Rods installed 12/6/75

APPENDIX C. LOGS OF BORINGS AND TEST PITS

Note: Locations of boreholes and test pits are indicated in Figures 7 and 9.
Abbreviations: w = water content
cs = claystone
ss = sandstone
s-cracks = shrinkage cracks
wx = weathered
br = brown
gr = gray
l.t. = less than
ms = mudstone
bl = black

Depth (ft)	
	C-1 (8/17/74)
0.0	dk gr silty clay;dry;minimal s-cracks
3.0	yellow br silty clay;moist; w g.t. Plastic Limit;wx cs;no structure
16.0	yellow br ss;soft, wx and moist
17.0	bottom
	C-2 (8/17/74)
0.0	dk gr silty clay;dry; small s-cracks
5.0	dk gr to bl silty clay;dry
10.0	dk yellow br slty clay; w increases with depth;becomes lighter colored with depth
18	bottom; wx cs; gradational contact; soft,moist; no structure
	C-3 (8/17/74)
0.0	dk gr silty clay; small s-cracks
5.5	wx cs; yellow br;moist, plastic, soft
10.0	bottom; becomes lighter colored; contains scattered fragments of greenish cs
	C-4 (8/17/74)
0.0	dk gr to br silty clay; large to med. s-cracks
5.0	yellow br wx cs
5.5	becomes stiffer
12.0	bottom
	C-5 (8/17/74)
0.0	dk br silty clay; dry; large s-cracks
5.0	yellow br cs; highly wx;becomes lighter colored with depth
12.0	bottom
	C-6 (8/17/74)
0.0	sandy silt; light gr to br;dry
5.5	refusal; ss
	C-7 (8/18/74)
0.0	dk br silty clay; dry
4.5	wx cs; yellow br; soft, plastic
6.0	bottom

C-8 (8/18/74)

0.0	dk br silty clay; dry; med. s-cracks
5.5	yellow br ss; highly wx;soft; slightly plastic
6.0	yellow br cs; soft; becomes lighter colored with depth
11.0	bottom

C-9 (8/18/74)

0.0	dk br silty clay
5.0	yellow br; highly wx cs; moist, soft
11.5	bottom

C-10 (8/18/74)

0.0	dk gr to bl silty clay
5.0	becomes moist
9.0	yellow br wx cs; soft, moist
12.0	bottom

C-11 (8/18/74)

0.0	dk br to bl silty clay; lg to med s-cracks
6.0	becomes moist
10.0	silty clay; reddish br; gradual color change
15.5	soft gr cs; abrupt contact; plastic, moist
18.0	bottom

C-12 (8/20/74)

0.0	dk gr to gr silty clay; dry; small s-cracks
5.0	becomes moist; dark br to bl
10.0	dk reddish br; gradational change
14.0	bottom

C-13 (8/20/74)

0.0	dk gr to bl silty clay; large s-cracks
3.5	becomes moist
10.5	reddish br; gradational change
14.2	refusal

C-14 (8/20/74)

0.0	dk gr to bl silty clay; med to large s-cracks
4.0	becomes moist
9.0	reddish br sandy clay
10.0	yellow br wx cs; sandy
12.0	bottom

C-15 (8/20/74)

0.0	light br to br silty sand; dry, loose
1.5	clayey sand; dry; loose
4.0	br ss; moist, friable
5.0	bottom

C-16 (8/20/74)

0.0	br silty sand; fn gr, dry, loose
3.0	becomes moist
3.5	wx clayey sand; yellow to br
4.0	yellow br ss; firm
5.5	bottom

C-17 (8/20/74)

0.0	dk br silty sand; loose; dry
1.0	becomes light br
2.0	yellow br ss; friable
4.0	bottom

C-18 (8/20/74)

0.0	silty sand; br gr; loose, dry
3.0	yellow br wx cs; soft, moist
8.0	bottom

C-19 (8/20/74)

0.0	br gr silty sand; dry; loose
3.0	yellow br sandy clay; grades to light br sandy wx cs
12.0	bottom

C-20 (8/20/74)

0.0	br to gr silty sand; loose
1.0	becomes light br
3.0	yellow br sandy clay
6.0	light br ss; friable
6.5	yellow br sandy cs; wx
8.0	bottom

C-21 (8/20/74)

0.0	light br silty sand; fine, dry, loose
2.5	clayey sand; highly wx; plastic; yellow br
3.0	light br wx ss; friable
5.0	bottom

C-22 and C-23 (8/20/74)

0.0	br silty sand; loose; dry, fine
2.5	moist, clayey sand; plastic; light br
4.0	br wx fine gr ss
6.0	bottom

C-24 (8/20/74)

0.0	dark br sandy clay; dry; small s-cracks
4.0	yellow br silty clay; slightly plastic
5.0	yellow br wx cs; soft, plastic, moist
11.0	bottom

C-25 (8/20/74)

0.0	dk gr to br silty clay; med to lg s-cracks
4.5	dk br wx cs; becomes lighter colored with depth
12.0	bottom

C-26 (8/20/74)

0.0	dk br silty clay; dry; small s-cracks
4.0	yellow br wx cs; becomes lighter colored with depth
10.0	cs acquires greenish tint
11.0	bottom

C-27 (8/20/74)

0.0	dk br silty clay; dry; large s-cracks
4.0	br wx cs; becomes lighter colored with depth
11.0	bottom; refusal in quartz (?) vein

C-28 (8/20/74)

0.0	light gr, fine grained silty sand; loose
3.0	yellow br wx cs
10.0	bottom

C-29 (8/20/74)

0.0	br fine grained silty sand; loose; dry
2.5	sandy clay; light br
3.5	wx cs; light br
12.0	bottom

C-30 (8/20/74)

0.0	dark gr silty clay; large s-cracks
9.5	color changes to yellow br; silty clay
18.0	bottom

F-1 (12/20/74)

0.0	dk br silty clay; moist; plastic
2.0	br to gr br silty sand; dry; w increases with depth; high dry strength
9.0	wx ms; moist

F-2 (12/23/74)

0.0	bl silty clay; slightly sandy; becomes br with depth
7.0	dark reddish br; silty clay; moist
7.5	silty sand; reddish br; slightly moist; some fine to med.-grained quartz; l.t. 10%; some large basalt frags (ca. 1 cm) becomes lighter colored with depth
9.0	dk br silty clay; moist; slightly plastic
10.0	light br to dark gr silty sand
12.0	wx loose ss
13.0	bottom

F-3 (12/24/74)

0.0	dk br to bl silty clay; minor sand (l.t. 5%); dry; med to large s-cracks
5.0	br to reddish br silty clay; sand l.t. 10%
8.0	sand content begins to decrease
9.0	wx cs; light brown to buff;slightly moist; fine to med.-grained sand includes quartz and basalt (l.t. 5%); becomes lighter colored with depth
13.0	rock fragments increase to about 15%; mostly ms in various stages of weathering but also chert; no sand; moist; w decreases with depth
15.0	dry
18.0	bottom

F-4 (12/24/74)

0.0	bl silty clay; high organic content to depth of 1 ft.; slightly moist; w increases with depth
5.5	dark reddish br sandy to silty clay; minor quartz but sand-sized fraction consists mostly of fine to med.-grained rock fragments basalt; dry
7.0	sandy clay; reddish br; sand about 15%; little quartz; amost completely rounded to angular rock frags; some are flat; slightly moist; w increases with depth; plastic; grain size fine to coarse;

	fine grains predominate; rock fragments decrease with depth
14.0	sand less than 5%
15.0	wx cs; dark br green; sticky and plastic; low w
17.0	bottom

F-5 (12/24/74)

0.0	dk br to bl silty clay; med s-cracks
1.0	reddish br silty clay; becomes darker with depth; dry
8.0	reddish br sandy to silty clay; sand and larger fraction make up less than 10%; consists mainly of angular to subrounded rock fragments, some of which are ss (max. size about one cm); slightly moist; plastic
10.0	orange br wx siltstone; slightly moist; plastic; rock fragments less than 5%
12.0	bottom

F-6 (1/4/75)

0.0	dark gr silty clay; surface wet; w decreases with depth
6.0	gradational contact to wx cs; dark yellow br
7.0	light colored yellow br cs
11.5	bottom in wx cs

F-7 (1/4/75)

0.0	dark gr to bl silty clay
2.5	some ss frags in bl silty clay
5.0	becomes dark reddish br
9.5	yellow br high wx clayey ss
11.5	refusal

F-8 (1/4/75)

0.0	bl silty clay; moist; ss fragments at surface
5.0	becomes dark reddish br then grades to lighter reddish br
7.0	dark br sandy clay
9.5	coarse grained wx ss; brown
10.0	sandy clay
15.0	br coarse ss; clean sand
17.0	bottom

F-9 (1/4/75)

0.0	bl silty clay; slightly moist; abundant basalt pebbles and cobbles on ground surface
6.0	turns brown; moist
9.5	basalt fragments increase with depth
12.5	refusal; basalt

F-10 (1/4/75)

0.0	bl silty clay; moist; highly plastic; abundant basalt pebbles and cobbles
5.0	turns dark br then lighter colored with depth
15.0	refusal in basalt

B-1 (7/22/74)

0.0	bl sandy clay
5.5	wx ms; brownish clay (gypsum chips)
6.5	bottom

B-2 (7/22/74)

0.0	bl sandy clay soil; surface cracks much more pronounced than at B-1
6.0	br clay (gypsum chips)
6.5	bottom; tan gray clay

B-3 (7/22/74)

0.0	bl sandy clay
6.0	brownish clay; gypsum chips
38.0	clay begins to turn grayish from initial brown color
40.0	bottom

B-4 (7/23/74)

0.0	gr clayey sand
4.0	br clay; gypsum chips
12.0	no change

B-5 (7/23/74)

0.0	gr clayey sand
4.0	grades into brownish clay; gypsum chips
8.0	clay becomes grayish; harder to drill
8.5	bottom

B-6 (7/23/74)

0.0	bl sandy clay
4.5	grades into brownish clay
7.5	grahish clay
8.0	bottom; difficult drilling

B-7 (7/23/74)

0.0	bl sandy clay; large s-cracks
6.0	becomes grayish clay
6.5	bottom; difficult drilling

B-8 (7/23/74)

0.0	bl sandy clay
4.0	grayish clay; difficult drilling
5.0	bottom

B-9 (7/23/74)

0.0	gray sandy clay; more sand than in black sandy soil
4.5	br clay
8.5	bottom; no change

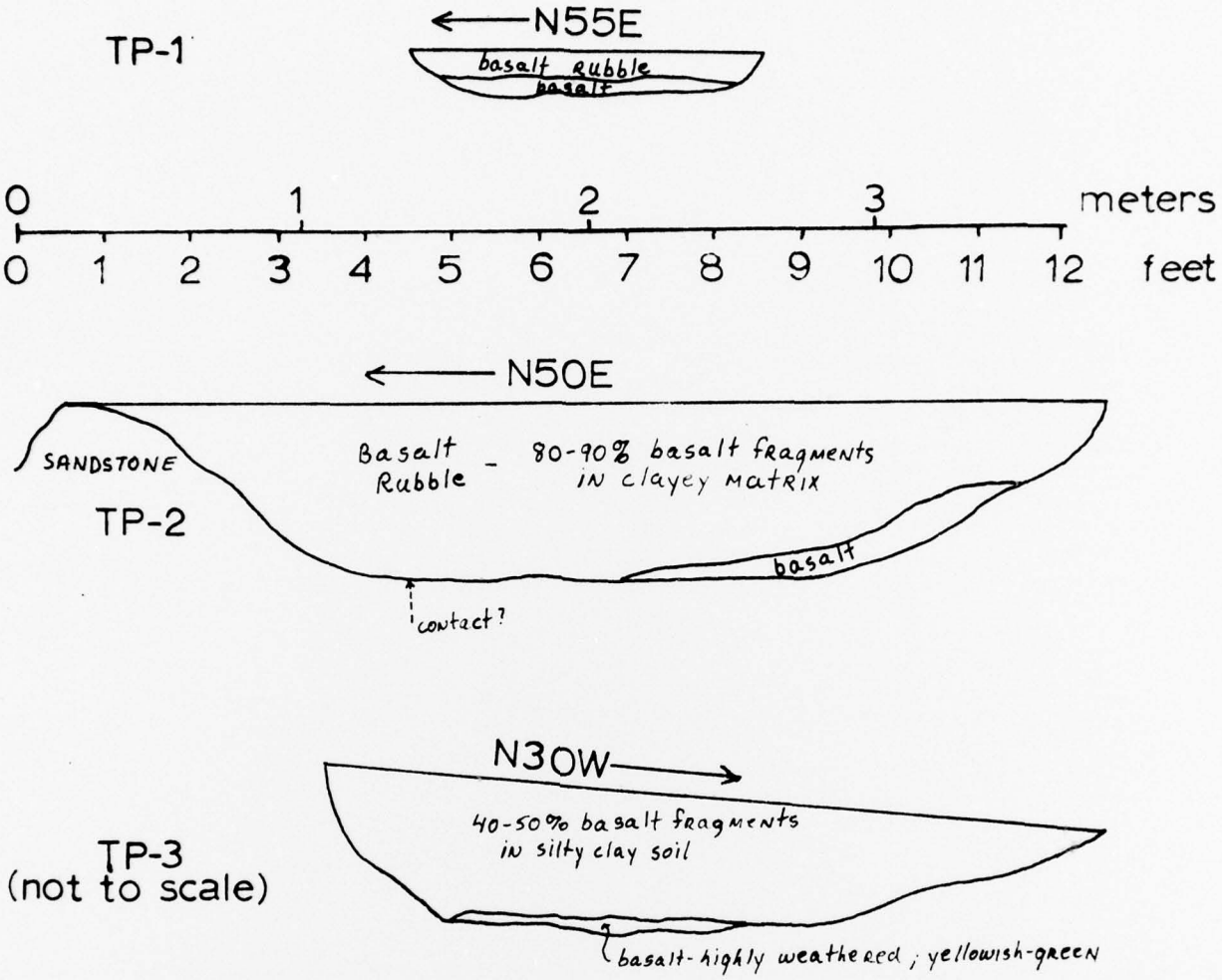
TP-1
N55E
basalt rubble
basalt
0 1 2 3 meters
0 1 2 3 4 5 6 7 8 9 10 11 12 feet
N50E
SANDSTONE
Basalt Rubble - 80-90% basalt fragments in clayey matrix
basalt
contact?
TP-2
N30W
40-50% basalt fragments in silty clay soil
basalt - highly weathered; yellowish-green
TP-3
(not to scale)

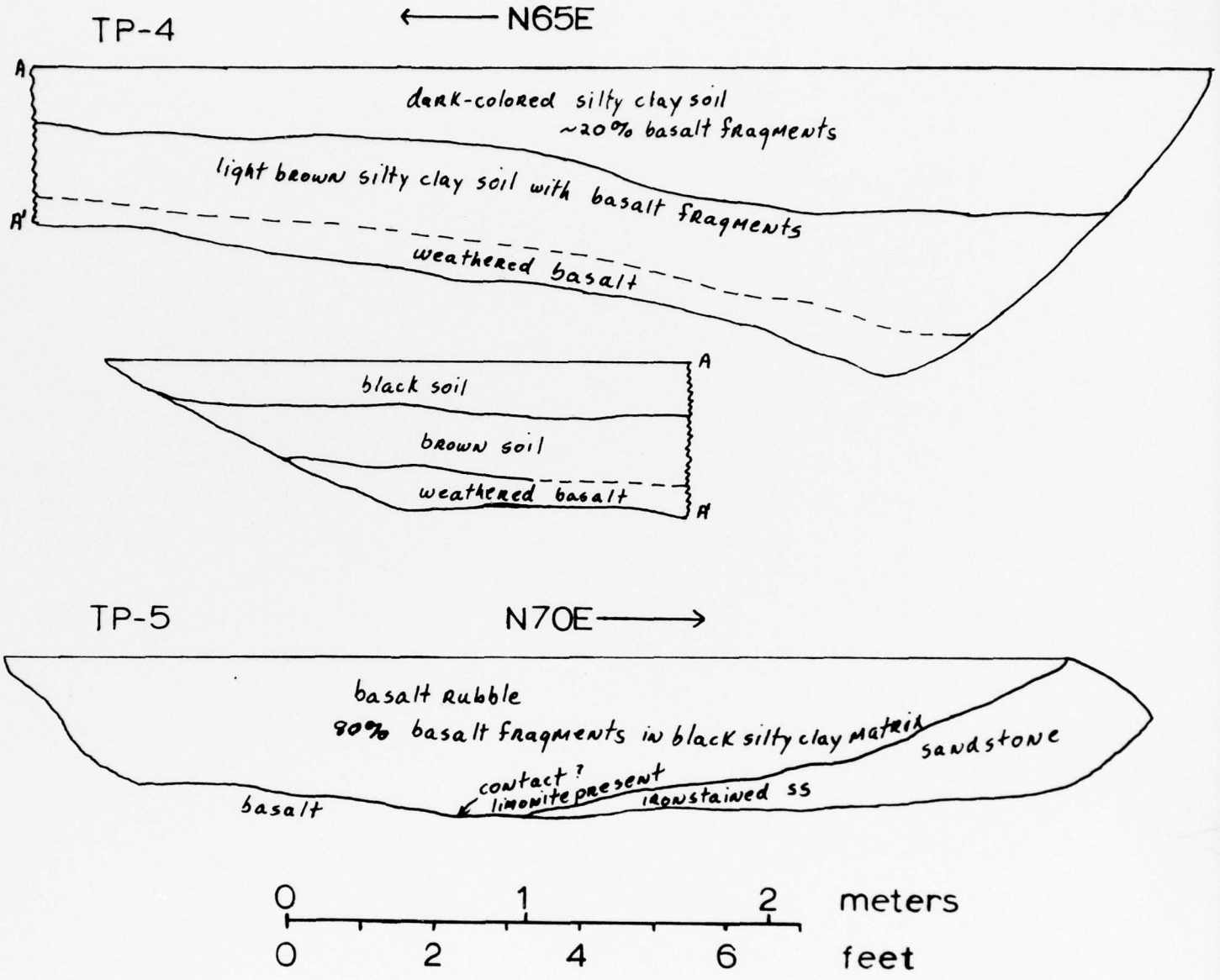
TP-4
N65E
A
A'
dark-colored silty clay soil
~20% basalt fragments
light brown silty clay soil with basalt fragments
weathered basalt
A
black soil
brown soil
weathered basalt
A
TP-5
N70E
basalt rubble
80% basalt fragments in black silty clay matrix
sandstone
contact?
limonite present
ironstained ss
basalt
0
1
2
meters
0
2
4
6
feet

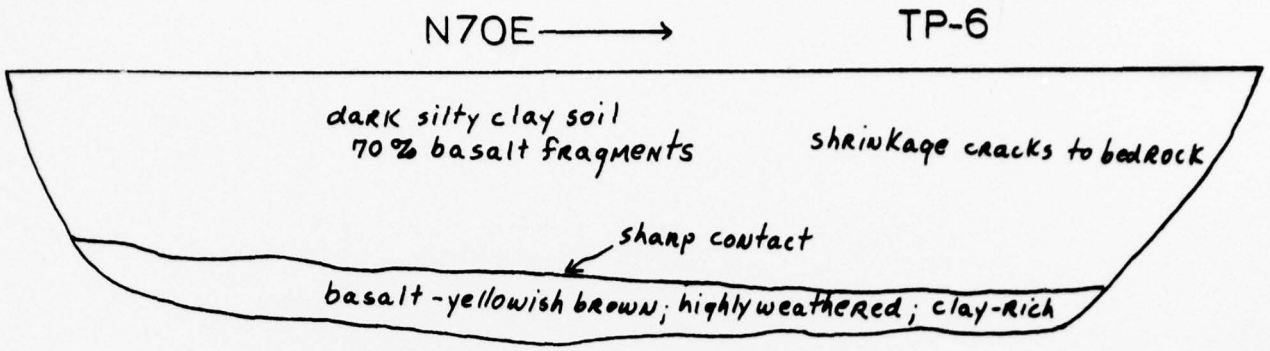
N70E
TP-6
dark silty clay soil
70% basalt fragments
shrinkage cracks to bedrock
sharp contact
basalt - yellowish brown; highly weathered; clay-rich

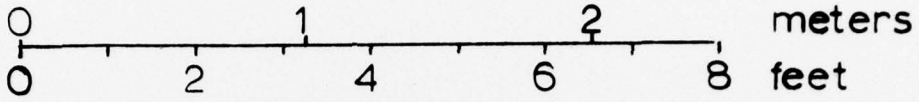
0
1
2
meters
0
2
4
6
8
feet

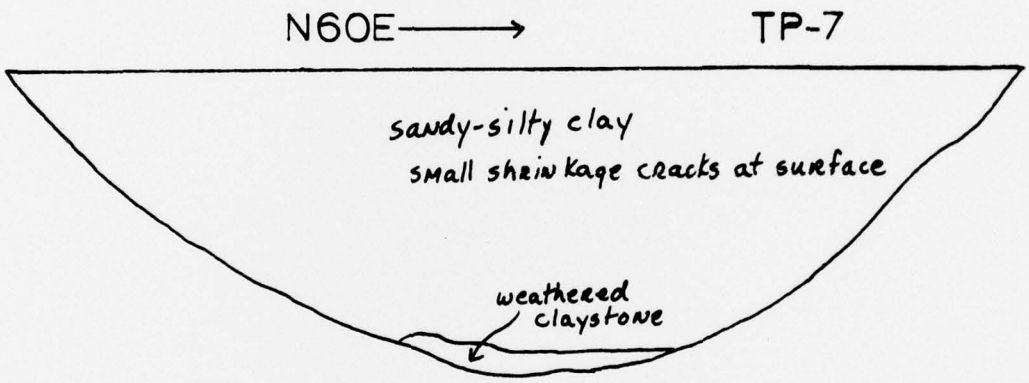
N60E
TP-7
sandy-silty clay
small shrinkage cracks at surface
weathered
claystone